ON THE GLOBULAR CLUSTER NGC 5694

By

Christian Hans Bernhard König

B. Sc. (Physics & Astronomy) University of British Columbia, 1992

A THESIS SUBMITTED IN PARTIAL FULFILLMENT OF

THE REQUIREMENTS FOR THE DEGREE OF

MASTER OF SCIENCE

in

THE FACULTY OF GRADUATE STUDIES
Department of
GEOPHYSICS AND ASTRONOMY

We accept this thesis as conforming

to the required standard

THE UNIVERSITY OF BRITISH COLUMBIA

December, 1994

In presenting this thesis in partial fulfilment of the requirements for an advanced degree at the University of British Columbia, I agree that the Library shall make it freely available for reference and study. I further agree that permission for extensive copying of this thesis for scholarly purposes may be granted by the head of my department or by his or her representatives. It is understood that copying or publication of this thesis for financial gain shall not be allowed without my written permission.

Department of Geophysics & Astronomy

The University of British Columbia
Vancouver, Canada

Date Dec 23rd 1994

DE-6 (2/88)

Abstract

We present CCD photometry of the distant globular cluster NGC 5694. Colour-magnitude diagrams and a colour-colour diagram using U, B & V data are shown. We find the reddening in the direction of NGC 5694 to be $E(B-V) = 0.10 \pm 0.02$. The metallicity is determined from $(U-B)_{1.0}$ as [Fe/H]$= -2.05 \pm 0.20$. We place an upper limit on the distance of NGC 5694 from the sun of R < 33.4 Kpc. We do not detect conventional Blue Straggler stars in NGC 5694. If these stars are present, they are in a magnitude range which is at the limit of our photometry. In addition to the known blue horizontal branch, we detect a sparsely populated red horizontal branch, which could be identified as an evolved population of Blue Straggler Stars. We also detect a very bright and blue population of stars in the core region of the cluster. The latter two populations can not be positively confirmed due to large photometric errors resulting from crowding in the cluster centre. A Michie-King model fit to the surface brightness profile yields a core radius of $r_c = 3''.51$ and a concentration parameter $c = 1.85$. We do not detect indications of a collapsed core in NGC 5694. We outline an improved method for finding the centres of globular clusters, which is used to determine the centre of the cluster to a high degree of accuracy.

Table of Contents

List of Tables

List of Figures

Chapter 1

Introduction

Studies of the globular cluster system of the Galaxy show that a large fraction of clusters exhibit features that indicate that they have reached or passed the evolutionary stage of core collapse (Trager *et al.* 1993 [38]). Binary stars are believed to play an important role in this process (Hut *et al.* 1992 [17]). Stellar populations in the cores of collapsed clusters are physically affected by the dynamical evolution of the cluster (See for example: Djorgovski *et al.* 1991 [9], Djorgovski & Piotto 1993 [10]). The cluster core, an environment of extremely high stellar densities seems to be conducive to the development of anomalous stellar populations such as blue straggler stars, while standard populations such as red giant stars seem to be under-represented (Auriere *et al.* 1990 [1]).

NGC 5694 ($\alpha = 14^h36^m41^s.6, \delta = -26°19'\ 25''$,1950) is a highly concentrated (Webbink 1985 [39]) globular cluster in the outer halo of the galaxy [16]. Only two Colour Magnitude Diagrams (CMDs) of NGC 5694 have been published. The first, by Harris 1975 [15], does not reach the horizontal branch (HB) and the other, by Ortolani & Gratton 1990 [28], does reach the main sequence turnoff but does not include the central regions of the cluster. The latter CMD shows a blue horizontal branch, typical of a metal-poor globular cluster. No unusual stellar populations are apparent in any of these investigations. Previous studies of the structure of the cluster classify it as having a Michie-King model morphology (Trager *et al.* 1993 [38]).

The intent of this study is to investigate both the stellar populations at the core of NGC 5694 and the morphology of the cluster.

Chapter 2

Observations

CCD observations of NGC 5694 were obtained by Gregory G. Fahlman and Ian B. Thompson at the 2.5m Dupont telescope of the Las Campanas observatory in May 1991 through standard U,B & V filters. The CCD used was a blue sensitive Tektronix chip with 1024x1024 pixels. The plate scale of the images is 0.″23 per pixel.

The data consists of 43 frames of standard stars and 6 frames of NGC 5694 obtained on May 12/13 1991 and 18 frames of NGC 5694 obtained on May 15/16 1991. The seeing varied during the observations; FWHMs in the program frames range between 0.″88 and 1.″47. Also obtained were flat fields and biases in the three colours. Flat fields from different nights were compared and show flatness to 0.1 %. Tables 2.1 to 2.4 summarise the data.

The observations of NGC 5694 include the cluster centre, which is not saturated in any of the frames. In all three colours visual inspection of the images reveals quasi-stellar objects very close to the cluster centre. A section of the U frame with the best seeing (# 429) is shown in Fig. 2, clearly showing the knotty structure in the centre.

Frame	Field	Filter	E.T. sec	Airmass X	FWHM (Arcsec)
412	NGC 5694	V	300	1.28	1.31
413	NGC 5694	V	300	1.24	1.47
414	NGC 5694	V	300	1.23	1.30
415	NGC 5694	V	300	1.22	1.38
416	NGC 5694	V	300	1.17	1.35
417	NGC 5694	V	300	1.15	1.26
418	NGC 5694	V	300	1.14	1.28
419	NGC 5694	V	300	1.12	1.22
420	NGC 5694	V	300	1.11	1.20
421	NGC 5694	V	300	1.10	1.23
422	NGC 5694	V	300	1.09	1.20
423	NGC 5694	V	300	1.07	1.04
424	NGC 5694	B	600	1.06	1.08
425	NGC 5694	B	600	1.05	0.95
426	NGC 5694	B	600	1.04	0.95
427	NGC 5694	B	600	1.02	0.87
428	NGC 5694	U	900	1.01	0.89
429	NGC 5694	U	900	1.00	0.88

Table 2.1: NGC 5694 observations on May 15/16 1991

Frame	Field	Filter	E.T. sec	Airmass X	FWHM (Arcsec)
307	NGC 5694	V	90	1.03	1.27
308	NGC 5694	V	300	1.03	1.47
309	NGC 5694	B	300	1.02	1.49
310	NGC 5694	B	150	1.02	1.49
311	NGC 5694	U	200	1.01	1.27
312	NGC 5694	U	500	1.01	1.38

Table 2.2: NGC 5694 observations on May 12/13 1991

Frame	Field	Filter	E.T. sec	Airmass X	FWHM (Arcsec)
260	RU 149	B	30	1.35	1.96
261	RU 149	B	30	1.36	1.82
262	RU 149	V	30	1.37	1.84
263	RU 149	V	30	1.38	1.78
264	RU 149	U	120	1.40	2.07
265	RU 149	U	120	1.41	1.86
271	PG 0918	U	120	1.21	2.03
272	PG 0918	U	120	1.21	1.93
273	PG 0918	B	30	1.22	1.88
274	PG 0918	B	30	1.22	2.25
275	PG 0918	V	30	1.22	1.90
276	PG 0918	V	30	1.23	2.12
286	Cen A	V	45	1.08	1.76
287	Cen A	V	45	1.08	1.83
288	Cen A	V	30	1.07	1.89
289	Cen A	B	45	1.07	2.04
290	Cen A	B	45	1.07	1.90
293	Cen A	U	100	1.06	2.28
294	Cen A	U	300	1.06	2.01
295	PG 1323	V	30	1.09	1.44
296	PG 1323	V	30	1.09	1.47
297	PG 1323	B	30	1.08	1.56
298	PG 1323	B	30	1.08	1.63
301	PG 1323	U	100	1.08	1.99
302	PG 1323	U	200	1.07	2.14
338	Cen A	V	30	1.84	1.86
339	Cen A	V	30	1.88	1.93
340	Cen A	B	60	1.90	1.99
341	Cen A	B	60	1.92	1.82
344	Cen A	U	300	1.98	2.28
345	Cen A	U	300	2.04	2.31

Table 2.3: Standard star observations on May 12/13 1991

Frame	Field	Filter	E.T. sec	Airmass X	FWHM (Arcsec)
355	SA110 AL-AO	B	40	1.19	1.44
356	SA110 AL-AO	B	80	1.20	1.73
357	SA110 AL-AO	V	40	1.20	1.65
358	SA110 AL-AO	V	40	1.21	1.58
359	SA110 AL-AO	U	240	1.21	2.09
360	SA110 AL-AO	U	240	1.22	2.00
361	SA110 CC-CF	V	40	1.24	1.80
362	SA110 CC-CF	V	40	1.25	1.81
363	SA110 CC-CF	B	40	1.25	1.75
364	SA110 CC-CF	B	40	1.26	1.78
367	SA110 CC-CF	U	240	1.28	1.84
368	SA110 CC-CF	U	240	1.30	1.91

Table 2.4: Standard star observations on May 12/13 1991

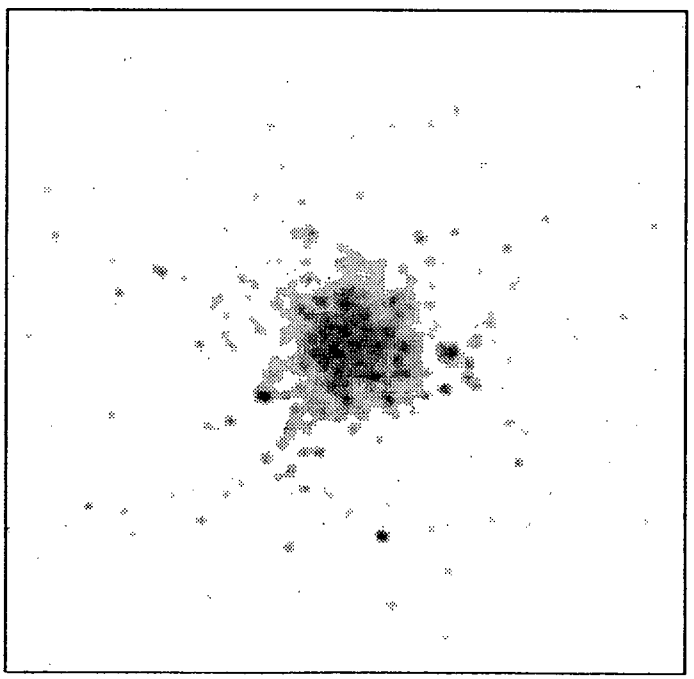

Figure 2.1: The central 56″.0 of U image # 429

Chapter 3

Data Reductions and Calibration

3.1 Preprocessing

Program and standard star frames were bias subtracted and flat fielded in standard fashion. Due to the long exposure times encountered in the data we felt it was necessary to remove cosmic ray events from the cluster frames and the standard star frames. To improve the signal to noise ratio of the data, the program frames in each of U,B & V were averaged. Ten V frames, 4 B frames and 2 U frames were used to create three deep frames.

3.2 Profile-Fitting Photometry

DAOPHOT (Stetson 1987 [34]) was used to reduce the data. The reduction procedure followed closely the procedure outlined in the *DAOPHOT User's Manual*, except that PSF stars were picked by hand and not by the PICK routine. The fact that PICK favours bright stars makes it prone to choose stars close to the cluster centre, which suffer from contamination by close neighbours. We chose a Moffat based DAOPHOT PSF to approximate the PSF shape observed in the data more closely. The PSF was not observed to vary across the frame, consequently we did not use the variable PSF option in DAOPHOT. ALLSTAR was used to perform the final reduction of the frames.

We encountered a problem with the PSF shapes in the averaged frames. Possibly corrupted in the adding procedure, the PSF could not be approximated closely enough

to permit a clean subtraction. We therefore used single frames with the best seeing in each colour in the subsequent analysis, in particular frames # 423, 427, 428 & 429 (See Table 2.1).

The averaged frames were used to create finding lists, which were more complete, due to the improved signal to noise characteristics of the averaged frames. These coordinate lists were used as coordinates in the reduction of the single frames.

We attempted to reduce the effect of the unresolved stellar component in the centre of the cluster on the accuracy of the photometry. The plan was to subtract a median filtered, star subtracted image from the frame, to remove part of the cluster background, as suggested by Stetson & Harris 1988 [37]. Due to unsatisfactory smoothness of the median filtered image, probably caused by rough subtractions of stars at the cluster centre, this plan was abandoned and the frames were reduced with the background in place. In addition to crowding, the unresolved stellar background is a probable source of increased photometric errors for stars close to the centre of the cluster. Stars will be superimposed not onto reasonably flat sky, but onto the slope of the unresolved cluster light. This can lead to a an error in the estimate of the sky brightness, which in turn influences the factor by which the model PSF will be scaled, i.e. the PSF magnitudes of the stars.

3.3 Aperture Correction

Since the PSF magnitudes returned by ALLSTAR have an arbitrary zero-point, which is different from frame to frame, corrections have to be applied to the magnitudes measured in different frames. In addition these corrections take into account that the ALLSTAR PSF only measures the stellar signal within a specified radius. The fraction of the signal in the wings of the stellar profile, outside the PSF radius, is determined by comparing

the stellar signal in apertures of increasing size. When increasing the size of the aperture does not yield a higher signal, the total signal of the star is contained in the aperture. It is then possible to relate aperture sizes to the fraction of the signal contained within.

All but the stars to be used in the determination of the aperture corrections[1] were subtracted from the data frames. Aperture photometry was carried out using DAOPHOT with the aperture radii specified by a geometric series. (See Stetson [36]) The program DAOGROW [36] was then used to perform the growth curve analysis and calculate the effective corrections for each frame.

3.4 Addstar Tests

To be able to better estimate the errors of our photometry, especially in the crowded central regions, we added artificial stars to the program frames and determined, after subsequent reductions, the accuracy with which we could recover the introduced artificial stars.

Using all the stars found in each of the program frames we binned the photometry by magnitude and plotted the log of the number of stars in each bin (Log N) vs. the central magnitude of the bin (m_c). The slope of this relation was used to generate artificial star lists with the right proportions of faint to bright stars. We chose to introduce only 150 stars per list so the number of additional stars per frame would not increase the crowding. We introduced stars at the same positions in all three frames, so matching would be carried out for more than one frame, more closely duplicating the procedure followed in the original reduction. Two hundred of these frames were created and reduced in each colour, yielding a total of 30000 artificial stars per program frame. When matching the ALLSTAR files after the subsequent reductions, we only accepted stars found in frames

[1]We used the same stars that were used earlier as PSF stars

of all three colours and in the artificial star list. Estimates of the photometric uncertainty or completeness as a function of magnitude and distance from the cluster centre will be given in later sections where applicable.

3.5 Transformation to standard magnitudes

DAOPHOT was used to carry out aperture photometry on the 37 standard stars distributed over 43 CCD frames. Aperture radii were chosen in a geometric series as described by Stetson ([36]). Standard magnitudes and colours were taken from Landolt 1992 [22].

The standard star data was fit to equations of the form:

$$v = V + a_1 + a_2(B-V) + a_3(X-1.25) + a_4(X-1.25)(B-V)$$

$$b = B + b_1 + b_2(B-V) + b_3(X-1.25) + b_4(X-1.25)(B-V)$$

$$u = U + c_1 + c_2(U-B) + c_3(X-1.25) + c_4(X-1.25)(U-B)$$

where u,b & v are the aperture magnitudes, U,B & V are the magnitudes in the standard system and X represents the airmass.

For fitting the coefficients of the transformation equations we used the fitting package MINUIT , a multi-parameter chisquare minimization routine developed at CERN. Stars in the frames listed in Table 2.4 were initially allowed to have a constant offset to allow for the possibility of a changing sky brightness. It was found that this offset was very small compared to the errors of the fitting coefficients and it was ignored. Table 3.1 lists the determined coefficients. The errors were determined through a standard bootstrap procedure[2]. By picking with replacement from the available standard star data we created

[2]See *Numerical Recipes in Fortran 2nd ed.* [27] p.686f

Coefficient	U	±	B	±	V	±
1	3.7610	0.0083	2.0047	0.0054	1.7083	0.0047
2	-0.12365	0.0135	-0.087797	0.0068	-0.021944	0.0045
3	0.43494	0.0238	0.23941	0.0246	0.10669	0.0256
4	0.0031815	0.0348	-0.046111	0.0274	0.012886	0.0219

Table 3.1: Fit Parameters

100 randomised sets that were analysed in the same fashion as the set of original standard stars. The sigmas listed in Table 3.1 are calculated from the output of the bootstrap fits.

To estimate the accuracy in our calibration we used the standard values in the literature and calculated the expected magnitudes for the standard stars in the different frames. Figure 3.1 shows the difference between calculated and standard magnitudes in the three colours. The rms scatter in the three colours is found to be $\sigma_U = 0.046, \sigma_B = 0.025, \sigma_V = 0.022$ mags. No systematic trends with magnitude are visible.

Extreme ($\Delta > 0.2$) outliers were identified by eye and removed from the list. The fitting procedure was then repeated to yield the final parameters shown in Table 3.1.

3.6 Photometric accuracy

To check the accuracy of our photometry we compared calibrated magnitudes for stars in common to the study of Ortolani & Gratton (1990)[28]. We identified six stars far from the cluster centre in both data sets and compared the existing photometry to our calibrated results. We list these data in Table 3.2. The agreement is excellent, we find offsets (in the sense Δ_m = our results - Ortolani & Gratton results) of $\Delta_V = -0.0062$ and $\Delta_B = -0.0198$.

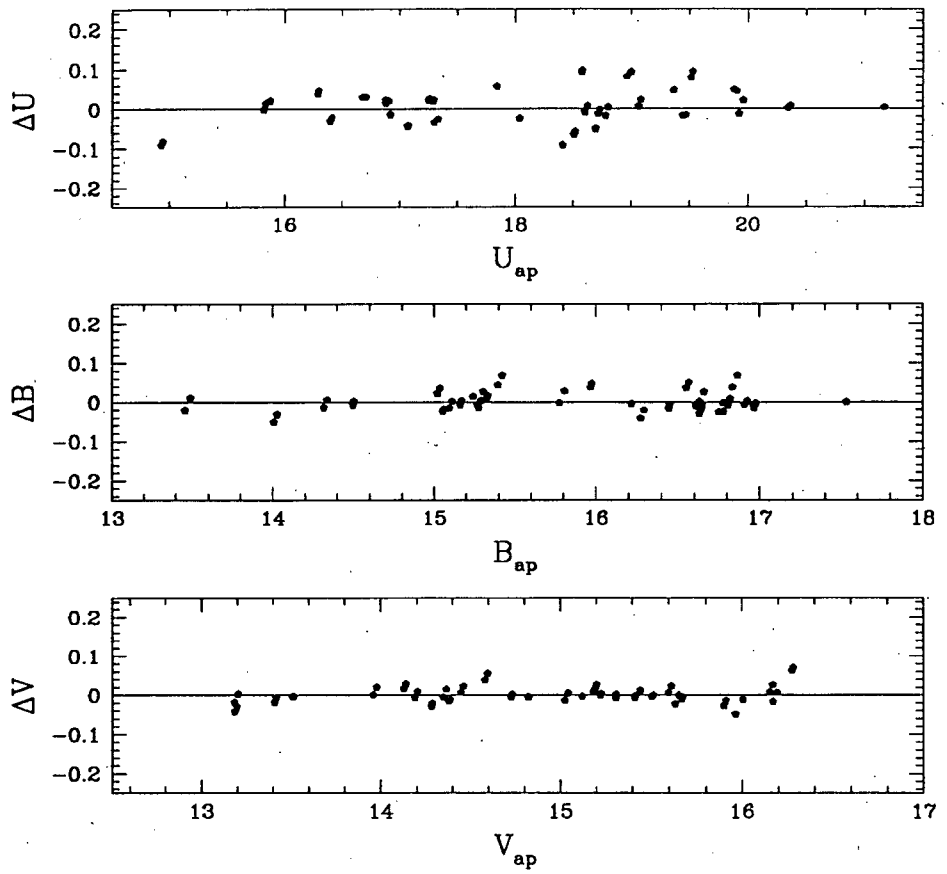

Figure 3.1: Calibration residuals

Star	V_O	V	B_O	B	ΔV	ΔB
1	18.437	18.428	19.096	19.098	-0.005	0.002
2	19.495	19.467	19.481	19.452	-0.028	-0.029
3	19.518	19.527	20.240	20.248	0.005	0.008
4	19.682	19.662	20.406	20.400	-0.020	-0.006
5	19.810	19.811	20.579	20.530	0.001	-0.049
6	20.978	20.987	21.054	21.009	0.009	-0.045
μ					- 0.006	-0.019

Table 3.2: Comparison of our photometry to Ortolani & Gratton

Chapter 4

Colour Magnitude Diagrams and derived parameters

4.1 Cmds

Fig. 4.1 shows CMDs in V,B-V (4.1 a), U,U-B (4.1 c), V, U-V (4.1 d) and a colour-colour plot in the U-B,B-V plane (4.1 b). Selection criteria were not applied, except we required stars to be detected in one frame in each of B & V and in two U frames. This yielded the 1435 stars shown in Fig. 4.1. The photometry of these stars is tabulated in Appendix B. The V magnitudes range from $\sim$ 14.5 to $\sim$ 22.5. The main sequence turnoff is not apparent in the data displayed here. The study by Gratton & Ortolani [28] places it at $V \sim 22.0$. The red giant branch (RGB), asymptotic giant branch (AGB) and horizontal branch (HB) are well defined. Notable is the number of objects brighter and bluer than the AGB. These stars are especially noticeable in Fig. 4.1 c. The data points marked by pentagons are the central knots shown in Fig. 2.

Since distances of stars from the cluster centre will play an important role in some of the following discussions we also include CMDs that indicate the distance of stars from the cluster centre. Fig. 4.2 shows CMDs in V,B-V (4.2 a), U,U-B (4.2 c), V, U-V (4.2 d) and a colour-colour plot in the U-B,B-V plane (4.2 b). The size of the symbols depends on the distance of the star from the cluster centre; the bigger the symbol is, the closer the star is to the centre.

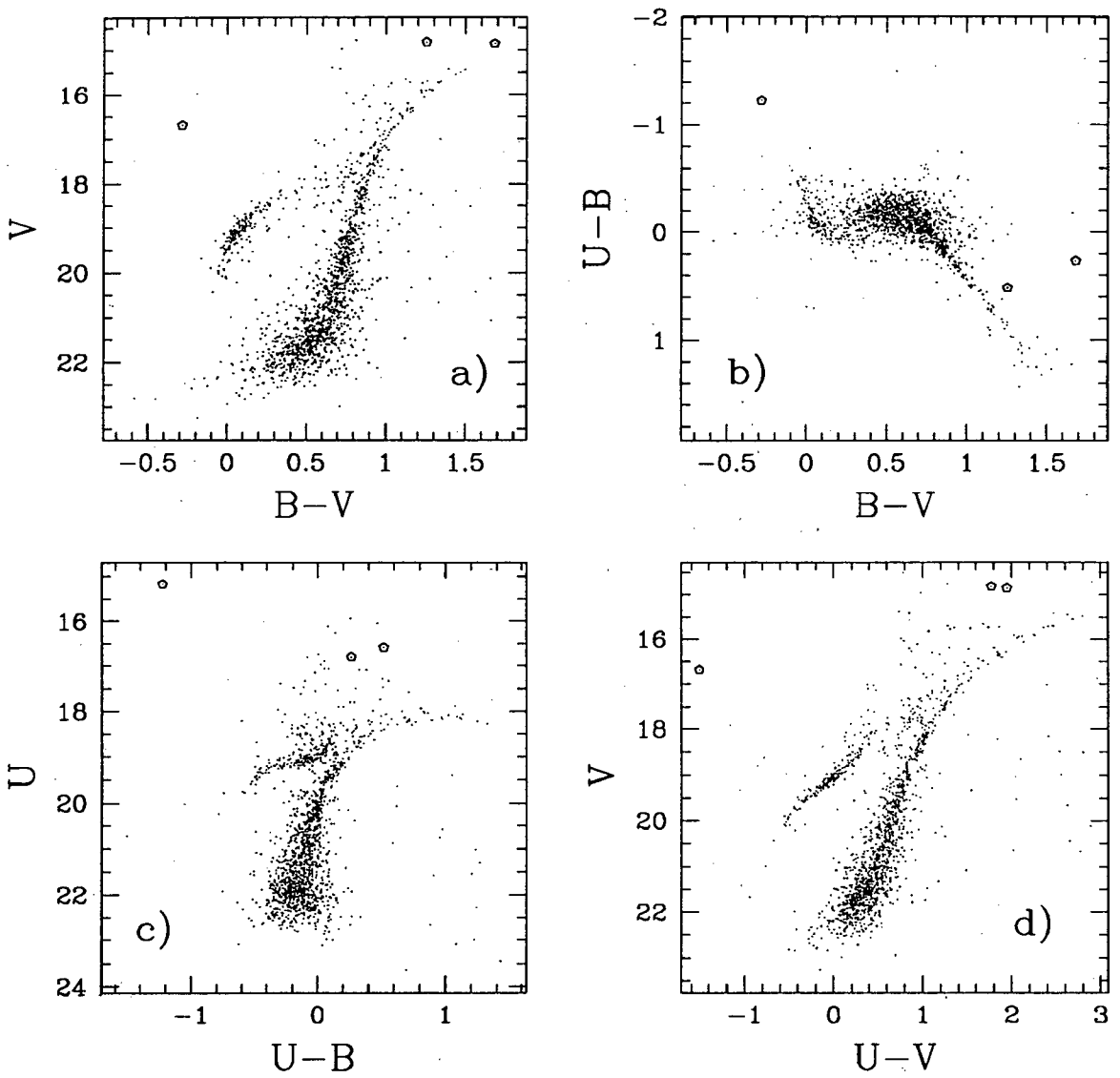

Figure 4.1: CMDs

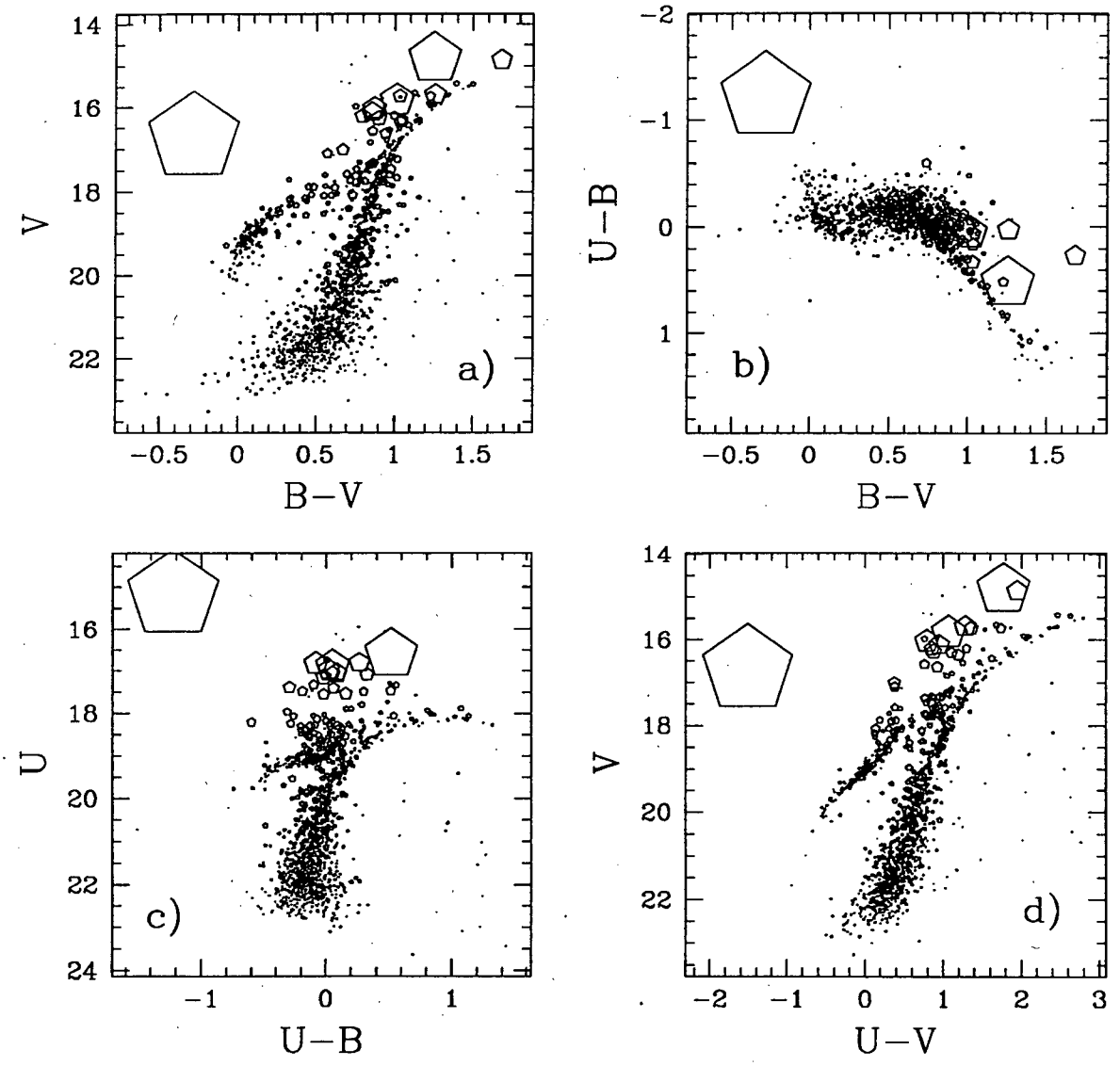

Figure 4.2: CMDs with indication of distance from center

4.2 Knots

Visual inspection of the knots reveals the following characteristics: Knot 1 (middle pentagon in Fig. 4.1 a) is starlike in appearance in frames of all three colours, knot 2 (the bluest in Fig. 4.1 a) is very weak in the V frame and displays a morphology wider than a typical star in the B and U frames. Knot 3 (the reddest in Fig. 4.1 a) seems to be a blend of three stars (3a-3c) with 3b and 3c visible in the V frame, all three visible in B and only 3a and 3b visible in U.

An attempt to simulate the magnitudes of the central knots was made by treating them as blends of two or three standard sequence stars. The limitations placed on those blenders were (1) they had to be stars occurring in the data and (2) their magnitude could not be brighter than 18.0 in U. This latter restriction was introduced to insure that stars of unusual magnitudes were not used in the trials. The results are shown in Fig. 4.3. A pentagon marks the data for the knot, a line leads to the value closest in UBV space achieved by adding signal from two or three stars. This point in turn is connected to the stars used in the blending.

It is apparent that it is impossible to replicate any of the values for the three knots by superposition of two stars. If one superimposes three stars, the agreement with observed values becomes better.

The reddest knot, which by its location in the V,B-V plane could be suspected of being a very bright AGB/RGB star is not well simulated. The middle knot in the diagram is well represented by three RGB/AGB stars, which is almost contradictory since it is the most starlike in appearance. The data of the knot on the blue of the CMD can not even approximately be replicated.

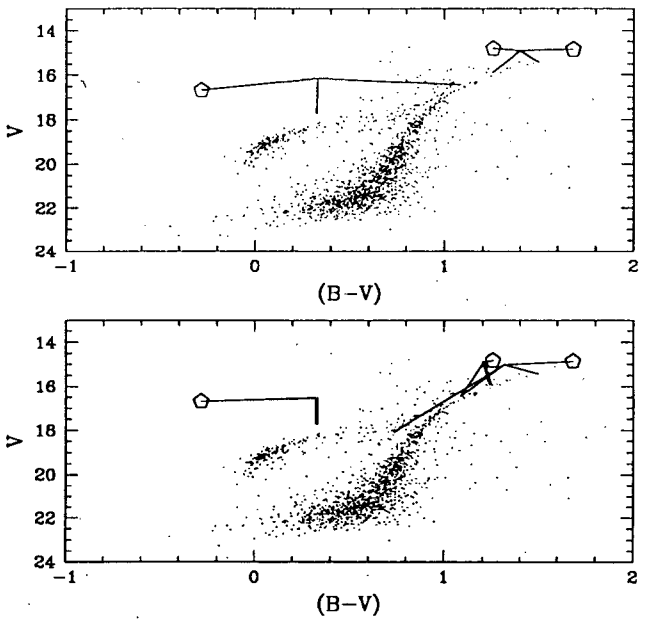

Figure 4.3: Simulation of magnitudes for central knots : Two (top panel) and three (bottom panel) component stars

4.3 Blue central Population

Strengthened by recent observations, primarily by HST, evidence is mounting that the stellar population in the cores of globular clusters can be modified by the extreme stellar densities. Djorgovski *et al.* 1991 [9] report colour gradients in the cores of the post corecollapse globular clusters NGC 6284, 6293, 6397 & 6558, in the sense of becoming bluer towards the center[1]. This effect is attributed to a different stellar population in the inner regions of the cluster. HST observations of M15 show an excess of blue stars and a deficiency of red giants in the core. [8]

[1]A reddening of the stars toward the center would be the effect of photometry being compromised by crowding. [9] Overestimating the brightness of stars by a false sky estimate is equivalent to interpreting part of the unresolved cluster background as signal of the stars. Since the cluster background is comprised mostly of red main sequence stars, this effect is more pronounced in V than in B or U. A reddening of the stellar colours is the result.

While it is tempting to identify the stars scattered $\sim$ 1 mag above or $\sim$ 0.25 mags to the blue of the AGB (See Fig. 4.2 a) as such a modified population, the artificial star tests conducted (Sect. 3.4) suggest that these data points could just be the result of photometric errors. This population is most apparent in the U,U-B CMD (Fig. 4.2 c), and this is what we concentrated our experiment on. We analyzed the artificial star test, trying to find which percentage of stars that were reported by ALLSTAR to have magnitudes of $U < 18.0$ actually were placed into the frame in this magnitude range. As is apparent in the CMD (Fig. 4.2 c), most of the stars in question are located in the inner part of the cluster. We therefore concentrated our analysis on an area of radius 50 pixels centred on the cluster centre.

Table 4.1 shows the result of this experiment for stars within R $<$ 50 pixels. Only stars that were artificially introduced **and** recovered were counted. The columns in Table 4.1 show at which magnitude stars were added into the frame, the label being the centre of the magnitude bins of width 1. The rows correspond to measured magnitudes. Ideally all the off-diagonal elements would be zero, i.e. all stars are measured at their true magnitudes. To aid the reader, the relevant magnitude ranges in Table 4.1 are bracketed by lines. Of the 13 stars measured in the magnitude range $16 < U < 18$ only 10 (or 77%) were introduced at this magnitude and 3 are scattered up from the magnitude bin below. The situation is even worse if we consider only stars with $17 < U < 18$. Out of 7 stars found only 4 (or 57%) were introduced in this magnitude range. Unfortunately we deal with small number statistics at small radii, but as expected, photometry in this magnitude range suffers close to the cluster centre.

Number counts in the U,U-B CMD (Fig. 4.2 c) yield 19 stars with $17 < U < 18$, 43 stars with $18 < U < 19$ and 9 stars with $19 < U < 20$. Table 4.1 shows that the number of stars with introduced magnitudes of $18 < U < 19$ is greater by a factor of 1.5 (6/4) than the number that is observed. From this we can estimate that the number of

U_{out} \ U_{in}	13.5	14.5	15.5	16.5	17.5	18.5	19.5	20.5	21.5	22.5
13.5	0	0	0	0	0	0	0	0	0	0
14.5	0	1	0	0	0	0	0	0	0	0
15.5	0	0	2	0	0	0	0	0	0	0
16.5	0	0	0	6	0	0	0	0	0	0
17.5	0	0	0	0	4	3	0	0	0	0
18.5	0	0	0	0	0	3	1	0	0	0
19.5	0	0	0	0	0	0	1	1	0	0
20.5	0	0	0	0	0	0	0	0	0	0
21.5	0	0	0	0	0	0	0	0	0	0
22.5	0	0	0	0	0	0	0	0	0	0

Table 4.1: Analysis of addstar tests in U for R $<$ 50 pixels

stars in NGC 5694 with $18 < U < 19$ within R $<$ 50 is on the order[2] of 65 (43×1.5). According to Table 4.1, half of these, or 32 stars would scatter into the magnitude range of $17 < U < 18$. This number is bigger than the number of observed stars in this range, which is 19. Thus we can not claim that the data with $U < 18$ represents the discovery of a modified blue population in the core of NGC 5694. Most of the data values could be artefacts of poor photometry[3].

4.4 Blue Straggler Stars

Recent observations have discovered large numbers of Blue Straggler Stars (BSSs)[4] in the cores of some globular clusters. For example De Marchi & Paresce 1994 [8] find large numbers of BSSs in the inner 2.″0 of M15. It has also been shown that BSSs in some

[2]The actual number is even larger, since the numbers in this magnitude range in Table 4.1 are affected by incompleteness.

[3]This discussion does not apply to **all** data in the specified magnitude range. While the photometry of the bluest of the central knots most certainly suffers from crowding effects, it is very unlikely that the star populates a standard sequence.

[4]I hereby register my protest. Being politically uncorrect, I prefer BSs.

Distance/pixels	Introduced	Recovered	Fraction recovered
$R > 300$	8735	7387	0.846
$300 > R > 175$	2150	1544	0.718
$175 > R > 100$	775	327	0.422
$100 > R > 50$	302	20	0.066
$50 > R$	89	0	0

Table 4.2: Completeness as a function of radius for $20.0 < V < 22.0$

globular clusters are centrally concentrated. In observations of the core of NGC 6397 Auriere *et al.* 1990 [1] discovered several bright BSSs and no RGB population. Lauzeral *et al.* 1992 [2] show that the BSSs in NGC 6397 are more centrally concentrated than other populations.

No BSSs are apparent in our CMD, some points in the relevant area could well be photometric scatter. But, if BSSs in NGC 5694 are also positionally biased toward the center we should not expect to find considerable numbers of them in our data. In NGC 5694 we would expect to find the BSSs in a magnitude range of $20 < V < 22$. One expects crowding in the cluster core to affect the completeness of the photometry. Table 4.2 shows the results of addstar tests. Listed is the fraction of stars introduced in a magnitude range of $20.0 < V < 22.0$ that were recovered in this same magnitude range as a function of radius from the cluster centre.

It is apparent that the fractions of stars in this magnitude range that is detectable at small radii is very low. If a large population of BSSs existed in the core of NGC 5694, we would not have detected them. To aid the reader in interpreting the radii in Table 4.2 : a radius of 100 pixels corresponds to 23.″0. At a distance of 33.4 Kpc[5] this angular size corresponds to a dimension of 3.72 pc. The core radius[6] of NGC 5694 is only on the

[5]See Sect. 4.6
[6]See Sect. 6.1

order of 15 pixels, which corresponds to a linear size of 0.55 pc.

While we can not expect to detect BSSs at $20 < V < 22$ if they are centrally concentrated, stars at brighter magnitudes could be found in the centre of the cluster.

4.4.1 Evolved BSSs

While information on BSSs in globular clusters is accumulating, data on their progeny is still speculative. Renzini & Fusi Pecci 1988 [32] and Fusi Pecci *et al.* 1992 [14] suggest that evolved BSSs will populate the horizontal branch at red magnitudes. Using ZAHB models by Seidl *et al.* 1987 [35] for stars ranging in mass from $0.66M_{\odot}$ to $1.7M_{\odot}$, Fusi Pecci *et al.* show that BBSs, due to their higher mass, are expected to appear at brighter and redder magnitudes than other HB stars in the cluster.

Figure 4.4 shows CMDs in V,B-V for different annuli centered on the cluster centre. Fig. 4.4 a) shows all stars, b) stars at R< 100 pixels, c) stars with $100 < R < 300$ pixels and d) stars with R> 100 pixels. Inspection shows that at radii $R < 100$ pixels we detect stars populating the red horizontal branch. While photometric scatter seems to be present, a definite sequence is detectable. Could this population of stars be a detection of evolved BSSs?

Since we have problems with photometric accuracy in the central region of the cluster we want to rule out that these points are the result of photometric errors. Using the results of the addstar tests, we estimated the accuracy of the photometry as a function of distance from the cluster centre. The results are shown in Table 4.3. The relevant magnitude ranges are bracketed by lines. Of the 11 stars found in the magnitude range $17 < V < 19$ only 8 (or 73%) were introduced at this magnitude and 2 are scattered up from the magnitude bin below, 1 even from two bins below.

Analagous to the conclusion in Sect. 4.3, we can not confidently conclude that we have detected a real population of stars. While stars in the AGB need photometric

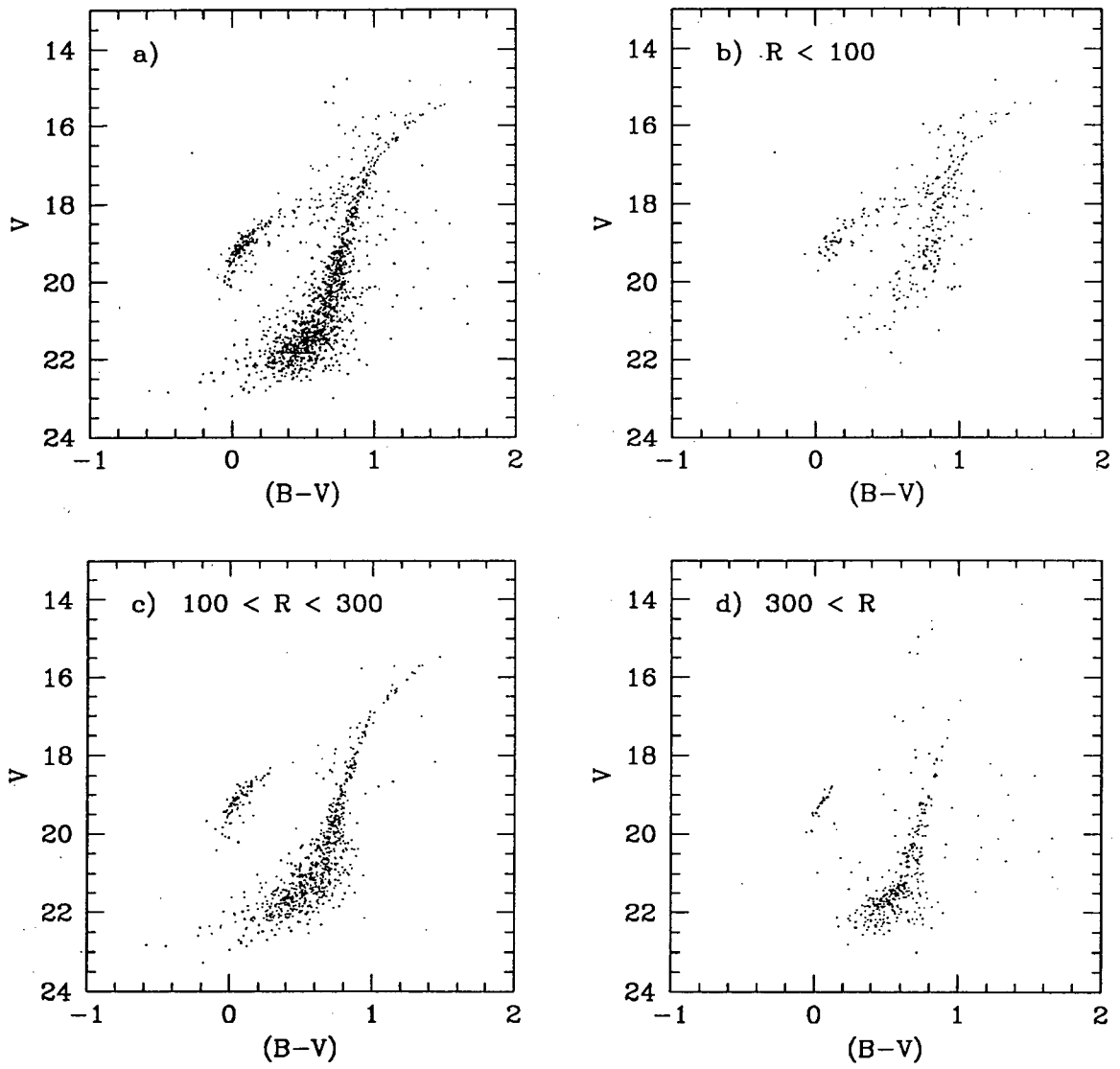

Figure 4.4: V,B-V CMD for radial annuli delimited by 100 & 300 pixels

V_{out} \ V_{in}	13.5	14.5	15.5	16.5	17.5	18.5	19.5	20.5	21.5	22.5
13.5	0	0	0	0	0	0	0	0	0	0
14.5	0	1	0	0	0	0	0	0	0	0
15.5	0	0	2	2	0	0	0	0	0	0
16.5	0	0	0	4	2	0	0	0	0	0
17.5	0	0	0	0	2	5	0	0	0	0
18.5	0	0	0	0	0	1	2	1	0	0
19.5	0	0	0	0	0	0	0	0	0	0
20.5	0	0	0	0	0	0	0	0	0	0
21.5	0	0	0	0	0	0	0	0	0	0
22.5	0	0	0	0	0	0	0	0	0	0

Table 4.3: Analysis of addstar tests in V for R $<$ 50 pixels

errors of $\sim$ 1 mag to be scattered into the area of the CMD relevant for a central blue population, inspection of Fig.4.1 a shows that stars found in the red HB would have to be scattered up from the subgiant branch by $\sim$ 2 magnitudes. While there are certainly enough stars in the subgiant branch to create a large enough population in the red HB by upscattering, on first thought one would not expect to see a reasonably well defined sequence of stars in this scenario. The impression of a sequence is partly caused by the sparcity of stars below the red HB. Unfortunately, this sparcity could simply be the result of incompleteness at magnitudes $V > 19$. Table 4.3 shows that no stars with $V > 19$ are detected at distances of R $<$ 50.

Since we only introduced stars of one colour in the addstar tests, we can not carry out a proper analysis of errors in colour. Thus we cannot rule out a scattering in colour from the blue HB or the giant branch into the relevant colour range.

4.5 Interstellar Reddening and Metallicity

The top part of figure 4.5 shows blue horizontal branch stars (V< 19.75, B-V < 0.2) superimposed onto the luminosity class V fiducial ([24],Table 3-3), which has been reddened by values of E(B-V)= 0.07, 0.10 & 0.13 using a reddening vector slope of 0.72. The blue horizontal branch stars were used to estimate the extent of the reddening since they are hot enough so their position in the diagram is not affected by metallicity. The fiducial reddened by E(B-V)= 0.10 was chosen as best representing the data. We estimate our error in the determination of E(B-V) to be ~ 0.02, the uncertainty could be greater if systematic errors in one of the magnitudes are significant, which does not seem to be the case. This reddening is consistent with results of other studies, most notably $E(B-V) = 0.16$ by Kron and Guetter (1976) [21], $E(B-V) = 0.10$ by Zinn (1980) [40] and $E(B-V) = 0.07$ by Reed *et al.* (1988) [31]. The maps by Burstein & Heiles (1982)[5] indicate a value of $0.09 < E(B-V) < 0.12$.

We also attempt to estimate the metallicity of NGC 5694. Since our photometry does not reach below the main sequence turnoff, we can not use the $\delta(U-B)_{0.6}$ vs. [Fe/H] relation (Richer & Fahlman 1984 [33]) for main sequence stars. Instead, we use a relation employing the ultraviolet excess at $(B-V)_0 = 1.0$, $\delta(U-B)_{1.0}$. The bottom panel of Figure 4.5 shows all stars dereddened and superimposed onto the class V fiducial. At $(B-V)_0 = 1.0$ we find an offset between the fiducial and the data of $\delta(U-B)_{1.0} = 0.273$ with a spread of $\sigma = 0.083$ and a standard error of the mean of $\sigma_m = 0.016$. These values were obtained by calculating the offset of 25 stars in the colour range $0.9 < (B-V)_0 < 1.10$ from the fiducial. Since a clear sequence is evident in this colour range, we only used stars with an offset of $0.07 < \Delta(U-B) < 0.4$ from the fiducial. We obtained fiducial values at the $(B-V)_0$ colours of the stars by linear interpolation between values of the fiducial at $(B-V)_0 = 0.85$ and 1.16. Our value of

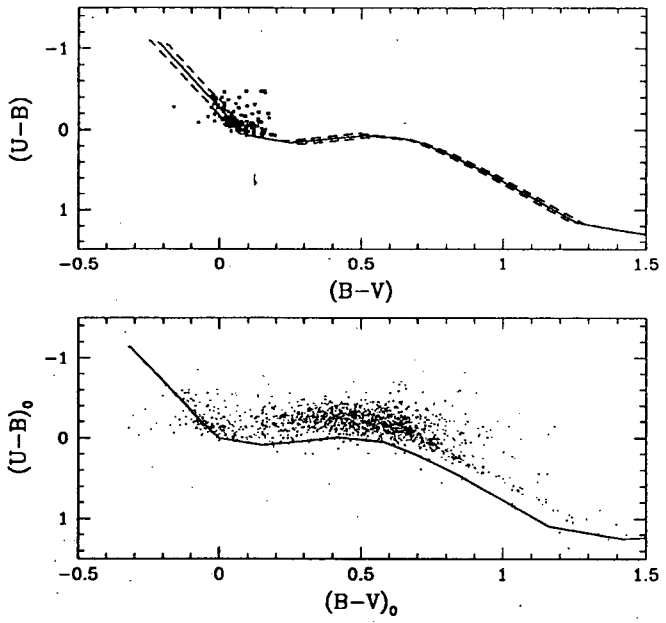

Figure 4.5: Estimation of Reddening toward NGC 5694

$\delta(U-B)_{1.0}$ can be related to the metallicity of the cluster. Buser and Kurucz 1992 [6] used model atmospheres to calculate a theoretical $\delta(U-B)_{1.0}$ vs. [Fe/H] relation applicable to globular cluster subgiants. Placing our value of $\delta(U-B)_{1.0} = 0.273 \pm 0.02$ on this relation, we estimate [Fe/H]$\sim -2.05 \pm 0.20$. This value is consistent with estimates of the iron abundance in previous studies, most notably [Fe/H]$= -1.91$ by Djorgovski 1993 [12], and [Fe/H]$= -1.92 \pm 0.15$ by Zinn & West 1984 [41]. The value of [Fe/H]$= -1.65 \pm 0.06$ by Ortolani & Gratton 1990 [28] does not seem plausible.

4.6 Distance Modulus

Ortolani & Gratton [28] find an apparent distance modulus of $(m - M)_V = 17.82 \pm 0.15$. Harris's [15] photometry does not reach the horizontal branch, but he estimates $V_{HB} = 18.2 \pm 0.3$ and $(m-M)_0 = 17.3$.

Due to the slope of the horizontal branch and the lack of red stars in the outer region of the cluster, the magnitude of the horizontal branch[7] is difficult to determine. Using data far from the cluster center to avoid artificially brightened stars we place a faint limit of $V_{HB} \leq 18^m.45$ on the horizontal branch magnitude. We estimate our error in this limit to be $+0^m.1, -0^m.3$. For further analysis we accept a value of $V_{HB} = 18^m.25$. Using $M_V(RR) = 0.37\,[Fe/H] \pm 1.24$ by Buonanno *et al.* 1989 [4] and a value of $[Fe/H] = -1.92$[8] obtain $M_V(RR) = 0.53$. This leads to a value for the distance modulus of $(m - M)_0 = 17.42$ with a limit of of $(m - M)_0 < 17.62$, where we also include the effect of absorbtion. The corresponding distance is 30.5 Kpc with an upper limit of 33.4 Kpc.

4.7 Contamination by field stars

The contamination of the CMDs by foreground field stars was estimated from simulations using the Bahcall-Soneira Galaxy model ([3]), in the direction of NGC 5694 (Ratnatunga & Bahcall 1985 [30]). The values were scaled to a field size of 15.408 square arcminutes[9]. Table 4.4 shows the number of stars presented in the CMDs in various colour and magnitude ranges compared to the number of expected foreground stars. In most ranges relevant to the analysis the estimated contamination by foreground stars is negligible.

To illustrate the probability of finding field stars in the cluster centre, compared to the area of the frames, we compiled a list of scaling factors to obtain the expected number of field stars within various distances from the cluster centre, which are shown in Table 4.5. Since the probabilities of finding field stars and finding the cluster center are independent[10] the number of expected field stars scales directly with area.

---

[7]Since we are dealing with a *diagonal* branch, horizontal branch stands for ZAHB at the colour of an RR Lyra star

[8]Here we use the spectroscopic value by Zinn & West 1984. We believe that a direct measurement is more accurate than a value derived from a secondary parameter.

[9]Corresponding to a plate scale of $0''.23$/pixel and an image size of 1024×1024 pixels

[10]N.B.: We assume independence in the small field of the frames of the observations. In general

Colour Range	14	16	18	20	22
$(B-V) < 0.8$	1/0.80	5 /2.00	131/4.31	440/13.4	578/7.7
$0.8 < (B-V) < 1.3$	2/0.43	48/2.31	145/6.01	53/7.86	12/16.9
$1.3 < (B-V)$	1/0.17	8 /0.37	3/2.16	4/8.94	1/24.7
TOTAL	4/1.4	61/4.8	279/12.5	497/30.8	591/49.3

Table 4.4: Count of Observed stars / Expected foreground stars

Radius	Multiplication factor
100	3.0×10^{-2}
50	7.5×10^{-3}
25	1.8×10^{-3}
10	3.0×10^{-4}
3	2.7×10^{-5}

Table 4.5: Probability of observing field stars within a certain radius from centre

independence is not given, there would be no point for a Galaxy model otherwise.

Chapter 5

The centre of NGC 5694

5.1 Motivation

The accurate determination of the centres of globular clusters is of great relevance to several fields of astronomy. The positions of pulsars can be known to sub-arcsecond accuracy and the precision of positions of X-ray sources observed by the Einstein HRI instrument is on the order of 3 arcseconds. Since many of these phenomena are observed within globular clusters, one needs to know the centre of the cluster core to a comparable accuracy to determine whether these phenomena originate in the core. Other needs for accurate centre positions arise in the calculation of radial profiles. If the centre is inaccurately measured, profiles will be faulty, in particular the calculated central density will be lower than the value that would be obtained with an accurate centre ([12]).

According to the importance of the subject, much effort has been placed in limiting the errors of the existing methods. For a review of the available methods and their accuracies the reader is referred to Picard & Johnston 1994 [29].

Making matters more complicated, it is not always clear which quantity determines the centre of a globular cluster. Ideally the maximum of the stellar density, the maximum of the received flux and any fitted maximum to the flux density would coincide in the same position. This of course would only be true if all stars were of the same mass and luminosity and had a *continuous* distribution. Unfortunately real stars come in different luminosities and are extremely non-continuous. In any image of a globular cluster one

expects a slight offset between the centre of the light distribution (luminosity centre) and the centre of the stellar distribution (gravitational centre) due to the presence of bright stars and to the discreteness of the stellar distribution.

The centres of gravity and luminosity can also be distinct. Calzetti *et al.* [7], for example, show that for 47 TUC the two centres are different by approximately 6 arc-seconds. Since this angular divergence would be smaller for more distant clusters, it is necessary to develop centre finding methods with high enough accuracy to detect such a phenomenon.

5.2 Results

The methods used to estimate the centre of NGC 5694 are outlined in Appendix A. We concentrated our efforts of determining the centre on one U image of NGC 5694 (Frame 429, see Table 2.1). The image was chosen for the procedures because it has the best seeing and the biasing effect of red giants is smallest in U (King 1985 [19]). Table 5.1 shows centres obtained using some of the methods listed in Appendix A. The following abbreviations are used: SCC= Self Cross Correlation, MACF= Mirrored Auto Correlation Function, NP= Non Parametric density estimation.

As seen in Table 5.1, the centres determined by runs of the SCC and MACF methods using different window sizes are very similar and fall in the same region as the centre determined by the projection method. It is noteworthy that all these methods use the light- distribution.

A very different centre was determined using the NP method, which used stellar positions determined by DAOPHOT. No limits on magnitudes were placed on stars used in this analysis, since incompleteness is a radially symmetric process[1].

[1]Assuming uniform sky brightness, etc.

No	Method	Window Size	X centre	Y centre
1	Projection	N/A	739.0	470.1
2a	NP	50	753.8	458.7
2b	SCC	128	754.4	454.6
3	SCC	128	739.4	469.8
4	MACF	128	740.4	470.2
5	SCC	256	738.5	470.6
6	MACF	256	738.2	470.8
7	SCC	64	740.8	469.2
8	MACF	64	740.8	470.0
	For 3-8			
	$\mu_{+(0.5,0.5)}$		740.2	470.6
	σ		1.16	0.58

Table 5.1: Centres obtained using different methods

While the spread of the results of the SCC & MACF methods was $\sigma_r = 1.3$ pixels[2], the centre determined by the NP method is located 18.1 pixels from the mean of the results of the correlation methods.

The question arises, whether this difference is due to the use of star counts vs. light distribution or to an intrinsic bias of one of the centre-determining algorithms. To test this, we used the DAOPHOT routine ADDSTAR to create an artificial image, populated by stars of a constant brightness[3] at positions determined by the ALLSTAR file. This image has stars in all the right places, but is lacking the contribution from bright stars and the underlying light distribution, originating from unresolved stars in the cluster. Thus if analyzed by the SCC method, one expects to find a centre similar to the one determined by the NP method run on the stellar position data. And indeed, the result, listed as item 2b in Table 5.1, shows the centre close to the one determined by the NP method.

[2] $\sigma_r^2 = \sigma_x^2 + \sigma_y^2$
[3] $m_{psf} = 19.0$

5.3 Two distinct centres ?

The notion of distinct centres of gravity and luminosity in NGC 5694 is intriguing, especially when viewed in the context of other unusual properties of NGC 5694. Taking into account NGC 5694's unusually high space velocity and its large distance from the Galactic centre, Harris & Hesser 1976 [16] conclude that the cluster is in a gravitationally unbound orbit, and suggest that tidal interaction with the Magellanic clouds could be responsible for the hyperbolic orbit.

Since the centre of luminosity agrees very well with the peak of the signal of the unresolved cluster background, the difference in centres would have to be attributed to the positions of the resolved stars[4]. Could tidal interaction have disturbed the gravitational centre of stars either only above, or only below the main sequence turnoff? In order to determine the significance of the different centres found by the methods using starcounts vs light distribution, we conducted two tests.

The first test was a Monte Carlo analysis using the NP method. We determined the cumulative distribution of stellar positions in X by fitting a cubic spline to the number of stars in bins of width 1 pixel. A deviate of the X position was obtained from this distribution whereupon a cumulative distribution in Y was calculated using a strip 10 pixels wide centered on the accepted X position[5]. This procedure was repeated 3072 times to create a sample as big as the original one. One thousand artificial data sets were created and analyzed in the same fashion as the original data set. The centres found are plotted in Fig. 5.1.

Since the scatter of points is not as symmetrical and concentrated as one would

[4]The stars which were used by the NP method in determining the centre of gravity.

[5]The determination of this strip- width was *ad hoc*, attempting to make the strip wide enough to have a reasonable number of stars included, but not so wide as to sample a different distribution of Y positions too far away from the accepted X position

expect[6], we devised a method to reject values beyond a certain threshold. The rejection method used was based on the following reasoning. Assuming the 1000 points are distributed normally, one expects ~ 683 points to fall within $\mu \pm 1\sigma$. We can also calculate the approximate distance in σs at which the probability for a point falls below 0.5, i.e. a distance from the mean beyond which we should not expect more data given our sample size. For 1000 points this probability is equal to $\frac{1}{1000} \times 0.5 = 0.05\%$ and corresponds to $\sim 3.5\sigma$ (99.5 %). A sample with less points reaches this threshold at a lower σ. In an iterative process we recalculated the mean and standard deviation of the sample of detected centres, in each step rejecting data that was further than the threshold from the mean, until the sample contained no more points beyond the threshold.

From the remaining points we extracted the mean and the standard deviation, which are listed in Table 5.2. In this table we also list the median and confidence limits[7] obtained from the cumulative distribution of the complete sample of detected centres. Table 5.2 shows that the σ calculated with rejection and the confidence limit for 68.3 % (determined without rejections) are not very different, indicating that the apparently deviant points in Fig. 5.1 do not have much influence on the result.

The second test carried out arose from interest in how single stars would affect the outcome of the SCC method. In order to test this we created test images in which we subtracted a certain number of the brightest stars to remove a corresponding fraction of the total light contributed by stars. Fig. 5.2 shows the relation between the number of stars and corresponding fractions of the total light. The squares indicate points at 10 % intervals of the total light.

DAOPHOT was used to subtract the number of stars corresponding to the light fractions from the original image. Then the SCC method was run on this image in a

[6]We believe computational inaccuracies in the code to create the artificial coordinates are responsible for this.

[7]Here 1σ stands for the interval that contains 68.3 % of the data points.

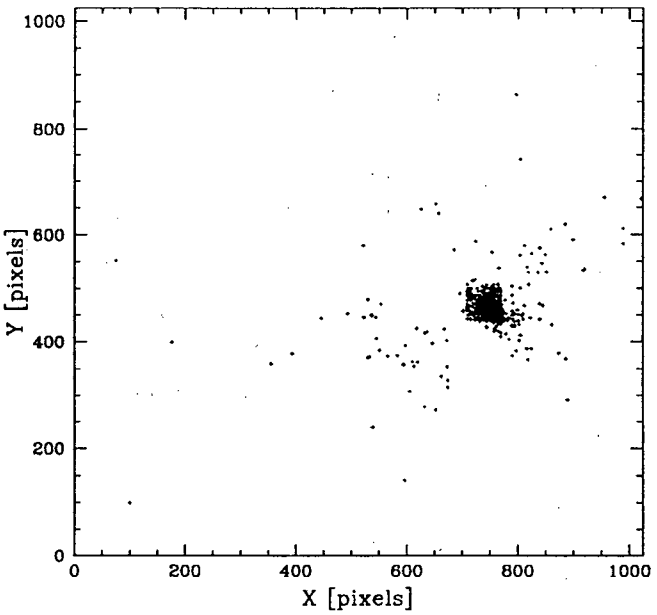

Figure 5.1: Centres found in the Monte Carlo analysis

Parameter	X	Y
μ	753.8	459.8
σ	14.3	15.4
Median	754.5	457.2
1σ	14.9	16.7
2σ	43.0	42.6
3σ	292.1	384.7
4σ	730.7	465.6

Table 5.2: Parameters derived from Monte Carlo analysis

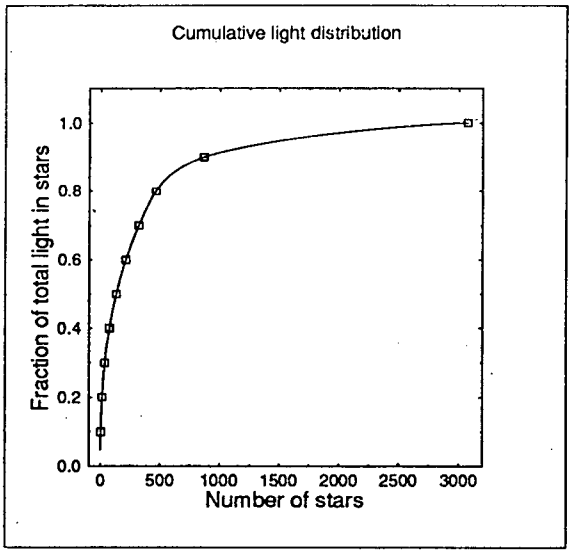

Figure 5.2: Total light as a function of number of contributing stars

fashion identical to the original run. Fig. 5.3 shows the distance of the centre determined in this fashion from the centre determined on the original image. Here the method shows its stability, even when all the stars are subtracted the centre determined by this method only changes by a maximum of ~3 pixels. Table 5.3 lists the locations of the determined centres which are plotted in Fig. 5.4. The size of the symbols is related to the fraction of stellar light removed before analysis, i.e. the largest symbol corresponds to all stellar light removed and the smallest symbol to the original image.

5.4 Adopted centre

Based on the results of the two tests conducted in the previous section, we can not claim that NGC 5694 has a gravity centre different from its luminosity centre. The centre determined by the NP method is quite uncertain. The detected separation of the two

Fraction of light removed	X	Y
0.0	740.168	470.598
0.1	739.895	470.328
0.2	739.521	470.488
0.3	739.769	470.647
0.4	739.511	470.547
0.5	740.011	473.098
0.6	742.093	473.059
0.7	742.081	473.064
0.8	740.132	471.132
0.9	741.974	472.968
1.0	741.997	472.996

Table 5.3: Centres determined for partially subtracted images

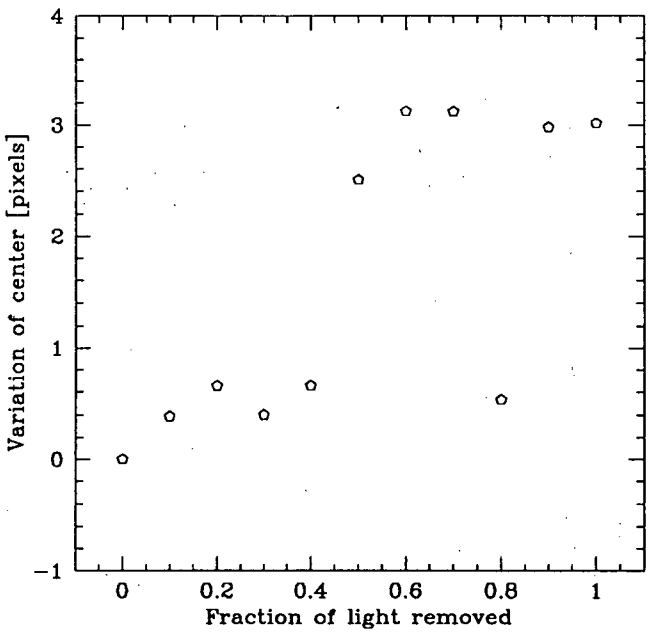

Figure 5.3: Error as a function of removed fraction of light

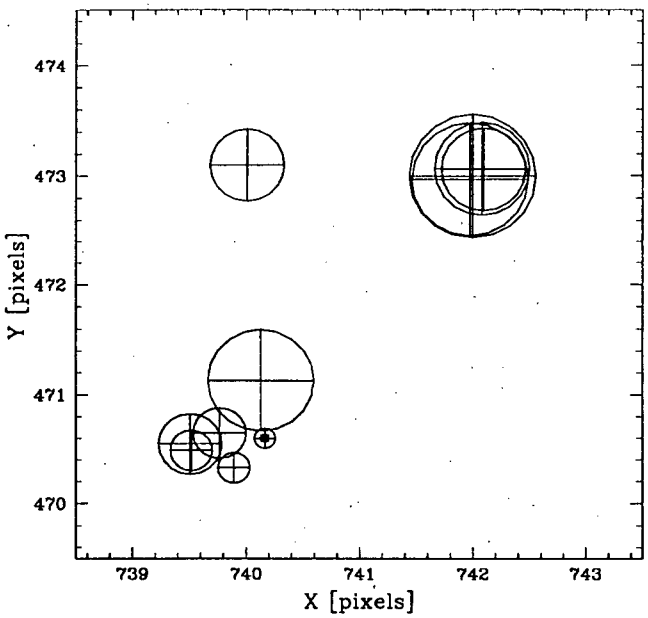

Figure 5.4: Detected centres

centres of $\Delta_r = 18.1$ pixels (Table 5.1) is less than one standard deviation of the results of the NP method, which we calculate as $\sigma_{r(NP)} = 21.0$ pixels[8].

We find the output of the SCC method to be very robust; subtraction of all resolved stars does not perturb the result by more than 3.2 pixels. Based on these results and Table 5.1 we accept a value of (741.0, 471.0) ($\pm 3., 3.$) as the luminosity centre in U for subsequent analysis.

[8] $\sigma_r^2 = \sigma_X^2 + \sigma_Y^2$

Chapter 6

Structure of NGC 5694

6.1 Radial profiles

The surface brightness profiles of most Galactic globular clusters are well represented by Michie-King (MK) models (Michie 1963 [25], King 1966 [18]). All of the previous studies of NGC 5694 that fit MK models to the surface brightness profile show a highly concentrated cluster morphology. Webbink 1985 ([39]) lists a concentration parameter of $c \equiv \mathrm{Log}(r_t/r_c) = 2.40$, while a more recent study by Trager, Djorgovski & King 1993 [13] finds a core radius of $r_c = 3''.72$ and a concentration of $c = 1.84$. Here r_t and r_c are two scale parameters used in a MK model fit, tidal- and core radius respectively.

Aperture photometry of a light distribution can be carried out with the IRAF task PHOT. The standard procedure to determine errors in a radial profile is to perform aperture photometry on an image divided into eight sectors. The error of the surface brightness in a radial annulus is then obtained from the standard deviation of the values in the eight sectors (See [12]). PHOT does not provide an option to divide the image into sectors, and consequently we would not have been able to derive realistic errors in the profile. We therefore wrote our own code, which determines the surface brightness using aperture radii equi-distant in logarithmic coordinates. The program divides the image into eight sectors, and determines uncertanties in the profile in the standard manner mentioned above. The program uses the dimensions of the CCD frame to calculate what part of the area of apertures partially extending off the frame is to be used in the

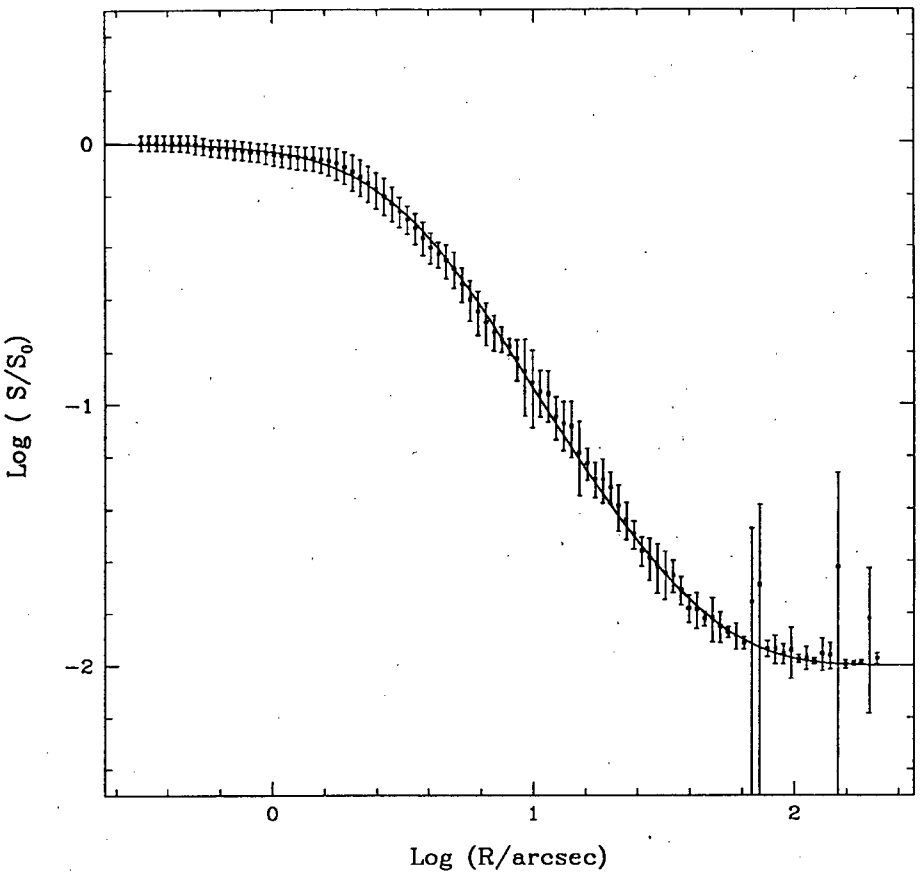

Figure 6.1: Surface brightness profile in U

calculation of the surface brightness, making it possible for apertures to cover all of the image out to the corner furthest from the centre.

As centre for the apertures we used the luminosity centre as determined in Sect. 5.4. A surface brightness profile derived from U frame # 429 is shown in Fig.6.1. Superimposed onto the data is a MK model (solid line) with parameters as determined in the next paragraph. While the model does not follow the data exactly, it is well within the errorbars.

Instead of determining and subtracting a background[1] a priori, we included the background as a parameter in the MK model fitting procedure. We used CERN's MINUIT fitting package to fit one dimensional, single mass MK models to the surface brightness profile. We carried out a bootstrap analysis (See *Numerical Recipes in Fortran 2nd ed.* [27], p.686f) to estimate uncertainties in the fit. By analyzing 100 randomised variants of the surface brightness data we determined the following parameters: $r_c = 15.28 \pm 0.16$ pixels or $3''.51 \pm 0''.04$ and $c = 1.85 \pm 0.02$. The tidal radius of the cluster was found as $r_t = 1086 \pm 40$ pixels or $249''.8 \pm 9''.2$, beyond our field of view. The quoted errors are standard deviations of the values obtained in the 100 bootstraps and should be interpreted as internal uncertainties of the fit, not as definite limits on the model parameters.

To gain independence from the effects of bright cluster stars we calculated surface brightness profiles for the partially subtracted images used in Section 5.3. Unclean subtraction of the stars in the centre compromised the quality of these profiles. The profiles were visibly un-King-like and could not be well fitted by MK models.

6.2 Is a collapsed core detectable ?

NGC 5694 is one of the most concentrated globular clusters next to the well known core collapsed clusters M15 and M30 according to the compilation of Webbink [39]. The question arises whether we would be able to detect indications of a collapsed core at the distance of NGC 5694.

De Marchi & Paresce 1994 [8] have shown the core of the classical core collapsed globular cluster M15 to be of size 0.13 pc ($2''.2$). This dimension at the distance of NGC 5694 [2] would yield an angular size of $0''.95$. This is certainly beyond the ability of the present data to detect. In radial profiles of M15 by Djorgovski & Penner 1985 [11] the

[1] In this case contributions from sky and field stars.

[2] Here we use a distance of 30.5 Kpc, derived in Sect. 4.6

characteristic powerlaw of slope -1 extends to ~ 0.6 pc. At the distance of NGC 5694 this would correspond to $\sim 4''.0$ (17 pixels). Although this seems large enough a scale to be recognised in the radial profile in Fig. 6.1, seeing can redistribute the light from the centre to larger radii, camouflaging the signature of a collapsed core. King 1985 [19] and Lugger *et al.* 1985 [23] show that in collapsed core clusters the powerlaw only extends inward to the seeing radius (HWHM of the PSF). Within this radius the profile flattens out.

Corresponding to a FWHM of $0''.88$, we would place the seeing radius in Fig. 6.1 at Log(R) $= -0.36$. If NGC 5694 had a collapsed core, we would expect to find the signature of a powerlaw at Log(R) ≥ -0.3. Based on this argument and the good fit by a MK model, we conclude that there is no evidence suggesting the presence of a collapsed core in NGC 5694.

Chapter 7

Conclusions

CCD photometry of NGC 5694 including the cluster centre is presented and values for reddening, metallicity and distance modulus are derived. Most values are in agreement with results of previous studies.

In an investigation of the stellar population close to the cluster core, we detect stars populating the red HB, possibly the progeny of BSSs. Also detected is a bright blue population of stars near the cluster core, including three very bright knots near the cluster centre. Photometric errors close to the centre and the limited resolution of the data do not permit us to draw firm conclusions about these populations. HST data will indubitably provide better resolution and allow us to (1) reduce photmetric errors for stars near the centre of the cluster and (2) resolve the peculiar knots at the centre into their components.

An improved method for determining the centres of globular clusters is presented and used to find the centre of NGC 5694 to a high degree of accuracy. A Michie-King model fit to a surface brightness profile yields structural parameters consistent with previous studies of this cluster. No indication of a collapsed core is found; NGC 5694 is well fit by a conventional Michie-King model.

References

[1] Auriere, M., Ortolani, S. & Lauzeral, C. 1990, *Nature*, **638**

[2] Lauzeral, C., Ortolani, S., Auriere, M. & Melnick, J. 1992, *A&A*, **262**, 63

[3] Bahcall, J.N. & Soneira, R.M. 1984, *ApJ Suppl.*, **55**, 67

[4] Buonanno, R., Corsi, C.E. & Pecci, F.F. 1989, *A&A*, **216**, 80

[5] Burstein,D. & Heiles,C. 1982, *AJ*, **87**, 1165

[6] Buser, R. & Kurucz, R.L. 1992, *A&A*, **264**, 557

[7] Calzetti, D., De Marchi, G., Paresce, F., & Shara, M. 1993, *ApJ Letters*, **402**, L1

[8] De Marchi, G. & Paresce, F. 1994, *ApJ*, **422**, 597

[9] Djorgovski, S., Piotto, G., Phinney, E.S. & Chernoff, D.F. 1991, *ApJ Letters*, **372**, L41

[10] Djorgovski, S. & Piotto G. 1993, in:*Structure and dynamics of Globular Clusters, ASPCS 50*, eds: S.Djorgovski & G. Meylan, (ASP:San Francisco),p. 203

[11] Djorgovski, S. & Penner, H. 1985, in: *Dynamics of Star Clusters, IAU Symposium No. 113*, eds: J. Goodman & P. Hut (D. Reidel Publishing : Dordrecht/Boston/Lancaster), p.73

[12] Djorgovski, S. 1988, in: *The Harlow Shapley Symposium on Globular Cluster Systems in Galaxies, IAU Symposium No. 126*, eds: J.E. Grindlay & A.G.D. Philip (Kluwer Academic : Dordrecht/Boston/London), p.333

[13] Djorgovski, S. 1993, in: *Structure and dynamics of Globular Clusters ASPCS 50*, eds: S.Djorgovski & G. Meylan, (ASP:San Francisco), p.373

[14] Fusi Pecci, F., Ferraro, F.R., Corsi, C.E., Cacciari, C., & Buonanno, R. 1992 *AJ*, **104**, 1831

[15] Harris, W.E. 1975, *ApJ Suppl.*, **29**, 397

[16] Harris, W.E. & Hesser, J.E. 1976, *PASP*, **88**, 377

[17] Hut, P., McMillan, S., Mateo, M. Phinney, E.S., Pryor, C., Richer, H.B., Verbunt, F. & Weinberg, M. 1988, *PASP*, **104**, 981

[18] King, I.R. 1966, *AJ*, **71**, 64

[19] King, I.R. 1985, in:*Dynamics of Star Clusters, IAU Symposium No. 113*, eds: J. Goodman & P. Hut (Reidel Publishing: Dordrecht/Boston/Lancaster), p.1

[20] König, C.H.B. 1995, *A&A* , in preparation

[21] Kron, G.E. & Guetter, H.H. 1976, *AJ*, **81**, 817

[22] Landolt, A.U. 1992, *AJ*, **104**, 340

[23] Lugger, P.M., Cohn, H. & Grindlay, J.E. 1985, in:*Dynamics of Star Clusters, IAU Symposium No. 113*, eds: J. Goodman & P. Hut (Reidel Publishing: Dordrecht/Boston/Lancaster), p.89

[24] Mihalas, D. & Binney, J. 1981, in: *Galactic Astronomy, Structure and Kinematics*, (W.H. Freedman and Company: New York), p.108

[25] Michie, R.W. 1963, *MNRAS*, **125**, 127

[26] Merrit, D. & Tremblay, B. 1994, *AJ*, **108**, 514

[27] Press, W.H., Teukolsky, S.A., Vetterling, W.T. & Flannery, B.P. 1992, in: *Numerical Recipes in Fortran*, (Cambridge University Press: Cambridge/ New York)

[28] Ortolani, S. & Gratton, R. 1990, *A&A Suppl.*, **82**, 71

[29] Picard, A. & Johnston, H. 1994, *A&A*, **263**, 76

[30] Ratnatunga, K.U. & Bahcall, J.N. 1985, *ApJ Suppl.*, **59**, 63

[31] Reed, B.C., Hesser, J.E. & Shawl, S.J. 1988, *PASP*, **100**, 545

[32] Renzini, A. & Fusi Pecci, F. 1988, *ARAA*, **26**, 199

[33] Richer, H.B. & Fahlman, G.G. 1984, *ApJ*, **277**, 227

[34] Stetson, P.B. 1987, *PASP*, **99**, 191

[35] Seidl, E., Demarque, P. & Weinberg, D. 1987, *ApJ Suppl.*, **63**, 917

[36] Stetson, P.B. 1990, *PASP*, **102**, 932

[37] Stetson, P.B. & Harris, W.E. 1988, *AJ*, **96**, 909

[38] Trager, S.C., Djorgovski, S. & King, I.R. 1993, in: *Structure and dynamics of Globular Clusters, ASPCS 50*, eds: S.Djorgovski & G. Meylan, (ASP:San Francisco), p.347

[39] Webbink, R.F. 1985, in: *Dynamics of Star Clusters, IAU Symposium No. 113*, eds: J. Goodman & P.Hut (Reidel Publishing : Dordrecht/Boston/Lancaster), p.541

[40] Zinn, R. 1980, *ApJ Suppl.*, **42**, 19

[41] Zinn, R. & West, M.J., 1984, *ApJ. Suppl.*, **55**, 45

Appendix A

Centre finding algorithms

We list four algorithms used in the estimation of the centre. The first is a *quick and dirty* method that directly yields a result. The other three share the fact that an extra procedure is required to interpret their output.

A.1 Projection onto axes

This method is of a rather simplistic nature and is only expected to work well for a smooth brightness distribution. The pixel values along columns and rows of an image are added and projected onto the x and y axes respectively. A spline is then fit to the maxima of these curves. The maximum values of the fits are then taken as the centre coordinates in x and y. Typical output of this method is shown in Fig. A.1. The result is for an image of NGC 5694 in the U filter.

A.2 Mirror Autocorrelation Function method (MACF)

This method is described by Djorgovski 1988 [12] and Picard & Johnston 1994 [29]. A grid of trial centres is placed on the original image and for each trial center at frame coordinate (i,j) the MACF

$$F(i,j) = \sum_{k=i-W}^{k=i+W} \sum_{l=j-W}^{l=j+W} f(i+k, j+l)\, f(i-k, j-l)$$

is calculated. Here $f(i,j)$ is the image value of pixel (i,j), W is the width of the window determining the area used in the calculation for each test centre. The centre can then be

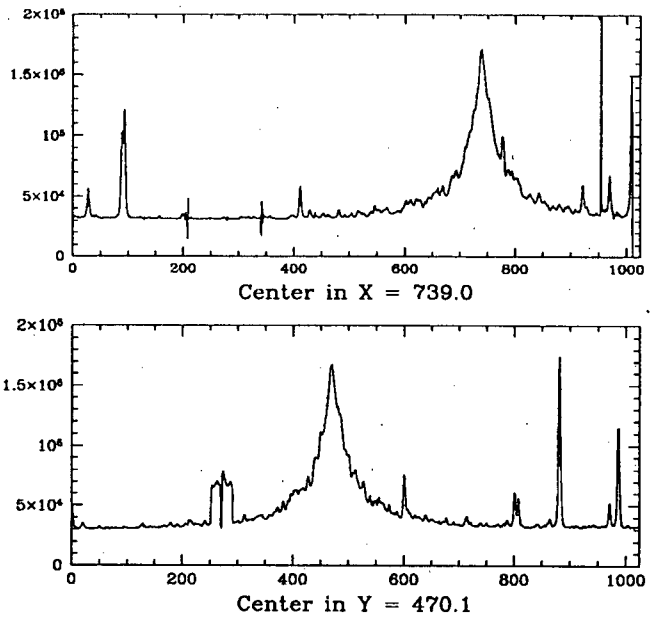

Figure A.1: Output of the projection method.

taken as the maximum of the resultant amplitude map with points at the test centers or an additional procedure can be used to fit the amplitude map.

A.3 Self Cross-Correlation (SCC)

The SCC method is similar in idea to the MACF method mentioned earlier. Again a grid of test centers is placed on the original image. At each test centre a *window* is placed on the original data and the data in this window is taken as a subimage S. This subimage S is then mirrored according to the rule

$$S'(i,j) = S(W-j+1, W-i+1),$$

where W is the width of the window and the dimension of the subimages. The two dimensional cross correlation[1] between S and S' is then calculated and the value at (0,0)

[1]For a detailed description of one- and two-dimensional cross correlations see *Numerical Recipes 2nd ed.*[27] pages 519f & 538

lag[2] is taken as the result for the coordinate at the centre of the window, which, of course, corresponds to the test centre in the original image. Again, the centre can be taken as the maximum of the amplitude map created by the method at the test centres or an additional procedure can be employed to fit the map.

A.4 Adaptive kernel smoothing technique (NP)

Also employed was a nonparametric approach developed by Merrit & Tremblay 1994 [26]. We used their adaptive kernel smoothing technique to create an amplitude map of the stellar density as a function of position. Adaptive kernel smoothing places *bumps* of a user chosen shape and width at the observed positions of stars, then calculates the combined contributions from all *bumps*. Our *bump* of choice was a Gaussian. The *bump*-width, in our case the standard deviation of the Gaussian, determines the degree of smoothness of the resultant map. We tested several degrees of smoothing until we achieved a satisfactory result. The output of this method was subjected to our fitting procedure[3] to extract a centre. This is the only method we used that does not use the brightness distribution as its working data, but solves for the centre of the cluster using stellar positions.

A.5 Fitting

Traditionally the amplitude map obtained from the MACF method was subjected to a second processing step; a paraboloid was fit to the area of the highest data values (see Picard & Johnston 1994 [29] and Djorgovski 1988 [12]). We felt that this parametric approach was unsatisfactory since it leaves to judgement which region of the amplitude

[2]The ouput for each testcenter includes values for lags (shifts) from $-W/2$ to $+W/2$ in both X and Y. We are not interested in shifts, thus we take the (0,0) lag value as a measure of similarity between S and S'. Since S' is mirrored this yields a measure of symmetry.

[3]See Sect. A.5.

map to fit the paraboloid to. While the amplitude map is well described by a paraboloid in **some** central region, a paraboloid is **completely** inappropriate as a function for the map at a distance from the cluster centre. Instead of continuing towards negative infinity, the paraboloid develops wings and flattens out. Fitting a paraboloid to only a small area of the amplitude map, in an attempt to avoid areas deviant from a paraboloid, wastes most of the information in the amplitude map. Fitting the paraboloid to the whole amplitude map introduces systematic errors of unknown magnitude since the deviant region will *pull* the paraboloid from its true position, unless the peak of the paraboloid is exactly in the centre of the amplitude map.

We used an altogether different, nonparametric approach, which uses all the information in the amplitude map. A preliminary centre K is assumed, for each of the N data points in the amplitude map we then calculate its distance from that preliminary centre. These distances are sorted in ascending order and a statistic S is calculated by summing the differences between amplitudes A between neighbouring[4] points , i.e.

$$S_k = \sum_{i=2}^{N} |A_{k,i} - A_{k,i-1}|.$$

A plot of A_i vs. i is very similar in appearance to a one-dimensional representation of a stellar PSF[5] if the centre K coincides with the peak of the amplitude map. Points *line up* and differences in amplitude values between neighbouring points are minimised. If K is far from the peak, the A_i vs. i plot deterioriates into a scatter plot, since points adjacent in i can have very different amplitude values. Reducing the differences in amplitude between adjacent points, i.e. minimising S_k by varying K, will force K to coincide with the peak of the amplitude map.

While this method is similar to the string length method used to determine stellar

[4]Neighbouring in the sorted list of radii.

[5]Readers unfamiliar with this shape may use the IRAF task IMEXAMINE, place the cursor on a star, and hit the 'r' key.

pulsation periods, it is not identical. The string length method also takes into account the separation between data points along the horizonal axis ,which we do not, since this would introduce systematic errors, due to the centre being *pulled* towards the centre of the grid.

CERN's non linear least square fitting routine MINUIT is used for the minimisation. A first scan of the data by Minuit identifies the approximate location of the minimum. Minuit then varies K in the direction of lower S_k values until the minimum is found.

A.6 Testing MACF, SCC and fitting

Estimating the accuracy of centre finding algorithms is difficult. Only tests on artificial images, in which the true location of the centre is known, can reveal the true external errors of the method.

We obtained images of artificial globular clusters created by Picard & Johnston [29] (PJ hereafter). These frames served two important purposes. First, we were able to test the accuracy of our methods, given the known centres. Secondly, it allowed us to compare the accuracy of our methods **directly** to the accuracy of other methods, since the identical frames were used by PJ to test the accuracy of these other methods.

We ran extensive tests using MACF and SCC methods and our modified fitting procedure. For an extensive description of the test results see König 1995 [20]. The main points are : The results of the SCC and MACF methods are similar, fitting of the SCC method is less susceptible to local minima. PJ list an average error of 11.59 and 14.71 pixels for the MACF method depending on the parameters used in the paraboloid fitting. Our modified fitting procedure used in conjunction with MACF yields average errors of 6-8 pixels depending on the window size. When the fitting is used with the SCC method we obtain average errors of 6-7 pixels. A very important point is that both the MACF

and SCC methods used in conjunction with our fitting procedure yield more consistent output, being less dependent on the chosen window size. This consistency places the modified MACF and SCC methods second in the ranking of accuracy given by PJ, next to their own Maximal Axial Symmetry (MAS) method[6]. We decided not to use the MAS method due to its large number (5) of adjustable parameters. While fine-tuning the adjustable parameters on artificial images will yield small average errors on real data with comparable properties, we are not confident that this would be the case for our data of NGC 5694.

To relate the average errors obtained in the testing to the expected error in the value of our centre is non trivial. The artificial clusters have a core radius of $r_c = 20''.0$ and a pixel scale of $0''.2$ per pixel. The dimension of the core diameter in these clusters is thus 100 pixels, and an average error of 7 pixels corresponds to $1''.4$. Since NGC 5694 in our images is much more concentrated than the artificial clusters[7], the average error of our centre finding method will be much smaller than 7 pixels. A direct scaling would yield an average error for NGC 5694 of ~ 2 pixels (7 pixels $\times 30/100$), which is in good agreement with the observed scatter in centres for images of NGC 5694 in different colours. Direct scaling is of course only applicable if the observations have enough resolution, i.e. if scaling of this nature leads to an average error of 0.01 pixels the logic of the argument would have to be reconsidered.

[6]For a detailed description of the MAS method see PJ [29]
[7]The core diameter is on the order of 30 pixels

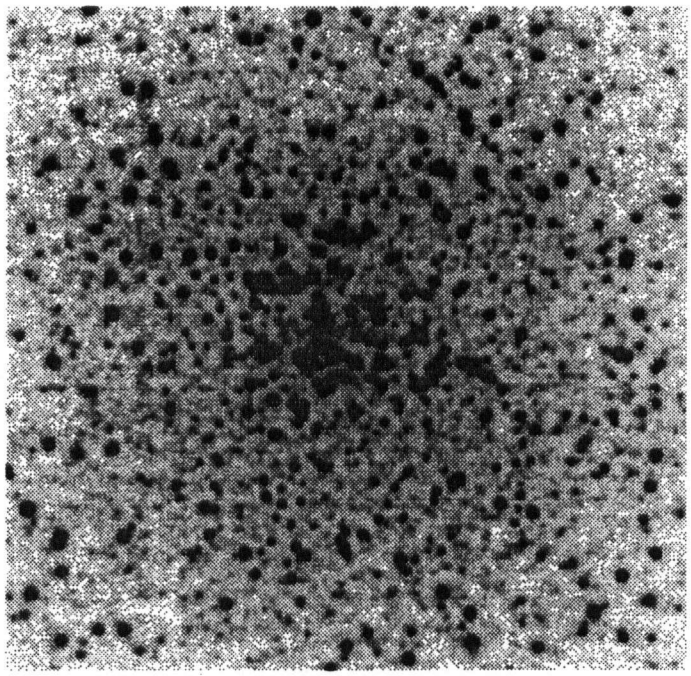

Figure A.2: Image of a simulated globular cluster

Appendix B

Photometry

In the following tables we show the photometry of 1435 stars. For each star the tables list the X and Y positions in frame number 429 (see Tab. 2.1) and the magnitude and formal uncertainty in each of U, B & V. The formal uncertainty was obtained by convolving the uncertainty-of-fit value returned by ALLSTAR with uncertainties determined for the transformation equations, the aperture corrections and offsets used in the calibration procedure. Convolution of errors was carried out by the method of partial derivatives, i.e. for a quantity

$$Z = f(I, J, K)$$

the error α is determined as

$$(\alpha Z)^2 = (\frac{\partial Z}{\partial I})^2 \times (\alpha I)^2 + (\frac{\partial Z}{\partial J})^2 \times (\alpha J)^2 + (\frac{\partial Z}{\partial K})^2 \times (\alpha K)^2.$$

The listed uncertainties are thus a combination of random scatter and possible systematic errors.

X	Y	U	σU	B	σB	V	σV
743.0	470.0	15.18	0.10	16.40	0.08	16.69	0.10
738.6	474.9	16.59	0.10	16.07	0.09	14.82	0.08
732.2	465.3	16.80	0.11	16.53	0.08	14.85	0.09
411.3	600.4	16.04	0.08	15.58	0.08	14.77	0.07
969.8	800.5	15.94	0.08	15.68	0.08	14.96	0.08
28.1	807.3	16.12	0.08	16.04	0.08	15.38	0.08
921.7	970.7	16.25	0.08	16.12	0.08	15.40	0.08
725.8	512.8	17.89	0.09	16.81	0.08	15.42	0.08
708.2	450.3	16.73	0.08	16.73	0.08	15.98	0.08
779.0	467.5	17.33	0.08	16.77	0.08	15.65	0.08
746.6	475.1	16.89	0.10	16.83	0.10	15.82	0.09
750.0	457.9	17.08	0.09	16.76	0.09	15.73	0.08
777.2	272.6	17.08	0.08	16.70	0.08	15.77	0.08
731.2	473.9	16.97	0.10	16.94	0.09	15.69	0.09
750.3	469.5	16.82	0.10	16.90	0.11	16.03	0.09
761.5	459.0	17.47	0.09	16.95	0.08	15.73	0.08
752.8	396.0	17.29	0.08	16.79	0.08	15.76	0.08
787.8	454.6	18.06	0.08	16.93	0.08	15.43	0.08
745.8	481.4	17.06	0.10	16.97	0.09	16.12	0.09
738.2	486.1	17.06	0.10	17.00	0.09	16.21	0.08
767.0	511.0	17.93	0.08	17.12	0.08	15.90	0.08
601.3	527.3	17.58	0.08	16.86	0.08	15.71	0.08
755.1	475.0	17.15	0.10	17.17	0.09	16.27	0.09
669.0	498.3	17.73	0.09	17.25	0.08	16.22	0.08
755.4	448.6	17.49	0.09	17.19	0.08	16.20	0.08
717.4	391.6	18.04	0.08	17.17	0.08	15.92	0.08
641.5	407.0	18.28	0.08	16.95	0.08	15.48	0.08
736.7	607.0	18.12	0.08	17.03	0.08	15.71	0.08
709.0	426.0	18.03	0.08	17.19	0.08	15.97	0.08
799.6	507.7	18.08	0.08	17.06	0.08	15.73	0.08
729.2	428.2	18.00	0.08	17.17	0.08	15.92	0.08
803.9	424.5	18.15	0.08	17.03	0.08	15.69	0.08
760.8	469.3	17.41	0.09	17.35	0.09	16.30	0.09
629.0	511.8	18.17	0.08	17.05	0.08	15.70	0.08
962.0	241.6	18.23	0.08	16.98	0.08	15.54	0.08

Table B.1: Photometry of NGC 5694

X	Y	U	σU	B	σB	V	σV
725.7	481.2	17.54	0.09	17.38	0.08	16.35	0.09
739.4	448.5	17.33	0.10	17.43	0.09	16.58	0.09
607.2	439.9	18.00	0.08	17.33	0.08	16.20	0.08
827.5	213.4	18.13	0.08	17.16	0.08	15.89	0.08
703.0	339.0	18.17	0.08	17.20	0.08	15.91	0.08
839.9	676.8	18.19	0.08	17.30	0.08	16.06	0.08
776.3	453.1	17.80	0.08	17.51	0.08	16.55	0.08
723.4	462.2	17.56	0.09	17.58	0.09	16.64	0.09
720.1	444.6	18.06	0.08	17.52	0.08	16.44	0.08
683.6	470.0	18.13	0.08	17.45	0.08	16.29	0.08
729.8	486.7	17.39	0.09	17.69	0.09	17.01	0.09
695.3	440.4	17.99	0.08	17.56	0.08	16.52	0.08
546.2	714.5	17.47	0.08	17.59	0.08	17.03	0.08
653.2	490.2	18.17	0.08	17.46	0.08	16.32	0.08
610.2	398.2	18.20	0.08	17.50	0.08	16.36	0.08
776.1	263.2	18.21	0.08	17.49	0.08	16.33	0.08
428.5	20.7	17.79	0.08	17.54	0.08	16.78	0.08
721.7	483.8	17.48	0.09	17.67	0.09	17.10	0.08
858.7	600.4	18.23	0.08	17.47	0.08	16.30	0.08
717.5	437.0	17.89	0.09	17.69	0.08	16.85	0.08
867.2	382.1	18.17	0.08	17.59	0.08	16.49	0.08
927.3	311.9	18.24	0.08	17.54	0.08	16.38	0.08
198.5	404.5	18.11	0.08	17.61	0.08	16.60	0.08
895.5	286.0	18.30	0.08	17.56	0.08	16.41	0.08
956.0	864.4	17.61	0.08	17.75	0.08	17.14	0.08
854.3	516.7	18.29	0.08	17.66	0.08	16.56	0.08
785.3	463.0	17.90	0.08	17.74	0.08	16.79	0.08
842.9	481.2	18.28	0.08	17.74	0.08	16.66	0.08
778.1	382.3	18.27	0.08	17.78	0.08	16.73	0.08
684.4	401.7	18.21	0.08	17.81	0.08	16.82	0.08
718.4	420.8	18.18	0.09	17.89	0.08	16.93	0.08
723.6	414.0	18.23	0.08	17.81	0.08	16.78	0.08
881.1	485.7	18.29	0.08	17.88	0.08	16.90	0.08
814.2	519.0	18.41	0.08	17.89	0.08	16.86	0.08
722.9	428.1	18.25	0.08	18.07	0.08	17.15	0.08

Table B.1: Photometry of NGC 5694

X	Y	U	σU	B	σB	V	σV
780.1	560.4	18.30	0.08	18.00	0.08	17.07	0.08
655.3	405.3	18.44	0.08	17.94	0.08	16.93	0.08
779.5	513.8	18.14	0.08	18.08	0.08	17.30	0.08
626.1	529.5	18.44	0.08	18.01	0.08	17.03	0.08
770.4	555.0	18.44	0.08	18.01	0.08	17.01	0.08
687.0	437.8	18.31	0.08	18.11	0.08	17.20	0.08
845.7	787.9	18.35	0.08	18.05	0.08	17.11	0.08
736.5	501.6	18.18	0.10	18.18	0.09	17.33	0.08
745.0	444.2	18.13	0.10	18.20	0.09	17.36	0.09
713.2	418.1	18.43	0.08	18.15	0.08	17.16	0.08
929.6	573.6	18.39	0.08	18.09	0.08	17.18	0.08
756.6	369.4	18.27	0.08	18.15	0.08	17.31	0.08
729.7	443.8	17.97	0.09	18.28	0.09	17.58	0.09
725.2	604.6	18.50	0.08	18.08	0.08	17.11	0.08
714.7	431.5	18.33	0.09	18.23	0.09	17.27	0.08
721.9	453.0	18.29	0.09	18.20	0.08	17.33	0.08
712.9	485.6	18.29	0.09	18.26	0.08	17.24	0.08
793.3	478.6	18.02	0.09	18.04	0.08	17.71	0.08
787.6	471.2	18.06	0.09	18.16	0.09	17.60	0.08
741.8	437.1	18.25	0.09	18.22	0.08	17.47	0.08
734.1	627.5	18.54	0.08	18.18	0.08	17.23	0.08
722.1	525.6	18.56	0.08	18.16	0.08	17.19	0.08
710.8	457.8	18.07	0.09	18.33	0.09	17.88	0.10
650.3	442.9	18.42	0.08	18.19	0.08	17.33	0.08
710.1	554.3	18.41	0.08	18.17	0.08	17.32	0.08
770.7	502.6	18.35	0.08	18.22	0.08	17.37	0.08
714.3	277.5	18.47	0.08	18.20	0.08	17.31	0.08
751.1	601.1	18.57	0.08	18.23	0.08	17.27	0.08
568.2	676.3	18.57	0.08	18.24	0.08	17.29	0.08
851.6	401.5	18.63	0.08	18.19	0.08	17.18	0.08
704.4	527.2	18.56	0.08	18.29	0.08	17.36	0.08
743.8	528.0	18.44	0.08	18.32	0.08	17.49	0.08
765.5	472.4	18.31	0.09	18.44	0.09	17.46	0.09
693.5	411.8	18.44	0.08	18.34	0.08	17.55	0.08
714.5	538.0	18.64	0.08	18.32	0.08	17.37	0.08

Table B.1: Photometry of NGC 5694

X	Y	U	σU	B	σB	V	σV
762.2	449.5	18.28	0.09	18.37	0.08	17.88	0.09
687.7	372.4	18.52	0.08	18.38	0.08	17.54	0.08
804.4	273.8	18.36	0.08	18.37	0.08	17.75	0.08
724.6	495.7	18.24	0.09	18.52	0.08	17.90	0.09
619.1	721.6	18.68	0.08	18.35	0.08	17.42	0.08
735.8	441.8	18.53	0.09	18.38	0.09	17.62	0.08
656.7	580.8	18.67	0.08	18.34	0.08	17.42	0.08
877.5	610.3	18.71	0.08	18.35	0.08	17.40	0.08
673.0	411.4	18.67	0.08	18.39	0.08	17.47	0.08
750.8	500.6	18.47	0.10	18.57	0.09	17.60	0.09
716.3	450.5	18.49	0.09	18.44	0.08	17.73	0.08
693.8	480.9	18.66	0.09	18.44	0.08	17.54	0.08
776.7	357.0	18.70	0.08	18.38	0.08	17.44	0.08
756.0	554.3	18.55	0.08	18.44	0.08	17.66	0.08
768.8	450.5	18.30	0.08	18.51	0.08	18.17	0.08
883.6	619.9	18.71	0.08	18.42	0.08	17.47	0.08
699.6	495.5	18.46	0.08	18.43	0.08	17.86	0.08
514.6	384.7	18.77	0.08	18.46	0.08	17.53	0.08
788.2	344.2	19.40	0.08	18.35	0.08	17.01	0.08
741.5	504.8	18.61	0.09	18.51	0.09	17.58	0.08
908.6	639.9	18.77	0.08	18.47	0.08	17.52	0.08
618.5	472.9	18.81	0.08	18.47	0.08	17.57	0.08
706.2	475.7	18.38	0.09	18.54	0.08	18.07	0.09
305.1	179.9	18.79	0.08	18.49	0.08	17.57	0.08
967.2	860.6	18.48	0.08	18.57	0.08	17.87	0.08
699.2	416.0	18.60	0.08	18.52	0.08	17.74	0.08
763.2	495.2	18.63	0.10	18.69	0.10	17.67	0.09
794.1	402.3	18.66	0.08	18.57	0.08	17.77	0.08
677.4	495.7	18.80	0.08	18.49	0.08	17.60	0.08
768.8	459.2	18.54	0.09	18.68	0.08	17.75	0.08
650.8	502.3	18.52	0.09	18.49	0.09	17.90	0.08
800.3	440.0	18.36	0.09	18.47	0.09	18.12	0.08
765.7	454.9	18.64	0.10	18.67	0.08	17.78	0.08
711.8	463.1	18.69	0.10	18.56	0.09	17.75	0.09
760.1	499.9	18.52	0.09	18.58	0.08	18.15	0.08

Table B.1: Photometry of NGC 5694

X	Y	U	σU	B	σB	V	σV
771.2	398.6	18.64	0.08	18.61	0.08	17.85	0.08
770.8	485.8	18.50	0.09	18.65	0.08	18.09	0.08
669.8	599.9	18.68	0.08	18.59	0.08	17.85	0.08
825.6	472.4	18.70	0.08	18.60	0.08	17.83	0.08
716.3	474.2	18.21	0.10	18.81	0.09	18.08	0.09
797.8	453.3	18.75	0.09	18.67	0.08	17.75	0.08
596.8	539.5	18.82	0.08	18.59	0.08	17.68	0.08
693.0	473.9	18.52	0.09	18.68	0.08	18.04	0.08
703.3	480.1	18.71	0.09	18.62	0.08	17.72	0.08
695.9	469.2	18.39	0.09	18.60	0.08	18.26	0.08
723.9	502.0	18.55	0.09	18.69	0.08	18.09	0.08
795.2	275.1	18.79	0.08	18.65	0.08	17.80	0.08
800.5	464.5	18.49	0.09	18.69	0.08	18.07	0.08
899.1	659.6	18.89	0.08	18.62	0.08	17.69	0.08
704.4	493.4	18.60	0.08	18.65	0.08	18.21	0.08
690.7	488.1	18.56	0.09	18.54	0.09	18.39	0.08
658.2	396.0	18.52	0.09	18.62	0.09	18.18	0.08
452.9	648.7	18.89	0.08	18.66	0.08	17.77	0.08
739.8	404.6	18.60	0.10	18.73	0.09	18.01	0.08
686.0	739.1	18.75	0.08	18.68	0.08	17.95	0.08
801.3	492.8	18.76	0.08	18.72	0.08	17.82	0.08
736.8	507.9	18.65	0.09	18.69	0.08	18.32	0.09
690.9	524.2	18.89	0.09	18.75	0.08	17.89	0.08
786.1	427.3	18.84	0.08	18.73	0.08	17.86	0.08
717.8	365.3	18.91	0.08	18.71	0.08	17.84	0.08
745.9	842.8	18.81	0.08	18.75	0.08	17.95	0.08
805.5	436.6	18.74	0.08	18.64	0.09	18.43	0.09
613.2	496.5	18.72	0.08	18.60	0.08	18.33	0.08
25.5	941.2	18.57	0.08	18.81	0.08	18.35	0.08
825.5	911.5	18.83	0.08	18.76	0.08	18.05	0.08
693.0	514.4	18.73	0.08	18.66	0.08	18.34	0.08
714.8	517.5	18.83	0.09	18.82	0.08	18.00	0.08
764.5	443.8	18.70	0.08	18.76	0.08	18.49	0.08
733.6	410.8	19.03	0.08	18.78	0.08	17.68	0.08
708.9	501.7	18.92	0.08	18.79	0.08	17.83	0.08

Table B.1: Photometry of NGC 5694

X	Y	U	σU	B	σB	V	σV
751.5	433.3	18.71	0.08	18.67	0.08	18.42	0.08
807.2	548.0	18.96	0.08	18.81	0.08	17.92	0.08
702.4	431.8	18.97	0.09	18.84	0.08	17.86	0.08
656.8	421.2	18.96	0.08	18.80	0.08	17.96	0.08
738.9	638.3	18.77	0.08	18.72	0.08	18.46	0.08
624.5	495.5	18.75	0.08	18.73	0.08	18.46	0.08
755.3	640.2	19.04	0.08	18.84	0.08	17.97	0.08
790.4	539.6	18.78	0.08	18.72	0.08	18.52	0.08
817.0	191.9	19.06	0.08	18.81	0.08	17.92	0.08
918.6	312.5	18.81	0.08	18.74	0.08	18.50	0.08
713.4	491.1	18.84	0.09	19.00	0.09	18.12	0.09
741.0	550.1	18.73	0.08	18.83	0.08	18.58	0.08
894.2	555.4	18.77	0.08	18.71	0.08	18.53	0.08
664.4	509.8	19.04	0.08	18.90	0.08	18.02	0.08
754.9	408.8	18.82	0.09	18.85	0.10	18.27	0.08
794.8	486.6	18.74	0.09	18.92	0.08	18.56	0.09
691.1	534.3	18.85	0.08	18.85	0.08	18.69	0.08
561.2	448.1	18.75	0.08	18.79	0.08	18.74	0.08
699.0	567.8	18.93	0.08	18.93	0.08	18.20	0.08
776.9	400.1	18.85	0.08	18.80	0.08	18.59	0.08
820.6	624.5	18.84	0.08	18.80	0.08	18.57	0.08
668.6	643.6	18.77	0.08	18.79	0.08	18.68	0.08
794.8	471.5	18.85	0.08	18.91	0.08	18.83	0.08
831.0	429.3	19.13	0.08	18.93	0.08	18.08	0.08
778.7	787.3	19.14	0.08	18.92	0.08	18.08	0.08
771.1	492.8	18.87	0.09	19.00	0.08	18.56	0.09
907.7	523.0	19.13	0.08	18.94	0.08	18.07	0.08
545.2	300.7	19.11	0.08	18.93	0.08	18.08	0.08
636.7	563.0	18.87	0.08	18.80	0.08	18.65	0.08
699.3	543.5	19.07	0.08	18.97	0.08	18.15	0.08
736.6	418.0	19.11	0.08	18.98	0.08	18.11	0.08
317.7	517.5	19.12	0.08	18.96	0.08	18.12	0.08
762.3	546.8	18.89	0.08	18.85	0.08	18.69	0.08
758.8	417.4	18.90	0.08	18.85	0.08	18.64	0.08
772.5	544.2	19.16	0.08	18.98	0.08	18.11	0.08

Table B.1: Photometry of NGC 5694

X	Y	U	σU	B	σB	V	σV
921.6	547.6	18.86	0.08	18.80	0.08	18.62	0.08
710.8	671.2	19.16	0.08	18.98	0.08	18.13	0.08
920.5	471.0	18.91	0.08	18.84	0.08	18.62	0.08
682.4	377.9	19.14	0.08	18.96	0.08	18.15	0.08
568.7	239.1	19.17	0.08	18.99	0.08	18.12	0.08
789.5	631.4	18.91	0.08	18.85	0.08	18.70	0.08
744.6	405.9	19.19	0.08	19.05	0.08	18.08	0.08
809.4	499.4	18.95	0.08	18.94	0.08	18.88	0.08
781.7	416.2	18.91	0.08	18.87	0.08	18.75	0.08
703.2	251.7	19.18	0.08	19.04	0.08	18.17	0.08
653.1	637.1	18.84	0.08	18.86	0.08	18.79	0.08
680.1	488.8	18.94	0.08	19.08	0.08	18.91	0.08
823.1	490.9	18.86	0.08	18.99	0.08	18.86	0.08
398.4	439.2	19.18	0.08	19.05	0.08	18.22	0.08
460.8	585.3	19.18	0.08	19.05	0.08	18.21	0.08
945.9	578.5	18.97	0.08	19.00	0.08	18.77	0.08
758.9	405.6	19.23	0.08	19.02	0.08	18.19	0.08
871.1	442.8	19.00	0.08	19.06	0.08	18.44	0.08
777.8	601.4	18.92	0.08	18.90	0.08	18.75	0.08
770.7	610.6	19.22	0.08	19.04	0.08	18.17	0.08
729.7	341.8	19.06	0.08	19.07	0.08	18.37	0.08
792.2	500.7	19.15	0.08	19.09	0.08	18.03	0.08
637.1	517.8	19.18	0.08	18.98	0.08	18.17	0.08
515.9	502.9	19.20	0.08	19.10	0.08	18.25	0.08
519.1	470.7	18.95	0.08	18.91	0.08	18.78	0.08
647.7	461.9	19.00	0.08	19.05	0.08	18.49	0.08
748.5	438.9	18.97	0.10	19.11	0.10	18.40	0.09
843.3	335.0	18.97	0.08	18.90	0.08	18.81	0.08
970.8	314.8	19.23	0.08	19.09	0.08	18.21	0.08
970.5	572.2	18.94	0.08	18.92	0.08	18.80	0.08
930.0	325.7	18.99	0.08	18.93	0.08	18.79	0.08
526.3	608.0	18.95	0.08	18.97	0.08	18.90	0.08
734.5	390.2	19.03	0.08	19.08	0.08	18.98	0.08
327.4	486.8	18.94	0.08	18.95	0.08	18.84	0.08
588.3	751.0	18.87	0.08	18.93	0.08	18.85	0.08

Table B.1: Photometry of NGC 5694

X	Y	U	σU	B	σB	V	σV
394.5	128.3	18.95	0.08	18.91	0.08	18.79	0.08
40.8	935.0	19.64	0.08	19.01	0.08	18.13	0.08
554.4	507.8	18.95	0.08	18.92	0.08	18.83	0.08
705.6	564.5	18.96	0.08	18.95	0.08	18.88	0.08
725.9	402.4	19.03	0.08	19.13	0.08	18.81	0.08
598.2	217.1	19.25	0.08	19.11	0.08	18.26	0.08
338.9	854.8	19.14	0.08	19.10	0.08	18.43	0.08
735.3	547.5	19.27	0.08	19.12	0.08	18.26	0.08
801.6	225.0	19.26	0.08	19.11	0.08	18.24	0.08
551.5	395.1	19.28	0.08	19.14	0.08	18.29	0.08
837.7	362.1	19.26	0.08	19.10	0.08	18.24	0.08
538.1	383.3	19.27	0.08	19.10	0.08	18.27	0.08
774.8	373.6	19.02	0.08	19.07	0.08	19.05	0.08
807.9	447.5	19.12	0.09	19.20	0.08	18.36	0.08
681.3	416.0	19.05	0.08	19.07	0.08	18.95	0.08
775.4	427.3	18.94	0.08	19.14	0.08	18.97	0.08
774.0	538.9	18.97	0.08	19.06	0.08	18.99	0.08
741.8	512.6	19.09	0.08	19.25	0.08	18.36	0.08
727.5	560.6	19.02	0.08	19.11	0.08	18.96	0.08
794.6	459.4	19.06	0.09	19.30	0.08	18.14	0.08
832.5	573.6	18.95	0.08	19.02	0.08	18.90	0.08
856.1	381.6	18.98	0.08	19.12	0.08	19.07	0.08
622.1	465.8	19.02	0.08	19.00	0.08	18.96	0.08
741.6	390.7	19.05	0.08	19.14	0.08	19.12	0.08
614.1	508.4	19.09	0.08	19.15	0.08	19.03	0.08
751.8	427.0	19.10	0.09	19.08	0.08	18.53	0.08
668.1	401.8	19.04	0.08	19.16	0.08	19.10	0.08
808.3	567.8	18.90	0.08	19.10	0.08	18.98	0.08
761.5	559.7	18.68	0.10	19.17	0.09	19.01	0.09
620.5	414.2	19.28	0.08	19.16	0.08	18.33	0.08
835.2	524.2	19.03	0.08	19.05	0.08	18.90	0.08
659.8	540.2	19.27	0.08	19.13	0.08	18.41	0.08
745.9	215.5	19.03	0.08	19.03	0.08	18.94	0.08
797.6	497.9	18.98	0.09	19.21	0.08	18.96	0.08
810.8	554.9	19.33	0.08	19.19	0.08	18.33	0.08

Table B.1: Photometry of NGC 5694

X	Y	U	σU	B	σB	V	σV
707.8	49.7	19.06	0.08	19.04	0.08	18.93	0.08
804.0	343.4	19.35	0.08	19.19	0.08	18.33	0.08
912.9	437.7	18.97	0.08	19.04	0.08	18.96	0.08
813.1	711.7	18.99	0.08	19.11	0.08	19.05	0.08
563.8	497.3	18.99	0.08	19.09	0.08	18.99	0.08
842.6	491.6	19.29	0.08	19.20	0.08	18.33	0.08
694.1	389.4	19.33	0.08	19.18	0.08	18.37	0.08
842.9	343.5	19.02	0.08	19.09	0.08	18.98	0.08
685.0	516.7	19.05	0.08	19.09	0.08	18.96	0.08
749.7	377.0	19.09	0.08	19.18	0.08	19.07	0.08
691.1	428.3	19.09	0.08	19.26	0.08	19.17	0.09
658.6	514.4	19.07	0.08	19.17	0.08	19.10	0.08
565.7	506.9	19.05	0.08	19.12	0.08	19.01	0.08
709.8	441.3	19.12	0.09	19.21	0.08	19.28	0.09
732.8	372.3	19.05	0.08	19.28	0.08	19.01	0.08
746.0	276.3	19.02	0.08	19.09	0.08	19.07	0.08
644.6	572.1	19.01	0.08	19.11	0.08	19.13	0.08
828.2	538.6	19.07	0.08	19.09	0.08	18.98	0.08
601.9	611.6	19.01	0.08	19.09	0.08	19.04	0.08
691.3	461.2	19.27	0.09	19.34	0.08	18.31	0.08
848.7	497.6	19.34	0.08	19.26	0.08	18.40	0.08
562.9	335.2	18.99	0.08	19.12	0.08	19.09	0.08
642.4	564.3	19.03	0.08	19.17	0.08	19.15	0.08
794.6	177.5	19.20	0.08	19.25	0.08	18.59	0.08
844.8	523.5	19.12	0.08	19.16	0.08	19.11	0.08
778.6	529.1	19.32	0.08	19.25	0.08	18.45	0.08
602.7	361.3	19.08	0.08	19.12	0.08	19.08	0.08
430.0	669.8	19.05	0.08	19.13	0.08	19.07	0.08
626.4	482.4	19.40	0.08	19.25	0.08	18.43	0.08
712.7	287.2	19.10	0.08	19.14	0.08	19.08	0.08
669.2	454.6	19.03	0.09	19.33	0.08	19.08	0.09
713.3	402.4	18.99	0.09	19.46	0.08	19.31	0.09
766.9	347.9	19.38	0.08	19.26	0.08	18.44	0.08
356.5	298.2	19.38	0.08	19.30	0.08	18.46	0.08
824.0	1003.3	19.03	0.08	19.13	0.08	19.04	0.08

Table B.1: Photometry of NGC 5694

X	Y	U	σU	B	σB	V	σV
537.5	421.8	19.41	0.08	19.28	0.08	18.47	0.08
741.4	356.0	20.57	0.09	19.60	0.08	18.16	0.08
987.0	434.3	19.39	0.08	19.30	0.08	18.46	0.08
659.4	319.2	19.10	0.08	19.18	0.08	19.14	0.08
1004.8	528.2	19.10	0.08	19.15	0.08	19.06	0.08
732.0	384.1	19.14	0.08	19.41	0.08	19.34	0.08
982.8	206.9	19.09	0.08	19.22	0.08	19.17	0.08
700.5	501.2	19.35	0.09	19.38	0.08	18.32	0.08
203.0	392.8	19.12	0.08	19.26	0.08	19.21	0.08
571.1	168.4	19.08	0.08	19.14	0.08	19.06	0.08
890.7	531.7	19.05	0.08	19.27	0.08	19.24	0.08
773.2	331.1	19.02	0.08	19.29	0.08	19.30	0.08
786.1	507.3	19.31	0.09	19.35	0.09	18.58	0.09
753.4	619.4	19.07	0.08	19.39	0.08	19.33	0.08
817.8	447.2	19.13	0.08	19.32	0.08	19.27	0.08
827.0	522.4	19.14	0.08	19.26	0.08	19.23	0.08
680.6	519.9	19.39	0.09	19.29	0.08	18.64	0.08
272.5	259.9	19.13	0.08	19.19	0.08	19.12	0.08
982.4	267.0	19.47	0.08	19.35	0.08	18.50	0.08
682.6	539.4	19.43	0.08	19.34	0.08	18.53	0.08
804.9	587.0	19.45	0.08	19.33	0.08	18.49	0.08
847.8	307.2	19.44	0.08	19.36	0.08	18.52	0.08
645.0	548.0	19.08	0.08	19.26	0.08	19.19	0.08
872.0	840.8	19.46	0.08	19.35	0.08	18.50	0.08
693.2	933.1	20.06	0.08	19.44	0.08	18.22	0.08
554.0	521.9	19.07	0.08	19.23	0.08	19.23	0.08
685.1	771.2	19.45	0.08	19.36	0.08	18.53	0.08
795.8	541.9	19.08	0.08	19.39	0.08	19.26	0.08
768.0	655.8	19.47	0.08	19.36	0.08	18.52	0.08
660.2	586.7	19.12	0.08	19.30	0.08	19.26	0.08
622.3	125.8	19.14	0.08	19.21	0.08	19.14	0.08
775.0	510.3	19.45	0.09	19.44	0.08	18.48	0.08
502.2	381.0	19.09	0.08	19.23	0.08	19.21	0.08
727.0	552.1	19.45	0.08	19.38	0.08	18.59	0.08
848.1	615.5	19.48	0.08	19.41	0.08	18.55	0.08

Table B.1: Photometry of NGC 5694

X	Y	U	σU	B	σB	V	σV
850.1	455.9	19.53	0.08	19.38	0.08	18.53	0.08
791.9	431.2	19.42	0.09	19.37	0.08	18.62	0.08
852.9	502.7	19.18	0.08	19.37	0.08	19.39	0.08
774.0	436.5	19.47	0.09	19.40	0.08	18.48	0.08
348.1	619.8	19.13	0.08	19.25	0.08	19.21	0.08
619.7	274.3	19.17	0.08	19.29	0.08	19.28	0.08
519.9	600.1	19.10	0.08	19.20	0.08	19.17	0.08
850.4	366.4	19.53	0.08	19.42	0.08	18.60	0.08
310.4	228.3	19.18	0.08	19.32	0.08	19.29	0.08
157.4	771.2	19.18	0.08	19.46	0.08	18.98	0.08
817.8	574.1	19.50	0.08	19.43	0.08	18.58	0.08
880.7	533.8	19.20	0.08	19.30	0.08	19.25	0.08
527.1	522.3	19.50	0.08	19.45	0.08	18.63	0.08
719.4	690.8	19.15	0.08	19.30	0.08	19.26	0.08
752.5	514.3	19.53	0.09	19.49	0.08	18.58	0.08
676.4	273.7	19.13	0.08	19.34	0.08	19.20	0.08
878.8	219.3	19.19	0.08	19.35	0.08	19.26	0.08
636.4	493.4	19.25	0.08	19.40	0.08	19.44	0.08
451.6	598.5	19.17	0.08	19.49	0.08	19.48	0.08
621.2	779.4	19.18	0.08	19.35	0.08	19.33	0.08
750.8	584.5	19.23	0.08	19.51	0.08	19.68	0.08
997.0	626.6	19.55	0.08	19.48	0.08	18.66	0.08
440.6	960.0	19.06	0.08	19.45	0.08	19.47	0.08
635.7	467.5	19.20	0.08	19.42	0.08	19.37	0.08
754.6	614.1	19.23	0.08	19.62	0.08	19.56	0.08
607.6	651.0	19.17	0.08	19.41	0.08	19.39	0.08
829.6	495.6	19.56	0.08	19.51	0.08	18.66	0.08
822.1	507.7	19.25	0.08	19.54	0.08	19.44	0.08
679.3	302.1	19.23	0.08	19.45	0.08	19.44	0.08
568.8	554.4	19.55	0.08	19.48	0.08	18.73	0.08
794.0	440.5	19.21	0.09	19.71	0.08	19.09	0.09
777.8	438.4	19.52	0.09	19.55	0.08	18.68	0.08
504.2	587.1	19.19	0.08	19.49	0.08	19.50	0.08
784.5	407.8	19.62	0.08	19.51	0.08	18.69	0.08
620.2	558.3	19.19	0.08	19.46	0.08	19.44	0.08

Table B.1: Photometry of NGC 5694

X	Y	U	σU	B	σB	V	σV
555.4	566.3	19.55	0.08	19.53	0.08	18.73	0.08
832.9	903.8	19.21	0.08	19.48	0.08	19.47	0.08
801.4	367.2	19.57	0.09	19.55	0.08	18.76	0.08
651.5	519.7	19.15	0.08	19.41	0.08	19.44	0.08
655.0	739.5	19.20	0.08	19.54	0.08	19.56	0.08
550.6	884.5	19.14	0.08	19.52	0.08	19.53	0.08
791.1	786.8	19.22	0.08	19.59	0.08	19.56	0.08
705.6	538.1	19.20	0.09	19.60	0.08	19.21	0.08
611.4	231.5	19.61	0.08	19.57	0.08	18.80	0.08
460.4	312.1	19.56	0.08	19.59	0.08	18.84	0.08
584.1	484.1	19.25	0.08	19.57	0.08	19.59	0.08
665.7	420.4	19.65	0.09	19.55	0.08	18.83	0.08
642.8	366.1	19.24	0.08	19.69	0.08	19.53	0.08
731.4	566.4	19.27	0.08	19.74	0.08	19.72	0.08
686.3	611.0	19.68	0.08	19.64	0.08	18.86	0.08
889.3	501.6	19.33	0.08	19.79	0.08	19.89	0.08
629.8	640.3	19.70	0.08	19.65	0.08	18.87	0.08
609.8	420.2	19.36	0.08	19.79	0.08	19.84	0.08
832.3	489.6	19.70	0.09	19.69	0.08	18.91	0.08
540.8	572.6	19.28	0.08	19.68	0.08	19.71	0.08
797.3	709.1	19.34	0.08	19.73	0.08	19.72	0.08
707.0	467.2	19.53	0.10	19.80	0.09	18.96	0.09
876.4	419.6	19.75	0.09	19.71	0.08	18.92	0.08
155.6	914.1	21.02	0.09	19.78	0.08	18.48	0.08
783.4	502.4	19.68	0.09	19.67	0.08	19.06	0.08
708.4	386.5	19.73	0.08	19.70	0.08	18.93	0.08
901.8	387.5	20.76	0.09	19.80	0.08	18.66	0.08
842.2	320.6	19.34	0.08	19.76	0.08	19.76	0.08
746.4	539.2	19.73	0.09	19.76	0.08	18.95	0.08
683.8	337.3	19.76	0.08	19.73	0.08	18.92	0.08
587.6	529.6	19.80	0.09	19.75	0.08	18.98	0.08
686.0	414.2	19.81	0.08	19.78	0.08	18.83	0.08
765.4	525.9	19.87	0.09	19.74	0.08	18.88	0.08
806.8	457.1	19.76	0.09	19.84	0.08	18.95	0.08
649.0	474.9	19.75	0.09	19.83	0.09	19.00	0.08

Table B.1: Photometry of NGC 5694

X	Y	U	σU	B	σB	V	σV
749.0	942.9	21.31	0.09	20.04	0.08	18.51	0.08
766.0	388.7	19.71	0.09	19.85	0.08	19.08	0.08
734.0	536.0	19.75	0.09	19.86	0.08	19.01	0.08
809.7	278.3	19.85	0.08	19.79	0.08	19.00	0.08
687.7	492.6	19.92	0.09	19.76	0.08	18.90	0.08
714.2	323.1	19.82	0.08	19.83	0.08	18.79	0.08
540.1	529.3	19.33	0.08	19.81	0.08	19.71	0.08
731.6	839.2	19.45	0.08	19.91	0.08	19.96	0.08
787.6	528.2	19.78	0.09	19.80	0.08	19.08	0.08
899.0	653.2	19.86	0.08	19.80	0.08	19.02	0.08
866.1	835.1	19.85	0.09	19.83	0.08	19.03	0.08
832.7	622.1	19.87	0.08	19.84	0.08	19.03	0.08
841.8	425.5	19.83	0.08	19.83	0.08	19.10	0.08
1003.4	699.4	19.41	0.08	19.89	0.08	19.92	0.08
821.0	439.1	19.83	0.09	19.88	0.08	19.10	0.08
523.7	441.5	19.85	0.08	19.87	0.08	19.10	0.08
604.4	954.7	19.90	0.08	19.87	0.08	19.08	0.08
896.1	360.4	19.95	0.08	19.82	0.08	19.09	0.08
842.3	224.1	19.94	0.08	19.85	0.08	19.09	0.08
610.0	190.0	19.43	0.08	19.92	0.08	19.94	0.08
575.7	581.5	19.90	0.08	19.88	0.08	19.12	0.08
938.0	501.8	20.15	0.09	19.91	0.08	18.96	0.08
693.1	630.3	19.48	0.08	19.96	0.08	20.01	0.08
765.5	396.3	19.92	0.09	19.90	0.08	19.08	0.08
740.2	557.8	19.87	0.09	20.00	0.08	18.92	0.09
733.3	521.2	19.82	0.10	20.01	0.09	19.15	0.09
1003.7	127.5	19.97	0.08	19.92	0.08	19.11	0.08
679.6	532.0	19.84	0.08	19.94	0.08	19.19	0.08
793.8	259.2	19.59	0.08	20.08	0.08	20.09	0.09
42.5	7.9	19.74	0.08	19.95	0.08	19.39	0.08
777.8	482.2	19.84	0.09	19.99	0.09	19.24	0.10
891.3	578.3	19.93	0.09	19.98	0.09	19.16	0.08
674.0	531.1	19.92	0.08	19.96	0.08	19.19	0.08
777.7	505.5	19.68	0.09	20.02	0.09	19.34	0.09
752.3	248.5	19.52	0.08	20.04	0.08	20.08	0.08

Table B.1: Photometry of NGC 5694

X	Y	U	σU	B	σB	V	σV
617.1	511.6	19.91	0.09	19.98	0.08	19.27	0.08
416.3	711.7	19.97	0.08	19.94	0.08	19.20	0.08
848.7	589.8	19.93	0.09	19.95	0.08	19.22	0.08
829.9	579.5	19.98	0.08	19.97	0.08	19.20	0.08
518.2	781.5	19.97	0.08	19.97	0.08	19.23	0.08
690.3	553.2	20.02	0.08	19.94	0.08	19.23	0.08
661.8	468.0	19.77	0.09	20.52	0.10	19.55	0.08
580.3	424.7	19.98	0.09	19.97	0.08	19.26	0.08
738.8	426.1	19.85	0.10	20.05	0.09	19.30	0.09
716.4	712.5	19.98	0.08	20.02	0.08	19.24	0.08
676.7	556.6	19.99	0.09	20.00	0.08	19.24	0.08
495.3	389.6	19.96	0.08	19.99	0.08	19.24	0.08
945.0	568.5	20.04	0.08	20.01	0.08	19.21	0.08
584.6	664.0	19.99	0.08	20.01	0.08	19.26	0.08
662.0	555.7	19.90	0.10	20.02	0.09	19.30	0.08
808.1	312.4	19.58	0.08	20.11	0.08	20.12	0.08
811.0	413.3	20.03	0.09	20.01	0.08	19.21	0.08
626.8	143.4	20.03	0.08	20.03	0.08	19.25	0.08
702.5	409.3	19.92	0.09	20.07	0.08	19.24	0.08
554.0	874.3	20.05	0.08	20.00	0.08	19.27	0.08
87.2	532.8	20.15	0.09	19.98	0.08	19.23	0.08
752.7	591.2	20.03	0.09	20.04	0.08	19.27	0.08
595.6	173.6	19.79	0.08	19.88	0.08	19.75	0.08
821.7	503.4	19.75	0.08	20.34	0.08	20.07	0.08
137.6	180.6	20.04	0.08	20.05	0.08	19.27	0.08
804.0	519.8	20.10	0.08	20.08	0.08	19.06	0.08
696.1	455.1	20.02	0.10	20.11	0.09	19.48	0.09
736.6	529.6	20.03	0.09	20.09	0.08	19.37	0.09
809.6	746.0	20.09	0.08	20.09	0.08	19.31	0.08
761.2	517.8	19.97	0.10	20.20	0.10	19.34	0.11
612.2	604.3	20.08	0.09	20.07	0.08	19.37	0.08
643.7	456.2	20.11	0.09	20.09	0.08	19.33	0.08
623.2	371.4	19.78	0.08	20.27	0.08	20.22	0.08
730.0	527.1	20.13	0.09	20.12	0.08	19.35	0.09
797.5	614.3	20.09	0.09	20.11	0.08	19.37	0.08

Table B.1: Photometry of NGC 5694

X	Y	U	σU	B	σB	V	σV
459.4	638.0	21.54	0.09	20.33	0.08	18.99	0.08
782.7	482.2	20.06	0.09	20.15	0.10	19.49	0.10
116.5	647.5	20.12	0.08	20.11	0.08	19.37	0.08
638.0	549.4	20.08	0.09	20.12	0.08	19.41	0.08
938.7	492.7	20.12	0.09	20.15	0.08	19.36	0.08
770.8	590.0	20.15	0.09	20.15	0.08	19.35	0.08
411.9	71.3	20.17	0.09	20.15	0.08	19.38	0.08
810.8	461.1	19.99	0.09	20.26	0.09	19.47	0.09
351.9	414.9	20.39	0.08	20.09	0.08	19.28	0.08
844.0	406.9	20.16	0.09	20.17	0.08	19.43	0.08
884.5	572.9	20.14	0.08	20.18	0.08	19.44	0.08
742.3	519.7	20.12	0.09	20.31	0.09	19.73	0.11
810.2	289.9	20.18	0.08	20.17	0.08	19.46	0.08
994.5	559.5	20.21	0.09	20.18	0.08	19.42	0.08
320.2	374.5	20.18	0.09	20.22	0.08	19.45	0.08
781.6	648.4	19.76	0.08	20.34	0.08	20.43	0.08
516.3	141.7	20.20	0.08	20.21	0.08	19.46	0.08
802.7	373.3	20.11	0.09	20.28	0.08	19.53	0.08
816.6	150.0	20.23	0.09	20.23	0.08	19.48	0.08
450.7	162.5	20.25	0.09	20.25	0.08	19.48	0.08
807.1	482.0	20.31	0.09	20.28	0.08	19.42	0.08
800.5	560.7	20.24	0.09	20.26	0.08	19.47	0.08
602.0	263.9	20.23	0.08	20.24	0.08	19.52	0.08
982.8	416.4	20.23	0.08	20.28	0.08	19.48	0.08
649.0	619.8	20.18	0.08	20.26	0.08	19.58	0.08
545.5	427.6	20.19	0.09	20.27	0.08	19.53	0.08
877.9	350.1	20.29	0.09	20.29	0.08	19.51	0.08
465.2	986.4	20.34	0.09	20.25	0.08	19.53	0.08
710.4	306.7	20.25	0.09	20.28	0.08	19.57	0.08
603.1	574.4	20.24	0.09	20.28	0.08	19.58	0.08
398.5	216.2	20.20	0.09	20.27	0.08	19.60	0.08
667.5	467.0	20.37	0.09	20.31	0.08	19.45	0.08
672.5	480.8	20.24	0.09	20.32	0.08	19.63	0.09
706.0	419.3	20.17	0.09	20.34	0.08	19.66	0.09
464.7	612.7	20.87	0.09	20.28	0.08	19.33	0.08

Table B.1: Photometry of NGC 5694

X	Y	U	σU	B	σB	V	σV
815.5	509.7	20.25	0.09	20.37	0.08	19.56	0.09
793.1	737.6	20.28	0.09	20.31	0.08	19.55	0.08
809.5	524.5	20.22	0.09	20.34	0.08	19.58	0.09
710.5	611.3	20.32	0.09	20.31	0.08	19.58	0.08
837.2	430.1	20.24	0.09	20.37	0.08	19.60	0.08
748.5	410.1	20.36	0.09	20.34	0.08	19.53	0.09
616.2	688.3	20.29	0.09	20.36	0.08	19.59	0.08
751.4	328.9	20.30	0.09	20.34	0.08	19.61	0.08
853.3	480.9	20.35	0.09	20.35	0.08	19.56	0.08
694.5	538.1	20.32	0.09	20.36	0.08	19.59	0.08
667.7	448.5	20.26	0.09	20.44	0.09	19.61	0.08
809.8	493.2	20.24	0.09	20.43	0.09	19.67	0.09
717.8	633.1	20.34	0.09	20.33	0.08	19.64	0.08
663.7	442.4	20.32	0.09	20.38	0.09	19.62	0.08
802.2	686.9	20.32	0.09	20.37	0.08	19.63	0.08
723.3	376.9	20.40	0.09	20.40	0.08	19.55	0.08
767.4	267.8	20.33	0.09	20.34	0.08	19.87	0.11
775.7	585.5	20.36	0.09	20.42	0.08	19.63	0.08
691.5	594.0	20.36	0.09	20.41	0.08	19.64	0.08
606.1	563.2	20.33	0.09	20.38	0.08	19.73	0.08
714.9	358.4	20.36	0.09	20.42	0.08	19.69	0.08
409.0	942.2	20.32	0.09	20.40	0.08	19.66	0.08
593.7	616.4	20.36	0.09	20.39	0.08	19.69	0.08
962.6	469.3	20.45	0.09	20.32	0.08	19.48	0.09
566.3	255.3	20.40	0.09	20.41	0.08	19.66	0.08
632.7	478.3	20.35	0.09	20.41	0.08	19.70	0.08
581.3	549.2	20.37	0.09	20.43	0.08	19.66	0.08
880.9	550.8	20.37	0.09	20.41	0.08	19.68	0.08
814.6	407.2	20.40	0.09	20.44	0.08	19.67	0.08
860.6	444.3	20.28	0.09	20.45	0.09	19.72	0.09
959.8	332.8	20.42	0.09	20.47	0.08	19.70	0.08
646.0	354.5	20.38	0.09	20.46	0.08	19.77	0.08
815.2	472.3	20.46	0.09	20.35	0.09	19.79	0.08
868.3	451.6	20.40	0.09	20.47	0.08	19.71	0.08
660.4	462.2	20.28	0.09	20.49	0.09	19.83	0.09

Table B.1: Photometry of NGC 5694

X	Y	U	σU	B	σB	V	σV
695.4	581.6	20.48	0.09	20.46	0.08	19.75	0.08
838.5	353.4	20.49	0.09	20.49	0.08	19.76	0.08
492.2	513.2	20.44	0.09	20.52	0.08	19.79	0.08
672.5	486.4	20.44	0.09	20.53	0.09	20.01	0.10
505.0	412.3	20.43	0.09	20.52	0.08	19.81	0.08
587.1	477.3	20.52	0.09	20.54	0.08	19.77	0.08
483.9	1011.5	20.41	0.09	20.53	0.08	19.81	0.08
613.8	373.6	20.53	0.09	20.52	0.08	19.74	0.08
549.8	181.1	20.51	0.09	20.52	0.08	19.78	0.08
615.6	747.2	20.42	0.09	20.52	0.08	19.79	0.08
890.5	521.6	20.45	0.09	20.55	0.08	19.81	0.08
646.3	382.8	20.55	0.09	20.49	0.08	19.78	0.08
754.1	533.8	20.52	0.09	20.55	0.09	19.71	0.09
690.6	364.2	20.42	0.09	20.62	0.08	19.87	0.08
628.0	656.3	20.52	0.09	20.54	0.08	19.82	0.08
1004.0	440.1	20.51	0.09	20.58	0.08	19.81	0.08
767.6	427.9	20.42	0.09	20.50	0.09	19.92	0.09
681.3	512.9	20.65	0.09	20.58	0.08	19.75	0.09
444.9	640.1	20.53	0.09	20.55	0.08	19.86	0.08
809.2	98.5	20.56	0.09	20.58	0.08	19.80	0.08
688.0	620.8	20.49	0.09	20.56	0.08	19.92	0.08
986.8	529.0	20.48	0.09	20.58	0.08	19.83	0.08
562.4	511.3	20.49	0.09	20.59	0.08	19.88	0.08
856.5	343.2	20.56	0.09	20.57	0.08	19.87	0.08
791.3	382.3	20.64	0.09	20.62	0.08	19.72	0.08
12.2	368.4	21.57	0.09	20.67	0.08	19.52	0.08
346.4	650.9	20.60	0.09	20.62	0.08	19.90	0.08
718.5	577.3	20.56	0.09	20.64	0.08	19.95	0.08
743.3	384.9	20.52	0.09	20.59	0.09	20.15	0.09
842.2	24.2	20.47	0.08	20.62	0.08	20.06	0.08
294.1	713.3	20.59	0.09	20.64	0.08	19.93	0.08
792.5	594.0	20.56	0.09	20.68	0.08	19.95	0.08
661.1	366.4	20.58	0.09	20.64	0.08	19.98	0.08
846.0	395.4	20.56	0.09	20.69	0.08	19.94	0.08
703.9	557.0	20.52	0.09	20.67	0.08	20.01	0.08

Table B.1: Photometry of NGC 5694

X	Y	U	σU	B	σB	V	σV
890.4	416.9	20.60	0.09	20.64	0.08	20.00	0.08
766.7	263.8	20.58	0.09	20.72	0.09	19.98	0.10
767.7	359.7	20.76	0.09	20.58	0.09	19.78	0.09
121.9	613.9	20.60	0.09	20.67	0.08	19.97	0.08
720.1	590.9	20.68	0.09	20.68	0.08	19.89	0.08
696.5	331.1	20.68	0.09	20.67	0.08	19.97	0.09
869.5	489.0	20.69	0.09	20.70	0.08	19.97	0.08
851.1	105.9	20.58	0.09	20.68	0.08	20.02	0.08
717.3	371.6	20.59	0.09	20.76	0.09	20.07	0.10
911.3	690.6	20.63	0.09	20.72	0.08	19.97	0.08
742.2	585.5	20.51	0.10	20.73	0.09	20.15	0.09
672.3	431.7	20.49	0.09	20.73	0.10	20.19	0.09
824.7	452.5	20.63	0.09	20.73	0.08	20.06	0.08
515.7	977.2	20.23	0.09	21.01	0.08	20.99	0.09
751.5	357.0	20.69	0.09	20.76	0.08	19.97	0.08
615.1	564.2	20.69	0.09	20.75	0.08	20.01	0.08
618.6	202.2	20.68	0.09	20.71	0.08	20.05	0.08
818.1	486.4	20.55	0.09	20.74	0.08	20.35	0.09
766.1	422.6	20.70	0.09	20.65	0.08	20.08	0.09
1009.3	357.3	20.72	0.09	20.73	0.08	20.01	0.08
766.1	374.2	20.63	0.09	20.77	0.08	20.16	0.09
558.5	663.6	20.63	0.09	20.75	0.08	20.14	0.08
748.4	550.3	20.69	0.09	20.77	0.08	20.07	0.09
832.3	1003.9	20.68	0.09	20.78	0.08	20.09	0.08
80.7	536.1	20.72	0.09	20.76	0.08	20.03	0.08
835.5	509.0	20.86	0.09	20.77	0.08	20.00	0.08
823.1	433.0	20.76	0.09	20.75	0.08	20.07	0.08
673.8	426.4	20.78	0.09	20.80	0.08	19.98	0.08
626.4	460.6	20.63	0.10	20.79	0.09	20.12	0.09
276.1	295.4	20.76	0.09	20.80	0.08	20.05	0.08
778.3	1019.7	22.27	0.11	21.03	0.08	19.65	0.08
976.6	757.4	20.67	0.09	20.83	0.08	20.06	0.08
748.9	349.6	20.68	0.09	20.80	0.08	20.17	0.08
651.0	324.1	20.73	0.09	20.83	0.08	20.09	0.08
763.2	239.8	20.76	0.09	20.83	0.08	20.04	0.08

Table B.1: Photometry of NGC 5694

X	Y	U	σU	B	σB	V	σV
885.7	410.0	20.76	0.09	20.79	0.08	20.09	0.08
768.8	410.2	20.70	0.09	20.86	0.09	20.19	0.09
655.9	280.3	20.74	0.09	20.81	0.08	20.10	0.08
618.9	440.7	20.83	0.09	20.85	0.08	20.06	0.08
799.1	577.7	20.62	0.09	20.86	0.08	20.21	0.08
634.3	527.2	20.81	0.09	20.82	0.08	20.30	0.11
662.9	340.5	20.75	0.09	20.82	0.08	20.13	0.08
640.3	558.4	20.72	0.09	20.81	0.08	20.18	0.08
929.3	272.8	20.75	0.09	20.84	0.08	20.14	0.08
766.0	406.0	20.83	0.09	20.83	0.08	20.24	0.10
798.6	588.1	20.78	0.09	20.87	0.08	20.08	0.08
572.2	653.3	20.69	0.09	20.86	0.08	20.27	0.08
640.8	717.1	20.76	0.09	20.88	0.08	20.12	0.08
769.0	433.8	20.63	0.10	21.12	0.09	20.11	0.10
652.0	594.3	20.86	0.09	20.85	0.08	20.28	0.08
704.0	509.3	20.70	0.10	20.89	0.09	20.34	0.10
868.3	529.7	20.82	0.09	20.90	0.08	20.20	0.08
815.6	377.2	20.91	0.10	20.90	0.08	20.13	0.08
796.0	316.5	20.69	0.09	20.85	0.08	20.35	0.08
687.3	981.1	20.76	0.09	20.79	0.08	20.60	0.08
498.5	515.2	20.80	0.09	20.91	0.08	20.23	0.08
915.7	631.0	20.83	0.09	20.95	0.08	20.18	0.08
708.0	294.8	20.77	0.09	20.94	0.08	20.19	0.08
710.8	331.1	20.81	0.09	21.02	0.08	20.17	0.09
788.9	616.3	20.75	0.10	20.97	0.09	20.23	0.09
816.7	530.9	20.96	0.10	20.94	0.08	20.18	0.09
552.5	643.6	20.87	0.09	20.97	0.08	20.25	0.08
827.3	447.1	20.89	0.10	20.95	0.09	20.24	0.09
428.1	696.5	20.91	0.09	20.94	0.08	20.25	0.08
586.3	557.7	20.92	0.09	20.98	0.08	20.19	0.08
920.0	491.1	20.78	0.09	20.96	0.08	20.29	0.08
652.2	542.4	20.75	0.09	20.96	0.09	20.34	0.09
609.4	238.7	20.87	0.09	20.95	0.08	20.25	0.08
804.8	334.5	20.85	0.09	20.94	0.08	20.31	0.09
853.8	489.9	20.85	0.09	20.98	0.08	20.36	0.10

Table B.1: Photometry of NGC 5694

X	Y	U	σU	B	σB	V	σV
697.3	397.8	20.82	0.09	21.03	0.08	20.46	0.10
687.4	451.8	20.87	0.10	21.10	0.09	20.13	0.09
662.4	408.7	20.91	0.09	21.04	0.09	20.26	0.09
840.1	498.9	20.78	0.10	21.08	0.08	20.25	0.10
515.8	423.6	20.89	0.09	20.96	0.08	20.27	0.08
763.9	672.0	20.89	0.09	20.92	0.08	20.31	0.08
757.9	428.0	20.83	0.10	20.95	0.09	20.34	0.09
522.0	560.5	20.93	0.09	20.96	0.08	20.30	0.08
680.0	547.2	20.74	0.10	21.07	0.08	20.15	0.09
690.6	546.1	20.82	0.09	21.00	0.08	20.42	0.09
725.2	777.1	21.04	0.09	20.95	0.08	20.28	0.08
627.7	550.0	20.98	0.09	20.93	0.08	20.31	0.08
994.4	669.2	20.92	0.09	21.00	0.08	20.29	0.08
646.2	451.8	20.83	0.09	21.05	0.09	20.40	0.09
626.9	117.6	20.86	0.09	21.03	0.08	20.45	0.08
675.9	49.5	20.88	0.09	20.99	0.08	20.36	0.08
811.5	321.8	20.93	0.09	20.98	0.09	20.35	0.08
834.9	765.3	20.99	0.09	21.02	0.08	20.33	0.08
845.3	544.6	20.95	0.09	21.04	0.08	20.30	0.08
645.0	345.2	20.97	0.09	21.03	0.08	20.34	0.08
391.4	640.9	20.92	0.09	21.03	0.08	20.35	0.08
656.9	530.8	21.12	0.09	20.98	0.09	20.24	0.08
799.5	662.7	20.84	0.10	20.92	0.09	20.50	0.09
778.4	636.5	21.01	0.09	21.08	0.08	20.43	0.09
646.5	514.3	20.90	0.09	21.23	0.09	20.38	0.10
793.7	521.2	20.99	0.10	21.17	0.10	20.40	0.11
621.1	310.3	21.00	0.09	21.07	0.08	20.37	0.08
833.1	406.7	20.96	0.09	21.11	0.08	20.38	0.08
116.1	42.1	20.99	0.09	21.10	0.08	20.36	0.08
676.4	344.6	21.12	0.09	21.05	0.08	20.38	0.08
961.2	656.3	21.08	0.09	21.06	0.11	20.25	0.12
124.4	382.6	21.09	0.09	21.07	0.08	20.36	0.08
740.2	701.5	21.03	0.09	21.06	0.08	20.42	0.08
760.6	433.7	21.14	0.10	21.14	0.09	20.19	0.10
589.0	486.9	21.02	0.09	21.02	0.08	20.42	0.08

Table B.1: Photometry of NGC 5694

X	Y	U	σU	B	σB	V	σV
401.4	575.6	21.04	0.09	21.08	0.08	20.42	0.08
929.4	168.4	21.02	0.09	21.13	0.08	20.44	0.08
797.2	416.4	20.97	0.10	21.13	0.09	20.91	0.17
643.9	435.1	20.99	0.09	21.09	0.08	20.51	0.09
279.0	982.2	20.93	0.09	21.04	0.08	20.72	0.09
663.1	427.1	20.82	0.09	21.20	0.08	20.82	0.10
718.0	821.8	21.04	0.09	21.12	0.08	20.50	0.08
922.5	337.3	21.09	0.09	21.15	0.08	20.47	0.09
886.5	516.1	21.04	0.09	21.16	0.09	20.46	0.08
420.4	514.2	21.06	0.09	21.12	0.08	20.47	0.08
806.4	294.5	21.11	0.09	21.16	0.08	20.44	0.08
548.4	654.1	21.01	0.09	21.14	0.08	20.59	0.08
874.4	447.1	21.10	0.09	21.02	0.08	20.66	0.09
830.1	596.3	21.11	0.09	21.23	0.09	20.41	0.09
486.9	176.6	21.41	0.09	21.19	0.08	20.27	0.08
605.9	332.7	21.07	0.09	21.18	0.08	20.44	0.08
635.7	668.8	21.15	0.09	21.15	0.08	20.49	0.08
714.8	598.3	21.02	0.09	21.14	0.08	20.60	0.09
804.9	414.2	21.04	0.10	21.29	0.10	20.66	0.12
768.2	603.6	21.07	0.09	21.26	0.09	20.46	0.09
825.5	394.5	21.13	0.10	21.22	0.08	20.42	0.09
691.1	382.5	21.00	0.09	21.15	0.08	20.74	0.09
837.7	231.2	21.09	0.09	21.20	0.08	20.57	0.09
665.7	579.0	21.14	0.09	21.28	0.08	20.38	0.09
642.1	803.2	21.33	0.11	21.41	0.10	20.13	0.09
362.7	866.0	21.09	0.09	21.20	0.08	20.46	0.08
630.7	199.6	21.18	0.09	21.18	0.08	20.48	0.08
823.9	351.6	21.25	0.10	21.18	0.10	20.37	0.09
220.6	160.2	21.09	0.09	21.20	0.08	20.54	0.09
709.9	349.0	21.16	0.11	21.27	0.09	20.40	0.11
681.3	589.9	20.95	0.10	21.18	0.09	20.75	0.09
651.7	430.6	21.02	0.09	21.31	0.08	20.68	0.09
669.6	371.8	21.12	0.09	21.19	0.08	20.63	0.09
476.6	716.0	21.09	0.09	21.22	0.08	20.57	0.08
803.1	127.4	21.11	0.09	21.23	0.08	20.55	0.08

Table B.1: Photometry of NGC 5694

X	Y	U	σU	B	σB	V	σV
610.0	576.3	21.12	0.09	21.22	0.08	20.58	0.09
725.9	350.6	21.20	0.10	21.20	0.08	20.53	0.08
431.0	983.8	21.03	0.09	21.24	0.08	20.59	0.08
789.2	551.0	21.26	0.11	21.22	0.09	20.91	0.10
868.9	259.0	21.09	0.09	21.27	0.08	20.57	0.08
819.8	552.0	21.05	0.09	21.30	0.09	20.72	0.09
395.5	529.5	21.19	0.09	21.24	0.08	20.58	0.08
895.4	424.9	21.10	0.09	21.29	0.09	20.79	0.09
795.1	349.1	21.06	0.09	21.33	0.08	20.83	0.10
606.2	512.9	21.17	0.10	21.33	0.09	20.59	0.10
509.3	608.0	21.13	0.09	21.28	0.08	20.62	0.09
641.6	209.1	21.18	0.09	21.24	0.08	20.74	0.09
926.7	32.0	21.23	0.10	21.29	0.09	20.54	0.08
810.2	371.1	21.16	0.10	21.36	0.09	20.66	0.09
675.8	378.0	21.21	0.10	21.26	0.08	20.80	0.09
431.3	476.7	21.19	0.09	21.32	0.08	20.58	0.08
752.5	627.0	21.08	0.11	21.28	0.09	20.81	0.10
832.3	854.0	21.23	0.09	21.30	0.08	20.60	0.09
434.4	546.7	21.34	0.10	21.36	0.08	20.64	0.09
609.2	636.6	21.15	0.09	21.22	0.08	21.03	0.09
902.1	495.2	21.27	0.09	21.30	0.08	20.61	0.08
785.7	358.4	21.27	0.10	21.45	0.09	20.56	0.10
789.4	574.1	21.13	0.09	21.38	0.08	20.80	0.11
641.9	238.6	21.20	0.09	21.33	0.08	20.65	0.09
817.9	326.0	21.17	0.10	21.31	0.09	20.64	0.09
876.6	671.2	21.18	0.09	21.37	0.08	20.63	0.09
599.9	621.6	21.15	0.09	21.33	0.08	20.68	0.09
848.7	74.8	21.31	0.10	21.32	0.08	20.67	0.09
733.9	588.7	21.27	0.10	21.63	0.09	20.84	0.12
621.0	300.4	21.24	0.09	21.34	0.08	20.65	0.09
772.7	417.5	21.27	0.10	21.31	0.09	20.76	0.11
866.1	519.8	21.11	0.09	21.55	0.09	21.08	0.10
967.5	259.6	21.38	0.10	21.35	0.08	20.75	0.11
893.0	408.8	21.29	0.09	21.33	0.08	20.65	0.09
577.8	802.7	21.15	0.09	21.35	0.08	20.69	0.09

Table B.1: Photometry of NGC 5694

X	Y	U	σU	B	σB	V	σV
855.3	336.1	21.24	0.09	21.34	0.08	20.76	0.09
421.3	244.3	21.59	0.10	21.50	0.08	20.34	0.08
816.1	654.0	21.36	0.10	21.37	0.08	20.59	0.09
994.7	17.4	21.28	0.09	21.38	0.09	20.66	0.09
670.8	522.7	21.37	0.10	21.36	0.08	20.65	0.09
547.2	351.7	21.21	0.09	21.37	0.08	20.72	0.09
88.5	949.5	21.30	0.09	21.23	0.08	20.97	0.09
730.9	790.4	21.29	0.09	21.38	0.08	20.67	0.08
628.9	578.5	21.31	0.09	21.45	0.09	20.81	0.09
949.2	514.5	21.33	0.09	21.32	0.09	20.71	0.09
1004.7	426.5	21.37	0.09	21.36	0.08	20.72	0.08
750.5	577.6	21.21	0.09	21.36	0.08	20.89	0.09
312.7	164.5	21.45	0.09	21.36	0.08	20.65	0.08
693.0	655.9	21.27	0.09	21.38	0.08	20.76	0.08
802.4	382.5	21.08	0.09	21.57	0.09	20.87	0.09
1008.4	320.6	21.39	0.10	21.39	0.08	20.67	0.09
334.2	448.2	21.16	0.09	21.44	0.08	20.91	0.09
669.5	279.6	21.35	0.09	21.42	0.08	20.72	0.08
664.0	261.4	21.33	0.09	21.38	0.08	20.77	0.09
717.4	570.6	21.20	0.09	21.55	0.09	21.02	0.11
670.8	567.4	21.27	0.11	21.53	0.10	20.84	0.10
585.2	490.0	21.26	0.09	21.44	0.08	20.94	0.09
983.3	24.3	21.28	0.09	21.45	0.08	20.73	0.08
600.5	560.7	21.29	0.09	21.43	0.08	20.81	0.09
736.7	721.7	21.25	0.09	21.43	0.08	20.83	0.09
806.6	354.6	21.24	0.10	21.50	0.09	20.76	0.09
858.5	639.3	21.51	0.09	21.42	0.08	20.63	0.08
819.7	373.1	21.29	0.09	21.45	0.09	20.76	0.08
650.4	798.3	21.36	0.10	21.50	0.09	20.59	0.09
657.8	598.5	21.39	0.09	21.40	0.08	20.77	0.09
821.6	710.5	21.32	0.10	21.46	0.08	20.74	0.09
520.1	322.7	21.34	0.09	21.42	0.08	20.85	0.09
700.4	273.4	21.35	0.09	21.39	0.08	20.90	0.09
518.9	719.1	21.29	0.09	21.49	0.08	20.83	0.09
711.3	572.5	21.22	0.10	21.43	0.09	21.00	0.09

Table B.1: Photometry of NGC 5694

X	Y	U	σU	B	σB	V	σV
838.6	859.6	21.32	0.10	21.50	0.08	20.77	0.09
712.5	651.9	21.25	0.10	21.47	0.09	20.89	0.09
938.9	380.5	21.17	0.09	21.48	0.08	21.02	0.09
765.0	533.0	21.30	0.11	21.43	0.09	21.16	0.11
121.5	714.3	21.32	0.09	21.46	0.08	20.81	0.09
810.2	391.4	21.25	0.10	21.51	0.09	20.83	0.09
968.5	399.7	21.48	0.10	21.44	0.08	20.77	0.09
790.1	282.4	21.42	0.10	21.55	0.10	20.88	0.12
923.7	464.6	21.25	0.09	21.57	0.09	20.90	0.09
920.7	82.6	21.43	0.09	21.48	0.08	20.83	0.08
828.2	561.1	21.27	0.09	21.42	0.08	21.09	0.09
282.5	75.5	21.34	0.09	21.48	0.08	20.83	0.08
916.5	623.1	21.47	0.09	21.53	0.08	20.79	0.09
551.0	465.3	21.31	0.10	21.50	0.08	20.82	0.09
439.2	634.8	21.25	0.09	21.49	0.08	21.11	0.09
544.9	416.5	21.33	0.09	21.57	0.08	21.01	0.09
760.2	312.9	21.49	0.10	21.51	0.08	20.74	0.09
714.8	704.7	21.28	0.09	21.56	0.09	21.06	0.10
845.7	562.2	21.36	0.09	21.50	0.08	21.25	0.10
642.5	372.7	21.43	0.09	21.48	0.08	20.92	0.09
616.2	449.0	21.38	0.10	21.58	0.09	20.97	0.11
682.8	448.3	21.28	0.11	21.59	0.10	21.04	0.12
468.0	178.8	21.42	0.09	21.52	0.08	20.95	0.09
654.0	369.1	21.37	0.10	21.51	0.09	21.02	0.10
615.8	541.3	21.45	0.10	21.57	0.09	20.99	0.10
629.1	446.0	21.41	0.10	21.53	0.09	21.17	0.11
674.9	612.0	21.34	0.10	21.45	0.10	21.00	0.09
944.9	357.8	21.36	0.10	21.58	0.09	20.88	0.09
656.0	337.3	21.49	0.10	21.53	0.08	20.87	0.09
873.9	435.2	21.36	0.10	21.51	0.08	21.07	0.10
680.3	425.1	21.52	0.10	21.61	0.10	21.13	0.11
776.8	573.0	21.39	0.10	21.61	0.09	21.09	0.11
437.9	519.6	23.09	0.15	22.00	0.08	20.44	0.08
794.6	136.9	21.36	0.10	21.56	0.08	21.08	0.09
551.9	534.3	21.36	0.10	21.53	0.08	21.02	0.09

Table B.1: Photometry of NGC 5694

X	Y	U	σU	B	σB	V	σV
720.0	678.2	21.32	0.10	21.57	0.09	20.99	0.09
861.4	330.7	21.32	0.10	21.57	0.09	21.01	0.09
839.3	714.4	21.40	0.09	21.47	0.08	21.25	0.09
533.8	406.7	21.44	0.09	21.57	0.09	20.87	0.09
685.6	683.1	21.42	0.10	21.60	0.09	21.02	0.09
37.6	164.5	21.44	0.09	21.53	0.08	21.15	0.09
730.7	614.1	21.52	0.10	21.59	0.09	20.92	0.15
744.3	291.8	21.56	0.10	21.63	0.10	20.78	0.09
758.8	84.5	21.55	0.11	21.59	0.08	20.87	0.09
844.9	418.7	21.52	0.11	21.64	0.09	20.93	0.10
824.3	589.6	21.48	0.10	21.63	0.08	21.24	0.10
558.7	974.6	23.00	0.16	21.77	0.08	20.12	0.09
915.2	520.7	21.53	0.10	21.57	0.08	21.06	0.09
594.9	438.9	21.62	0.10	21.59	0.09	21.37	0.12
864.9	416.8	21.48	0.11	21.59	0.09	21.05	0.10
617.1	421.9	21.49	0.11	21.68	0.10	21.04	0.11
708.7	355.3	21.51	0.09	21.58	0.08	21.48	0.20
771.9	713.2	21.53	0.09	21.60	0.08	21.02	0.09
565.9	458.5	21.57	0.09	21.58	0.08	20.99	0.09
606.2	585.6	21.52	0.10	21.57	0.09	21.07	0.09
642.2	506.9	21.44	0.10	21.67	0.09	20.97	0.14
763.5	572.8	21.40	0.11	21.72	0.09	20.95	0.10
367.0	22.6	22.66	0.13	21.78	0.08	20.64	0.08
909.4	469.7	21.54	0.10	21.59	0.08	21.05	0.09
828.0	364.5	21.50	0.10	21.72	0.09	20.91	0.09
919.2	581.1	21.45	0.11	21.78	0.09	21.18	0.10
825.3	572.8	21.41	0.11	21.59	0.09	21.10	0.09
879.8	381.6	21.69	0.10	21.60	0.08	20.88	0.10
798.4	624.8	21.42	0.10	21.68	0.09	21.26	0.10
868.8	728.0	21.50	0.09	21.67	0.08	21.10	0.09
717.5	648.5	21.53	0.10	21.65	0.08	20.98	0.09
901.8	220.5	21.48	0.10	21.65	0.08	21.00	0.09
526.4	411.7	21.62	0.10	21.63	0.09	20.89	0.09
920.7	76.9	21.45	0.10	21.67	0.08	21.02	0.09
858.2	269.7	21.50	0.10	21.65	0.08	21.00	0.09

Table B.1: Photometry of NGC 5694

X	Y	U	σU	B	σB	V	σV
933.6	389.6	21.67	0.10	21.63	0.08	21.02	0.09
760.5	361.4	21.49	0.11	21.69	0.09	21.48	0.13
949.4	834.5	21.60	0.10	21.65	0.08	21.04	0.09
693.4	114.8	21.52	0.10	21.67	0.08	21.07	0.09
606.8	761.5	21.51	0.09	21.70	0.08	20.99	0.09
883.2	450.5	21.42	0.10	21.72	0.09	21.06	0.09
819.2	335.5	21.56	0.10	21.70	0.08	21.14	0.10
742.9	336.5	21.52	0.09	21.72	0.08	20.91	0.10
596.3	484.3	21.51	0.10	21.71	0.09	21.27	0.10
634.3	390.6	21.51	0.10	21.78	0.09	20.98	0.13
330.3	778.2	21.59	0.10	21.70	0.08	21.00	0.09
153.5	933.2	21.61	0.10	21.69	0.08	21.06	0.09
606.8	989.4	21.60	0.10	21.64	0.08	21.40	0.10
655.3	559.8	21.52	0.11	21.81	0.09	20.98	0.10
536.3	534.5	21.75	0.10	21.64	0.08	21.10	0.09
782.0	541.5	21.47	0.11	21.68	0.09	21.47	0.17
581.8	807.8	21.45	0.10	21.70	0.08	21.09	0.09
699.7	375.9	21.78	0.11	21.72	0.08	20.86	0.10
31.7	226.6	21.59	0.10	21.76	0.08	21.00	0.09
593.7	807.0	23.44	0.18	22.01	0.08	20.68	0.08
866.0	711.7	21.64	0.10	21.72	0.08	21.02	0.09
880.5	425.8	21.56	0.10	21.69	0.10	21.25	0.10
672.8	473.9	21.94	0.13	21.74	0.09	21.22	0.16
671.1	330.8	21.59	0.11	21.64	0.09	21.62	0.11
545.7	570.6	21.77	0.11	21.69	0.09	21.07	0.09
898.0	420.8	21.56	0.10	21.73	0.08	21.24	0.09
977.9	692.5	21.62	0.09	21.76	0.08	21.02	0.09
687.2	186.1	21.60	0.10	21.70	0.09	21.12	0.09
754.6	351.8	21.53	0.10	21.77	0.09	21.27	0.12
603.0	377.4	21.74	0.11	21.70	0.08	21.10	0.09
786.5	674.3	21.46	0.10	21.72	0.10	21.19	0.09
967.5	733.8	21.67	0.10	21.74	0.08	21.07	0.09
870.8	338.4	21.66	0.10	21.71	0.08	21.18	0.10
577.4	464.2	21.67	0.09	21.72	0.08	21.12	0.09
424.8	535.5	21.60	0.10	21.75	0.08	21.20	0.09

Table B.1: Photometry of NGC 5694

X	Y	U	σU	B	σB	V	σV
871.8	286.1	21.60	0.10	21.76	0.08	21.10	0.09
580.2	601.6	21.56	0.10	21.76	0.09	21.17	0.09
578.7	622.0	21.56	0.10	21.76	0.09	21.44	0.11
799.6	526.1	21.93	0.14	21.66	0.09	21.23	0.16
929.0	342.7	21.49	0.11	21.99	0.10	21.05	0.09
805.9	654.7	21.73	0.10	21.71	0.09	21.19	0.09
841.5	571.5	21.61	0.10	21.77	0.08	21.13	0.10
547.1	518.9	21.64	0.10	21.72	0.08	21.16	0.09
750.5	284.5	21.61	0.10	21.73	0.08	21.15	0.09
816.4	480.0	21.84	0.11	21.60	0.09	21.30	0.12
74.3	573.9	21.66	0.10	21.78	0.08	21.18	0.09
868.9	560.5	21.53	0.09	21.86	0.09	21.26	0.09
819.2	318.6	21.56	0.10	21.74	0.09	21.23	0.09
839.6	450.9	21.51	0.11	21.76	0.09	21.42	0.12
666.5	384.4	21.63	0.10	21.82	0.09	21.16	0.10
728.8	99.4	21.62	0.09	21.84	0.08	21.26	0.10
457.3	486.1	21.71	0.11	21.78	0.08	21.17	0.09
913.1	307.5	21.76	0.10	21.81	0.09	21.26	0.12
824.1	546.2	21.57	0.10	21.85	0.09	21.40	0.11
684.4	632.7	21.61	0.11	21.78	0.08	21.31	0.10
594.8	230.2	21.75	0.10	21.82	0.08	21.04	0.09
808.0	620.2	21.63	0.10	21.80	0.09	21.29	0.10
816.9	367.1	21.62	0.11	21.80	0.08	21.28	0.09
859.1	431.8	21.69	0.11	21.77	0.10	21.27	0.11
909.0	392.7	21.72	0.10	21.81	0.08	21.14	0.10
610.4	623.5	21.67	0.10	21.78	0.08	21.24	0.09
886.2	421.8	21.49	0.10	21.87	0.09	21.17	0.09
864.7	338.8	21.61	0.11	21.85	0.10	21.25	0.09
441.8	535.5	21.67	0.09	21.89	0.08	21.27	0.10
382.2	439.0	21.72	0.10	21.85	0.09	21.35	0.10
462.8	461.2	21.72	0.10	21.87	0.08	21.03	0.09
750.8	653.3	21.82	0.10	21.72	0.08	21.62	0.11
826.7	234.6	21.76	0.10	21.85	0.09	21.20	0.10
853.1	574.8	21.61	0.11	21.77	0.09	21.47	0.09
516.2	450.8	21.63	0.10	21.81	0.09	21.30	0.09

Table B.1: Photometry of NGC 5694

X	Y	U	σU	B	σB	V	σV
894.3	443.0	21.68	0.10	21.89	0.08	21.15	0.10
574.3	648.5	21.68	0.11	21.83	0.09	21.29	0.10
659.2	346.2	21.72	0.10	21.92	0.09	21.38	0.10
768.0	366.8	21.69	0.11	21.92	0.09	21.27	0.11
365.6	280.1	21.76	0.10	21.87	0.09	21.23	0.10
124.8	561.1	21.70	0.10	21.86	0.08	21.23	0.09
216.9	665.7	21.66	0.11	21.92	0.11	21.56	0.17
806.3	303.8	21.81	0.10	21.82	0.08	21.27	0.10
593.4	493.7	21.74	0.10	21.71	0.10	21.37	0.11
899.2	579.5	21.77	0.11	21.95	0.10	21.18	0.10
832.6	111.6	21.84	0.09	21.86	0.08	21.14	0.09
703.4	287.6	21.73	0.10	21.85	0.09	21.33	0.10
687.0	314.1	21.62	0.11	21.88	0.09	21.30	0.09
651.5	318.1	21.75	0.10	21.86	0.09	21.50	0.10
750.0	898.9	21.62	0.09	21.93	0.09	21.21	0.09
1004.0	360.4	21.70	0.10	21.92	0.09	21.43	0.10
939.4	391.5	21.57	0.10	21.89	0.08	21.39	0.10
527.4	297.0	21.70	0.11	21.83	0.08	21.33	0.10
868.9	679.4	21.72	0.11	21.85	0.08	21.24	0.09
44.5	469.6	21.71	0.11	21.85	0.08	21.31	0.09
658.8	710.5	21.64	0.10	21.83	0.08	21.44	0.09
872.3	472.0	21.76	0.11	21.81	0.09	21.38	0.12
195.6	789.5	21.67	0.10	21.95	0.08	21.19	0.10
540.3	542.1	21.73	0.09	21.86	0.08	21.46	0.10
783.6	856.0	21.66	0.10	21.89	0.09	21.28	0.09
828.0	629.1	21.66	0.11	21.83	0.08	21.34	0.09
779.5	342.0	21.73	0.10	21.97	0.09	21.78	0.16
417.4	409.1	21.75	0.09	21.90	0.08	21.27	0.09
861.2	352.4	21.79	0.11	21.80	0.09	21.42	0.09
928.8	562.8	21.69	0.11	21.88	0.08	21.41	0.12
885.7	645.1	21.74	0.10	21.95	0.08	21.24	0.09
807.1	632.1	21.59	0.10	21.96	0.09	21.33	0.10
885.6	859.3	21.66	0.10	21.89	0.08	21.27	0.09
847.4	659.5	21.77	0.10	21.99	0.09	21.28	0.12
581.5	165.8	21.75	0.10	21.86	0.09	21.31	0.09

Table B.1: Photometry of NGC 5694

X	Y	U	σU	B	σB	V	σV
461.4	382.8	21.80	0.10	21.86	0.08	21.46	0.10
822.6	815.4	21.75	0.09	21.88	0.08	21.44	0.10
679.0	189.9	21.82	0.10	21.88	0.09	21.23	0.09
663.8	30.4	21.70	0.10	21.90	0.08	21.31	0.09
573.8	595.6	21.72	0.10	21.94	0.09	21.23	0.09
276.8	701.7	21.74	0.10	21.90	0.08	21.31	0.09
478.5	769.7	21.72	0.09	22.02	0.08	21.42	0.10
256.1	728.8	21.67	0.10	22.01	0.09	21.35	0.09
525.9	285.2	21.79	0.10	21.93	0.08	21.24	0.10
890.8	264.7	21.88	0.10	21.85	0.08	21.60	0.12
1008.0	652.1	21.88	0.11	21.89	0.08	21.25	0.09
906.4	546.9	21.83	0.10	21.94	0.09	21.34	0.11
550.0	157.0	21.74	0.09	21.91	0.08	21.33	0.09
563.0	765.0	21.68	0.10	21.94	0.09	21.31	0.09
864.0	12.4	21.84	0.10	21.95	0.08	21.36	0.10
857.8	422.6	21.90	0.12	21.87	0.09	21.34	0.10
463.1	675.4	21.75	0.10	21.96	0.08	21.37	0.09
668.0	392.5	22.00	0.13	21.88	0.09	21.46	0.13
741.1	743.7	21.76	0.10	21.96	0.08	21.25	0.10
701.9	599.3	21.89	0.10	21.82	0.09	21.53	0.10
621.7	453.1	21.85	0.11	21.94	0.09	21.98	0.15
809.8	626.2	21.72	0.10	22.02	0.09	21.48	0.11
897.0	351.4	21.67	0.11	21.96	0.09	21.40	0.09
915.5	782.5	21.87	0.11	21.95	0.08	21.41	0.10
765.4	637.1	21.85	0.10	21.86	0.09	21.55	0.11
927.6	430.6	21.77	0.10	21.96	0.08	21.39	0.10
831.5	713.3	21.95	0.11	21.93	0.09	21.32	0.10
600.3	492.1	21.83	0.11	21.98	0.09	21.35	0.12
688.0	645.0	21.69	0.10	21.96	0.09	21.45	0.10
918.2	452.1	21.98	0.11	21.86	0.09	21.54	0.11
898.6	567.1	21.78	0.10	21.93	0.09	21.42	0.09
864.2	258.7	21.85	0.11	21.94	0.08	21.35	0.09
747.0	646.2	21.79	0.10	22.02	0.09	21.49	0.11
222.8	556.6	21.82	0.10	21.96	0.08	21.38	0.10
744.1	866.2	21.72	0.10	21.95	0.08	21.42	0.10

Table B.1: Photometry of NGC 5694

X	Y	U	σU	B	σB	V	σV
826.7	421.1	21.75	0.11	22.11	0.09	21.25	0.10
490.8	557.0	21.85	0.11	22.01	0.09	21.35	0.10
837.8	21.6	21.95	0.10	21.94	0.09	21.32	0.09
527.7	808.8	21.72	0.10	21.99	0.08	21.36	0.09
492.5	641.8	21.80	0.10	21.97	0.08	21.41	0.09
704.3	577.7	21.56	0.11	22.06	0.09	21.51	0.11
829.3	610.6	21.85	0.10	21.97	0.10	21.57	0.11
619.8	401.8	22.07	0.12	21.92	0.10	21.58	0.15
187.8	731.5	21.80	0.10	21.97	0.08	21.42	0.09
498.7	18.3	21.80	0.10	22.01	0.09	21.47	0.10
854.1	418.9	21.86	0.10	21.96	0.09	21.66	0.12
121.1	329.9	21.76	0.11	22.02	0.08	21.45	0.10
859.4	662.7	21.90	0.10	21.95	0.09	21.53	0.10
527.6	270.4	21.90	0.11	21.98	0.08	21.47	0.10
949.9	271.3	21.91	0.11	22.01	0.09	21.33	0.09
354.9	131.1	21.92	0.10	21.96	0.08	21.37	0.10
829.3	165.4	21.89	0.10	22.02	0.08	21.39	0.10
800.7	597.4	21.85	0.10	22.04	0.09	21.37	0.10
697.3	284.9	21.99	0.12	22.02	0.09	21.39	0.10
104.3	577.0	21.71	0.11	21.99	0.08	21.44	0.10
604.1	720.8	21.89	0.11	22.04	0.09	21.67	0.12
857.2	213.8	21.86	0.10	21.98	0.08	21.44	0.09
706.5	621.2	21.69	0.11	22.07	0.08	21.32	0.10
724.0	641.6	21.72	0.11	22.06	0.09	21.53	0.12
326.6	377.1	21.77	0.10	22.06	0.09	21.65	0.12
691.7	1000.9	21.83	0.10	22.03	0.09	21.55	0.10
881.9	270.0	21.86	0.11	21.99	0.09	21.50	0.10
300.1	548.8	21.80	0.10	22.01	0.08	21.62	0.10
913.3	480.4	21.86	0.11	21.94	0.09	21.52	0.10
213.1	871.5	21.84	0.10	22.05	0.09	21.48	0.10
462.0	290.5	21.88	0.11	22.02	0.08	21.38	0.09
862.2	322.6	21.74	0.10	22.11	0.10	21.38	0.09
933.2	630.7	21.81	0.10	21.99	0.08	21.58	0.10
748.6	968.3	21.79	0.11	22.11	0.09	21.38	0.09
912.7	227.0	21.84	0.10	22.02	0.09	21.44	0.10

Table B.1: Photometry of NGC 5694

X	Y	U	σU	B	σB	V	σV
932.8	442.6	21.82	0.11	22.04	0.09	21.66	0.10
904.4	331.6	21.94	0.11	22.05	0.09	21.57	0.11
646.8	333.8	22.00	0.11	22.04	0.09	21.53	0.10
937.9	693.9	21.90	0.10	22.04	0.08	21.62	0.11
596.3	645.6	21.85	0.11	22.12	0.08	21.45	0.10
413.1	854.5	21.92	0.11	22.03	0.09	21.52	0.10
930.2	480.2	22.07	0.12	21.97	0.09	21.51	0.10
559.9	579.8	21.90	0.10	22.05	0.08	21.40	0.10
877.2	311.6	21.79	0.09	22.16	0.09	21.63	0.10
817.0	803.3	21.93	0.10	22.04	0.08	21.50	0.10
568.0	689.2	21.79	0.10	22.14	0.09	21.45	0.11
876.1	564.2	21.89	0.11	22.01	0.09	21.78	0.12
492.9	626.5	21.80	0.10	22.03	0.08	21.66	0.10
686.8	293.1	21.83	0.10	22.13	0.09	21.47	0.10
487.7	873.4	21.78	0.10	22.07	0.08	21.46	0.10
396.0	192.0	21.91	0.11	22.05	0.09	21.45	0.10
597.2	475.7	21.55	0.11	22.08	0.09	21.98	0.14
121.7	74.4	21.87	0.10	22.11	0.09	21.54	0.10
872.4	251.8	21.97	0.11	22.09	0.09	21.47	0.10
474.2	421.1	22.07	0.11	22.04	0.09	21.26	0.09
744.5	987.4	21.75	0.10	22.07	0.08	21.69	0.11
717.7	270.4	22.07	0.11	22.05	0.09	21.51	0.12
778.1	678.3	21.86	0.10	22.05	0.09	22.02	0.39
740.3	991.4	22.01	0.11	22.03	0.08	21.52	0.10
491.7	460.2	21.92	0.10	22.07	0.08	21.54	0.10
997.3	726.1	21.83	0.11	22.05	0.08	21.54	0.10
735.8	207.3	21.83	0.11	22.02	0.08	21.58	0.10
742.3	317.2	22.05	0.11	21.96	0.09	21.50	0.10
226.8	952.2	21.85	0.10	22.08	0.08	21.54	0.11
363.9	702.0	21.97	0.11	22.05	0.08	21.55	0.10
702.9	282.0	21.78	0.11	22.01	0.09	21.63	0.10
742.0	246.8	21.92	0.10	22.05	0.08	21.58	0.10
946.1	282.4	21.94	0.11	22.05	0.08	21.60	0.11
760.3	793.5	21.77	0.10	22.13	0.09	21.51	0.10
913.5	586.7	21.87	0.10	22.13	0.08	21.53	0.11

Table B.1: Photometry of NGC 5694

X	Y	U	σU	B	σB	V	σV
729.4	323.4	21.88	0.10	22.05	0.09	21.62	0.10
431.1	555.0	21.89	0.10	22.10	0.08	21.44	0.10
588.6	733.2	21.92	0.11	22.16	0.09	21.48	0.10
831.9	645.8	21.89	0.11	22.10	0.09	21.50	0.09
911.3	568.5	22.00	0.12	22.06	0.09	21.48	0.11
818.7	259.5	22.03	0.12	22.00	0.08	21.61	0.11
761.2	662.9	22.02	0.12	21.96	0.09	21.83	0.11
571.6	618.6	21.92	0.10	22.06	0.08	21.66	0.11
110.8	587.1	21.92	0.10	22.08	0.08	21.52	0.10
532.7	593.3	21.93	0.10	22.12	0.09	21.80	0.11
577.0	396.5	21.92	0.11	22.08	0.08	21.69	0.11
647.1	265.6	22.13	0.10	21.98	0.09	21.71	0.11
493.0	406.7	21.87	0.12	22.09	0.09	21.45	0.10
375.6	473.0	21.93	0.12	22.08	0.09	21.59	0.10
437.1	372.0	22.09	0.10	22.10	0.08	21.46	0.09
579.3	282.7	21.94	0.10	22.05	0.08	21.70	0.10
972.5	582.1	21.88	0.10	22.11	0.09	21.67	0.11
562.2	742.3	21.94	0.10	22.09	0.09	21.65	0.11
187.4	607.3	21.94	0.11	22.09	0.09	21.52	0.10
787.4	637.9	22.17	0.13	22.02	0.09	21.43	0.11
617.6	615.2	21.86	0.10	22.12	0.09	21.51	0.10
905.4	738.4	22.00	0.12	22.09	0.08	21.45	0.10
861.1	493.1	21.96	0.11	22.09	0.10	21.58	0.11
762.5	696.0	21.92	0.10	22.10	0.09	21.58	0.10
898.0	95.2	21.91	0.10	22.10	0.08	21.53	0.10
895.5	627.6	21.78	0.11	22.14	0.09	21.86	0.16
585.7	470.7	21.93	0.10	22.08	0.09	21.63	0.10
760.5	341.9	21.93	0.11	22.07	0.08	21.94	0.12
768.0	324.9	22.04	0.11	22.00	0.10	21.63	0.11
781.2	587.6	22.02	0.11	22.13	0.09	21.49	0.11
895.3	545.1	22.00	0.11	22.07	0.08	21.60	0.10
859.5	169.0	21.98	0.11	22.08	0.08	21.50	0.10
444.3	370.4	21.94	0.11	22.11	0.08	21.64	0.11
721.3	328.3	21.94	0.11	22.08	0.09	21.55	0.11
733.0	820.0	22.09	0.11	22.07	0.08	21.58	0.10

Table B.1: Photometry of NGC 5694

X	Y	U	σU	B	σB	V	σV
849.3	423.2	22.03	0.10	22.07	0.09	21.54	0.10
641.2	607.9	22.13	0.12	22.05	0.09	21.52	0.10
876.4	661.3	22.07	0.11	22.06	0.09	21.65	0.11
647.9	530.8	21.92	0.12	22.09	0.09	21.86	0.14
356.5	654.3	21.90	0.10	22.16	0.08	21.69	0.11
694.1	355.0	22.17	0.13	22.30	0.11	21.68	0.19
857.4	753.0	21.94	0.10	22.14	0.09	21.72	0.11
669.3	364.7	21.98	0.12	22.07	0.09	21.78	0.12
1007.2	768.5	22.15	0.13	22.15	0.08	21.56	0.10
649.7	306.5	21.98	0.11	22.06	0.08	21.80	0.11
551.1	948.1	21.85	0.11	22.18	0.09	21.63	0.11
792.4	564.8	21.85	0.12	22.21	0.11	21.87	0.15
665.8	673.3	21.99	0.11	22.08	0.09	21.69	0.11
676.8	813.0	21.94	0.12	22.12	0.08	21.60	0.11
560.6	284.4	21.90	0.11	22.16	0.09	21.55	0.10
770.9	853.9	21.99	0.10	22.24	0.09	21.50	0.11
522.9	659.9	21.92	0.11	22.13	0.09	21.62	0.10
533.0	447.0	21.88	0.10	22.18	0.09	21.89	0.11
652.7	700.4	22.00	0.10	22.27	0.09	21.62	0.10
878.3	572.9	21.91	0.11	22.14	0.09	21.76	0.12
501.3	735.5	21.96	0.11	22.12	0.09	21.59	0.10
895.5	329.6	21.93	0.10	22.24	0.09	21.52	0.11
713.8	7.4	21.98	0.10	22.17	0.08	21.60	0.10
582.2	318.3	21.95	0.10	22.17	0.09	21.85	0.14
744.4	898.0	22.01	0.11	22.14	0.08	21.68	0.10
778.3	689.2	21.98	0.11	22.14	0.09	21.75	0.11
974.8	748.5	21.90	0.11	22.20	0.09	21.52	0.10
222.2	810.4	21.84	0.10	22.22	0.08	21.56	0.11
287.2	795.7	21.95	0.10	22.21	0.09	21.68	0.10
943.2	532.5	22.03	0.11	22.10	0.08	21.67	0.10
637.2	343.1	22.06	0.11	22.08	0.09	21.99	0.14
845.1	747.7	21.94	0.12	22.16	0.08	21.66	0.11
661.9	655.2	21.88	0.11	22.19	0.09	21.74	0.11
444.0	763.8	21.92	0.11	22.17	0.08	21.69	0.10
622.3	334.6	21.96	0.10	22.22	0.09	21.80	0.12

Table B.1: Photometry of NGC 5694

X	Y	U	σU	B	σB	V	σV
867.3	406.8	21.97	0.11	22.18	0.10	22.38	0.22
623.2	281.7	21.94	0.10	22.18	0.09	21.65	0.10
767.2	685.1	22.09	0.10	22.12	0.08	21.79	0.10
504.6	553.7	21.95	0.10	22.16	0.08	21.75	0.11
559.0	480.5	22.04	0.11	22.20	0.09	21.81	0.12
877.7	341.3	22.07	0.12	22.12	0.09	21.92	0.12
583.3	503.6	21.98	0.10	22.23	0.09	21.97	0.13
782.2	245.1	22.24	0.12	22.19	0.09	21.52	0.12
879.6	504.8	22.15	0.13	22.11	0.09	22.07	0.18
857.8	686.2	22.02	0.13	22.16	0.08	21.72	0.14
828.3	312.5	22.04	0.11	22.16	0.09	21.73	0.12
602.0	138.5	22.04	0.09	22.24	0.09	21.82	0.12
224.4	37.2	21.97	0.10	22.19	0.08	21.64	0.11
634.3	141.9	21.97	0.10	22.22	0.08	21.63	0.11
678.7	618.5	21.98	0.11	22.23	0.09	21.57	0.10
763.5	585.1	21.97	0.12	22.15	0.09	21.83	0.13
516.3	518.5	21.99	0.11	22.18	0.09	21.73	0.11
553.4	441.1	22.02	0.13	22.13	0.09	21.77	0.13
662.9	281.1	22.07	0.11	22.15	0.09	21.83	0.12
776.7	306.3	22.03	0.11	22.22	0.09	21.57	0.10
541.4	961.8	22.01	0.11	22.19	0.08	21.82	0.10
551.3	624.4	22.03	0.12	22.14	0.09	21.80	0.11
348.6	473.2	22.08	0.12	22.30	0.12	21.83	0.15
703.6	638.0	22.49	0.14	22.15	0.09	21.31	0.09
549.5	845.6	22.05	0.11	22.26	0.09	21.48	0.11
469.6	557.2	21.96	0.10	22.20	0.09	21.72	0.10
854.1	618.8	22.02	0.10	22.25	0.09	21.72	0.18
678.8	167.1	22.23	0.11	22.15	0.09	21.64	0.10
461.2	199.5	21.99	0.11	22.21	0.09	21.68	0.10
599.1	480.5	22.14	0.13	22.25	0.09	21.58	0.10
567.1	879.7	21.89	0.12	22.19	0.08	21.84	0.11
578.0	205.8	22.14	0.11	22.15	0.09	21.81	0.10
146.7	382.4	21.96	0.10	22.25	0.08	21.61	0.09
899.7	425.8	22.00	0.10	22.31	0.09	21.59	0.11
779.2	674.5	21.95	0.10	22.28	0.09	22.11	0.20

Table B.1: Photometry of NGC 5694

X	Y	U	σU	B	σB	V	σV
862.1	801.3	21.97	0.10	22.19	0.09	21.78	0.10
488.2	158.4	22.04	0.13	22.16	0.09	21.59	0.10
345.1	34.7	22.09	0.11	22.21	0.09	21.72	0.11
673.3	221.6	22.13	0.11	22.15	0.09	21.83	0.11
953.9	770.7	20.73	0.23	22.24	0.09	21.67	0.11
414.5	506.5	22.03	0.11	22.23	0.09	21.78	0.10
633.7	764.2	21.90	0.10	22.23	0.09	21.72	0.10
860.0	478.4	21.89	0.11	22.33	0.10	22.04	0.23
500.5	531.1	22.03	0.11	22.24	0.09	21.70	0.11
558.7	300.1	22.11	0.11	22.22	0.08	21.69	0.12
901.5	215.8	22.01	0.11	22.27	0.09	21.75	0.10
683.6	651.2	21.89	0.11	22.23	0.09	21.82	0.12
560.5	759.6	22.04	0.11	22.24	0.08	21.78	0.11
720.7	701.2	22.02	0.11	22.25	0.09	21.62	0.10
866.6	496.7	22.08	0.12	22.21	0.09	21.80	0.15
602.9	422.7	22.14	0.13	22.40	0.12	21.70	0.16
357.5	679.8	22.17	0.11	22.23	0.09	21.84	0.12
944.7	545.3	22.04	0.11	22.21	0.09	21.94	0.11
390.6	141.9	22.03	0.11	22.26	0.09	21.73	0.10
751.3	296.8	22.16	0.11	22.23	0.09	21.70	0.11
830.4	385.3	22.26	0.11	22.14	0.09	21.85	0.13
866.8	466.1	22.14	0.12	22.23	0.09	21.81	0.12
587.4	409.5	22.15	0.11	22.32	0.09	21.51	0.11
969.8	623.3	22.11	0.12	22.27	0.09	21.74	0.11
925.3	364.9	22.02	0.10	22.29	0.09	21.82	0.13
679.2	764.1	22.07	0.12	22.28	0.09	21.95	0.13
627.6	957.1	22.02	0.11	22.32	0.09	21.63	0.11
603.4	749.1	21.97	0.11	22.31	0.09	21.57	0.10
921.6	93.9	21.96	0.11	22.31	0.09	21.84	0.11
969.1	673.2	22.00	0.10	22.30	0.08	21.77	0.11
893.8	817.3	22.20	0.11	22.23	0.09	21.61	0.10
899.8	185.2	21.95	0.10	22.28	0.09	21.84	0.11
741.2	237.2	22.16	0.12	22.27	0.09	21.59	0.10
999.2	43.4	21.96	0.11	22.27	0.09	21.76	0.10
147.0	246.0	22.04	0.10	22.30	0.08	21.84	0.11

Table B.1: Photometry of NGC 5694

X	Y	U	σU	B	σB	V	σV
810.8	330.4	22.17	0.10	22.21	0.10	22.35	0.20
948.9	622.1	22.15	0.12	22.37	0.09	21.49	0.11
657.5	785.7	22.07	0.10	22.32	0.09	21.87	0.12
174.3	887.7	22.56	0.17	22.74	0.10	21.08	0.09
815.6	48.3	22.11	0.12	22.26	0.09	21.78	0.10
486.4	634.8	22.05	0.12	22.23	0.08	21.80	0.10
573.2	337.6	22.03	0.11	22.29	0.09	21.73	0.11
639.0	625.4	22.13	0.13	22.25	0.09	21.83	0.12
889.2	310.1	22.15	0.11	22.28	0.09	21.92	0.13
971.6	449.5	22.20	0.10	22.29	0.09	21.76	0.11
880.9	291.2	22.31	0.12	22.23	0.10	22.82	0.35
430.8	482.4	22.15	0.11	22.23	0.09	21.93	0.12
794.0	608.0	22.12	0.11	22.29	0.10	22.18	0.17
693.2	605.8	22.24	0.12	22.26	0.09	21.77	0.14
517.7	799.6	22.03	0.10	22.33	0.09	21.83	0.12
723.8	658.6	22.23	0.11	22.23	0.09	21.98	0.13
982.0	216.6	22.19	0.10	22.25	0.09	21.78	0.10
430.9	685.4	22.24	0.12	22.32	0.09	22.07	0.14
664.4	692.2	22.18	0.11	22.30	0.09	21.85	0.11
647.0	603.1	22.09	0.12	22.35	0.09	21.73	0.12
1006.5	567.3	22.02	0.11	22.28	0.09	22.12	0.13
977.8	640.0	22.09	0.11	22.34	0.10	21.91	0.12
564.8	622.5	22.20	0.12	22.29	0.10	21.73	0.10
464.0	129.3	22.04	0.11	22.33	0.09	21.80	0.11
856.4	558.6	22.18	0.12	22.31	0.10	22.15	0.14
239.4	643.1	22.06	0.12	22.35	0.09	21.91	0.13
873.7	591.7	22.12	0.11	22.45	0.10	22.06	0.21
642.2	292.8	22.20	0.12	22.26	0.09	22.16	0.14
575.8	392.8	22.43	0.15	22.33	0.09	21.71	0.12
599.7	823.3	22.12	0.10	22.39	0.08	21.82	0.11
365.5	748.3	22.10	0.11	22.32	0.09	21.84	0.12
696.7	241.0	22.09	0.11	22.28	0.09	22.33	0.17
862.3	304.4	22.18	0.10	22.39	0.09	22.04	0.13
905.3	461.6	22.48	0.14	22.21	0.10	21.81	0.12
780.5	124.7	22.30	0.11	22.31	0.09	21.77	0.11

Table B.1: Photometry of NGC 5694

X	Y	U	σU	B	σB	V	σV
887.8	36.1	22.29	0.11	22.34	0.09	21.86	0.12
803.0	603.9	22.17	0.13	22.40	0.09	21.84	0.12
506.8	203.3	22.28	0.13	22.32	0.09	21.96	0.13
676.4	981.0	22.25	0.11	22.35	0.08	21.80	0.12
214.1	190.5	21.92	0.11	22.68	0.11	21.86	0.13
812.9	335.4	22.21	0.11	22.34	0.09	21.85	0.13
921.7	741.1	22.22	0.11	22.39	0.09	21.84	0.11
753.9	768.8	22.21	0.12	22.37	0.09	21.96	0.13
816.3	537.4	22.38	0.14	22.36	0.11	21.83	0.19
330.7	200.4	22.15	0.12	22.38	0.09	22.05	0.13
224.4	127.4	22.04	0.11	22.40	0.09	21.81	0.12
556.5	476.7	22.21	0.12	22.30	0.09	22.26	0.14
678.0	575.5	22.10	0.13	22.30	0.10	22.00	0.12
731.2	251.8	22.19	0.11	22.38	0.10	22.15	0.13
942.0	1009.7	22.09	0.11	22.44	0.09	21.85	0.12
599.1	589.3	22.24	0.11	22.35	0.09	22.05	0.14
505.4	319.4	22.10	0.11	22.43	0.09	21.77	0.12
675.5	386.3	22.28	0.13	22.32	0.13	22.06	0.21
796.3	151.2	22.49	0.13	22.30	0.09	22.01	0.12
719.9	297.3	22.30	0.13	22.36	0.09	22.08	0.15
783.9	87.1	22.33	0.12	22.36	0.09	21.95	0.11
766.8	296.0	22.34	0.12	22.37	0.09	21.92	0.13
925.7	410.7	22.28	0.11	22.36	0.09	22.10	0.13
582.5	346.5	22.31	0.12	22.39	0.09	21.83	0.13
888.9	606.3	22.27	0.12	22.46	0.10	21.67	0.13
493.7	549.6	22.17	0.12	22.36	0.09	21.85	0.10
883.4	226.4	22.14	0.11	22.44	0.09	21.86	0.13
672.6	254.6	22.21	0.11	22.44	0.09	21.87	0.11
588.0	454.5	22.33	0.12	22.33	0.09	22.39	0.18
636.3	357.0	22.27	0.12	22.33	0.09	22.16	0.14
538.2	499.2	22.25	0.13	22.28	0.09	22.18	0.14
482.7	867.9	22.23	0.11	22.46	0.09	21.74	0.11
815.8	590.8	22.27	0.12	22.46	0.10	22.03	0.14
564.2	471.8	22.29	0.12	22.41	0.09	21.93	0.14
532.6	199.2	22.17	0.11	22.43	0.09	22.01	0.12

Table B.1: Photometry of NGC 5694

X	Y	U	σU	B	σB	V	σV
637.6	444.8	22.12	0.13	22.51	0.11	22.39	0.24
851.9	429.8	22.27	0.12	22.34	0.10	22.19	0.17
670.0	756.5	22.31	0.12	22.34	0.09	21.97	0.12
668.1	1016.8	22.17	0.10	22.48	0.09	22.02	0.12
719.3	228.5	22.24	0.12	22.41	0.09	21.96	0.11
682.5	641.2	22.10	0.11	22.50	0.10	21.89	0.12
827.7	697.3	22.66	0.24	22.40	0.09	21.78	0.11
446.8	86.5	22.11	0.12	22.51	0.09	21.91	0.12
776.7	662.0	22.48	0.13	22.39	0.09	22.23	0.14
757.6	974.2	22.51	0.14	22.59	0.09	21.47	0.09
667.4	716.5	22.23	0.11	22.40	0.09	22.09	0.13
969.5	53.0	22.50	0.13	22.42	0.09	21.63	0.10
591.4	385.0	22.43	0.12	22.45	0.09	21.79	0.13
725.5	960.8	22.11	0.11	22.46	0.09	21.91	0.10
568.7	727.2	22.22	0.12	22.46	0.09	22.06	0.13
741.8	779.7	22.21	0.11	22.45	0.09	22.06	0.13
644.6	678.1	22.14	0.11	22.45	0.09	22.19	0.15
882.3	475.0	22.31	0.13	22.36	0.10	22.59	0.24
794.0	676.7	22.17	0.11	22.47	0.08	21.95	0.13
957.8	493.6	22.15	0.11	22.45	0.09	22.03	0.13
278.0	912.7	22.24	0.14	22.43	0.10	21.85	0.11
284.8	493.8	22.34	0.11	22.40	0.09	21.94	0.11
409.2	691.5	22.39	0.12	22.38	0.09	22.15	0.13
777.2	113.8	22.29	0.13	22.50	0.09	21.94	0.12
769.5	176.1	22.17	0.12	22.46	0.09	21.96	0.12
624.1	60.3	22.18	0.11	22.46	0.09	22.20	0.15
583.3	650.5	22.26	0.12	22.49	0.11	21.99	0.12
970.7	181.5	22.14	0.11	22.50	0.09	22.03	0.12
231.0	63.3	22.26	0.13	22.47	0.09	22.11	0.13
935.4	367.1	22.26	0.12	22.44	0.09	22.04	0.12
733.5	318.1	22.33	0.12	22.42	0.10	22.12	0.14
715.8	108.0	22.29	0.12	22.46	0.09	21.97	0.12
553.2	139.9	22.10	0.10	22.61	0.09	21.88	0.12
853.7	150.4	22.17	0.12	22.55	0.09	22.06	0.13
683.4	675.2	22.33	0.12	22.48	0.09	22.13	0.14

Table B.1: Photometry of NGC 5694

X	Y	U	σU	B	σB	V	σV
607.6	469.6	22.30	0.13	22.42	0.10	22.54	0.16
701.7	148.7	22.31	0.11	22.45	0.08	22.06	0.12
895.4	708.3	22.32	0.10	22.61	0.10	21.88	0.13
569.3	710.3	22.55	0.13	22.44	0.09	22.08	0.12
857.2	467.7	22.42	0.15	22.40	0.11	22.84	0.34
226.5	694.6	22.29	0.13	22.50	0.09	21.89	0.11
794.5	194.0	22.29	0.11	22.61	0.09	21.84	0.11
720.9	319.6	22.36	0.16	22.43	0.10	22.12	0.15
517.1	355.8	22.26	0.11	22.50	0.09	22.01	0.12
759.2	806.2	22.26	0.12	22.53	0.09	21.98	0.14
674.0	322.7	22.40	0.12	22.50	0.10	22.21	0.13
775.9	746.5	22.37	0.12	22.54	0.09	21.99	0.12
855.7	297.3	22.25	0.11	22.52	0.09	22.32	0.15
554.8	808.3	22.32	0.12	22.51	0.09	22.22	0.13
150.5	358.9	22.42	0.13	22.52	0.09	22.24	0.14
525.1	839.1	22.18	0.13	22.58	0.09	22.18	0.14
886.3	339.1	22.44	0.11	22.55	0.10	22.10	0.14
813.5	677.6	22.50	0.13	22.57	0.10	22.03	0.13
591.7	375.0	22.35	0.12	22.58	0.11	22.05	0.12
676.5	202.0	22.35	0.12	22.50	0.09	22.22	0.15
548.8	737.0	22.44	0.12	22.55	0.09	22.17	0.13
929.6	757.4	22.30	0.11	22.63	0.09	22.04	0.12
559.2	248.3	22.42	0.12	22.55	0.10	22.14	0.13
781.1	761.1	22.36	0.12	22.53	0.09	22.11	0.12
851.0	931.4	22.17	0.10	22.80	0.10	22.06	0.12
538.0	753.1	22.35	0.12	22.61	0.09	21.96	0.12
652.2	209.0	22.47	0.12	22.52	0.09	22.12	0.14
489.8	835.4	22.25	0.13	22.62	0.09	21.98	0.12
859.2	200.3	22.49	0.11	22.57	0.09	21.98	0.12
912.3	335.6	22.57	0.13	22.49	0.10	22.06	0.13
690.1	169.8	22.37	0.12	22.58	0.09	21.98	0.12
329.8	685.1	22.49	0.13	22.52	0.09	22.35	0.14
598.0	991.2	22.36	0.15	22.58	0.09	22.02	0.13
481.6	537.6	22.35	0.13	22.60	0.09	22.24	0.14
720.8	78.4	22.76	0.13	22.60	0.09	21.74	0.10

Table B.1: Photometry of NGC 5694

X	Y	U	σU	B	σB	V	σV
529.5	890.0	22.30	0.12	22.65	0.10	22.16	0.12
837.7	808.0	22.22	0.12	22.62	0.10	22.22	0.14
999.9	795.5	22.38	0.12	22.70	0.09	22.12	0.13
235.0	895.6	22.40	0.12	22.67	0.09	21.97	0.12
907.1	837.8	22.31	0.14	22.63	0.09	22.11	0.13
631.0	383.1	22.55	0.17	22.54	0.09	22.42	0.16
875.2	824.8	22.39	0.12	22.68	0.10	22.39	0.17
310.6	763.4	22.17	0.12	22.66	0.09	22.31	0.16
941.0	441.0	22.52	0.13	22.64	0.09	22.01	0.12
868.0	395.0	22.68	0.16	22.62	0.10	22.26	0.28
912.0	789.1	22.44	0.12	22.59	0.09	22.24	0.14
259.1	528.3	22.46	0.15	22.62	0.09	22.16	0.14
289.0	115.2	22.37	0.11	22.72	0.09	22.24	0.15
592.8	47.5	22.44	0.13	22.79	0.09	22.05	0.11
535.8	505.8	22.45	0.14	22.68	0.11	22.58	0.21
462.5	355.5	22.60	0.12	22.60	0.10	22.17	0.13
950.3	591.0	22.47	0.12	22.65	0.09	22.31	0.16
914.8	165.1	22.69	0.14	22.70	0.09	22.26	0.15
982.8	539.4	22.26	0.13	22.71	0.10	22.48	0.18
634.5	350.4	22.39	0.14	22.76	0.10	22.26	0.14
566.7	531.8	22.62	0.15	22.64	0.10	22.31	0.17
1003.8	339.1	22.48	0.14	22.74	0.09	22.36	0.16
808.0	398.8	22.62	0.22	22.69	0.11	22.10	0.16
872.3	581.8	22.52	0.13	22.71	0.10	22.48	0.18
857.6	362.3	22.79	0.15	22.73	0.10	22.25	0.17
618.2	294.6	22.50	0.12	22.84	0.11	22.29	0.15
882.3	437.4	22.42	0.14	22.75	0.12	22.69	0.23
70.8	358.0	22.45	0.13	22.80	0.10	22.27	0.17
677.2	351.5	22.44	0.16	22.76	0.12	22.46	0.20
372.2	483.5	22.59	0.16	22.79	0.09	22.36	0.17
365.4	523.3	22.61	0.14	22.78	0.10	22.26	0.15
788.2	51.2	22.45	0.13	22.79	0.10	22.22	0.14
628.5	758.8	22.73	0.16	22.66	0.10	22.37	0.20
503.1	466.1	22.64	0.13	22.76	0.09	22.20	0.14
578.4	127.0	22.53	0.14	22.77	0.10	22.29	0.14

Table B.1: Photometry of NGC 5694

X	Y	U	σU	B	σB	V	σV
357.0	726.3	22.47	0.13	22.75	0.10	22.33	0.14
97.3	477.8	22.52	0.14	22.91	0.09	22.01	0.13
727.8	300.9	22.81	0.18	22.72	0.10	22.52	0.20
945.9	195.3	22.41	0.12	22.82	0.09	22.34	0.15
840.4	446.8	22.77	0.22	22.96	0.14	22.84	0.35
438.1	102.5	22.48	0.13	22.87	0.10	22.15	0.14
736.7	854.1	22.57	0.16	22.84	0.10	22.16	0.15
912.9	882.8	22.31	0.12	22.90	0.09	22.15	0.13
194.7	16.6	22.62	0.15	22.84	0.09	22.18	0.13
600.7	662.8	22.76	0.16	22.77	0.11	22.42	0.16
936.0	601.3	22.51	0.13	22.82	0.10	22.40	0.16
913.5	560.9	22.68	0.17	22.90	0.12	22.47	0.18
308.4	327.2	22.53	0.15	22.90	0.10	22.24	0.14
769.2	676.2	22.52	0.15	22.83	0.10	22.75	0.24
783.3	774.9	22.86	0.19	22.81	0.09	22.43	0.14
797.2	748.2	22.60	0.17	22.86	0.11	22.78	0.22
723.4	736.5	22.56	0.14	22.92	0.10	22.48	0.17
828.0	372.8	22.61	0.19	22.89	0.14	22.57	0.19
512.8	572.9	22.80	0.12	22.96	0.10	22.31	0.15
171.0	34.9	22.70	0.16	22.90	0.10	22.44	0.14
780.7	230.9	22.57	0.13	23.09	0.10	22.14	0.12
637.9	379.9	23.00	0.19	22.88	0.11	22.72	0.22
959.1	169.3	22.67	0.13	22.98	0.11	22.29	0.17
966.5	92.5	22.73	0.13	22.97	0.10	22.44	0.19
707.1	156.9	22.66	0.14	22.94	0.11	22.52	0.19
536.8	312.7	22.65	0.14	23.09	0.11	22.53	0.18
870.2	181.0	22.51	0.15	23.05	0.10	22.29	0.15
598.0	837.7	22.75	0.14	23.04	0.11	22.55	0.18
907.2	486.6	22.80	0.18	22.97	0.10	22.70	0.24
438.6	442.7	22.98	0.14	22.91	0.10	22.56	0.17
352.4	712.1	22.61	0.16	23.04	0.11	22.81	0.35
737.2	297.4	23.64	0.26	22.95	0.11	22.94	0.29
603.8	473.2	23.11	0.20	23.07	0.13	23.26	0.37
420.5	164.7	22.70	0.18	23.20	0.10	22.38	0.16

Table B.1: Photometry of NGC 5694